Contract No. 582-23-45978
Work Order No. 9
Tracking No. 2025-05
Task 6.2

Prepared for:

Texas Commission on Environmental Quality
12100 Park 35 Circle MC 164
Austin, TX 78753

Prepared by:

Katie Tuite, Ling Huang, Gary Wilson and Greg Yarwood
Ramboll Americas Engineering Solutions, Inc.
7250 Redwood Blvd., Suite 105
Novato, California 94945

June 30, 2025

Updating CAMx's Treatment of VCP/IVOC to Target SOA Precursor Emissions More Precisely

PREPARED UNDER A CONTRACT FROM THE
TEXAS COMMISSION ON ENVIRONMENTAL QUALITY

The preparation of this document was financed through a contract from the State of Texas through the Texas Commission on Environmental Quality.
The content, findings, opinions and conclusions are the work of the author(s) and do not necessarily represent findings, opinions or conclusions of the TCEQ.

Updating CAMx's Treatment of VCP/IVOC to Target SOA Precursor Emissions More Precisely

Final Report

Ramboll
7250 Redwood Boulevard
Suite 105
Novato, CA 94945
USA

T +1 415 899 0700
https://ramboll.com

Contents

Appendix

Table of Figures

Table of Tables

List of Acronyms and Abbreviations

AToM	Atmospheric Tomography Mission
AVOC	Anthropogenic VOC
BC	Boundary conditions
BVOC	Biogenic VOC
CAMx	Comprehensive Air Quality Model with extensions
CB	Carbon Bond
CG	Condensable gas
CMC	Chemical mechanism compiler
CPA	Chemical process analysis
D5	Decamethylcyclopentasiloxane
DDM	Decoupled direct method
DFW	Dallas-Fort Worth
EPA	Environmental Protection Agency
HOM	Highly oxidized molecule
IVOC	Intermediate volatility organic compounds
MIR	Maximum incremental reactivity
OA	Organic aerosol
OFR	Oxidation flow reactor
OPE	Ozone production efficiency
OSAT	Ozone source apportionment technology
PAH	Polycyclic aromatic hydrocarbon
PAM-OFR	Potential aerosol mass oxidation flow reactor
PAN	Peroxyacyl nitrates
PBL	Planetary boundary layer
PM	Particulate matter
$PM_{2.5}$	Particulate matter with a diameter of 2.5 micrometers or less
POA	Primary organic aerosol
PSAT	Particulate source apportionment technology
SAN	San Antonio
SIP	State implementation plan
SOA	Secondary organic aerosol
SVOC	Semivolatile organic compounds
TYL	Tyler
VOC	Volatile organic compounds
VCP	Volatile chemical product
VBS	Volatility basis set

Plain Language Summary

Secondary organic aerosol (SOA) contributes a large fraction of particulate air pollution in Texas. Emissions from volatile chemical products (VCPs), which include products such as solvents, paints, and cleaning products, are important contributors to SOA production, however many air quality models poorly characterize VCP emissions and chemistry. Ramboll updated the treatment of VCPs in the Comprehensive Air Quality Model with Extensions (CAMx), which is used by the TCEQ for particulate air pollution modeling. We performed model tests and found that the VCP-related updates caused a decrease in SOA concentrations. The updates will allow TCEQ to better understand SOA production in Texas and to develop more effective strategies to address particulate air pollution.

Executive Summary

Volatile organic compound (VOC) containing products such as solvents, paints, printing inks, adhesives, pesticides, cleaning agents and personal care products are often referred to as volatile chemical products (VCPs) (McDonald et al., 2018) and have emerged recently as a VOC emission category that is poorly characterized in air pollution models. In the Comprehensive Air Quality Model with extensions (CAMx), which the Texas Commission on Environmental Quality (TCEQ) uses for particulate matter (PM) modeling, many different organic compounds, including VCPs, are mapped to a single intermediate volatility organic species (IVOC). IVOC is important to secondary organic aerosol (SOA) formation, particularly in Texas urban areas, but the amount of SOA produced from IVOC emissions is uncertain, partly due to the poor characterization of VCPs which have a wide range of SOA forming potential. The purpose of this project was to improve the treatment of VCP chemistry and emissions in CAMx to target important SOA precursors more precisely. By updating the gas-phase mechanism, aerosol scheme, and emission speciation mapping to better represent VCPs and IVOC in CAMx, we improve the accuracy of TCEQ's PM modeling in Texas, which is critical for the development of State Implementation Plan (SIP) strategies.

The most recent Carbon Bond mechanism, CB7r1, was updated to CB7r2 by integrating the VCP mechanism developed by Yarwood and Tuite (2024), which includes 16 new emitted VCP species and their oxidation reactions. A number of other changes were made in CB7r2, including maintenance of the core mechanism (i.e., rate constant and photolysis frequency updates), addition of a new species to represent emitted hydrogen, and updates to the chemistry of organic nitrates, biogenic degradation products, and iodine species. The new CAMx aerosol scheme (CB7r2_CF3) was developed following an analysis of the U.S. Environmental Protection Agency's VCP emission dataset (VCPy) and a literature review of SOA yields. We defined three new SOA precursor species (IVC1, IVC2, and HPAR) and updated yields for existing species IVOA, which allows CB7r2_CF3 to efficiently represent SOA production from VCP emissions. IVC1 and IVC2 were developed based on glycol ethers but can be used to represent other VCPs with similar SOA yields. HPAR, which is a gas-phase species in CB7r2 used to represent large alkanes, is included in CB7r2_CF3 to represent SOA production from large alkanes. The SOA yields for IVOA, which represents organic aerosol produced from IVOC, were updated in CB7r2_CF3 based on recently published SOA yield data for the types of compounds represented by IVOA. CAMx probing tools and the emissions speciation mapping were updated accordingly to work with the new CB7r2 mechanism and CB7r2_CF3 aerosol scheme and the updated version of CAMx is referred to as version 7.32-CB7r2.

Proper implementation of CB7r2, CB7r2_CF3, and CAMx probing tool updates were tested using CAMx 2-box model scenarios for three Texas locations: Dallas-Fort Worth (DFW), San Antonio (SAN), and Tyler (TYL) in Northeast Texas. We conducted three sets of model runs for each location: 1) CB7r1 with CAMx v7.30, which is the latest publicly available version; 2) CB7r2 with CAMxv7.32-CB7r2, without emissions of new VCP species; and 3) CB7r2 with CAMxv7.32-CB7r2, with emissions of new VCP species. Emissions of new VCP species were incorporated in the 2-box model scenarios using VOC emissions and measurement data from Chen et al., 2024. Results show

that the CB7r2-related updates cause a decrease in concentrations of total SOA at all three locations. This decrease is primarily due to the updated IVOA yields in CB7r2_CF3. While IVOA remains the dominant SOA precursor for the urban DFW and SAN locations, it's relative contribution to SOA potential decreases from >70% in the CAMxv7.30- CB7r1 runs compared to 50-60% in the CAMx7.32-CB7r2 runs. Adding emissions of new VCP species causes an increase in SOA concentration due to additional emitted SOA precursors (IVC1, IVC2, HPAR, and IVOA). Changes to O_3 between the model runs were minor. CAMx7.32-CB7r2 model runs that employ the PM source apportionment technology (PSAT) probing tool show that area source emissions dominate SOA production at DFW and SAN, while the biogenic sources dominate at TYL.

1.0 Introduction

The TCEQ is preparing for particulate matter (PM) modeling that might be required because the U.S. Environmental Protection Agency (EPA) lowered the National Ambient Air Quality Standard for PM with a diameter of 2.5 µm or smaller ($PM_{2.5}$) from 12.0 to 9.0 µg/m^3. Secondary organic aerosol (SOA) contributes a large fraction of PM air pollution in Texas, and modeling indicates that intermediate volatility organic compounds (IVOC) emissions dominate SOA formation potential for Texas urban areas (>70% in both Dallas-Fort Worth and San Antonio; Ramboll, 2024a). Volatile organic compounds (VOC) containing products such as solvents, paints, printing inks, adhesives, pesticides, cleaning agents and personal care products are increasingly referred to as volatile chemical products (VCPs) (McDonald et al., 2018) and contribute to IVOC emissions. VCPs and IVOCs are poorly characterized in current emission inventories and air quality models, however, which makes their contribution to SOA formation uncertain. In the Comprehensive Air Quality Model with extensions (CAMx), many different organic compounds are mapped to a single IVOC species, including some VCP compounds with very low SOA forming potential. Ramboll recently completed a new VCP chemical mechanism (Yarwood and Tuite, 2024) for use with the Carbon Bond (CB) mechanism in CAMx. Updating TCEQ's CAMx and emissions modeling systems to use the new VCP mechanism can further improve the accuracy of TCEQ's $PM_{2.5}$ modeling by targeting important SOA precursors more precisely.

1.1 Project purpose

The purpose of this project was to update the latest CB mechanism (version 7 revision 1, CB7r1) to include VCP gas-phase chemistry (in a new CB7r2 mechanism) and update CAMx's treatment of SOA formation to account for VCP species (in a new CB7r2_CF3 SOA scheme). CAMx updates were designed to work with the $PM_{2.5}$ source apportionment (PSAT) and ozone source apportionment (OSAT) tools in CAMx and speciation mapping was updated to differentiate between VCP and IVOC species. CAMx 2-box model scenarios for several Texas cities were used to test and evaluate these updates.

1.2 Background

1.2.1 VCP mechanism

The new VCP mechanism developed by Ramboll (Yarwood and Tuite, 2024) includes more detailed speciation and reactions for alcohols, ethers, esters, siloxanes and larger alkanes that are characteristic constituents of VCP emissions. A total of 16 emitted VCP gas-phase species (Table 1-1), along with their OH oxidation reactions, were added to the Carbon Bond (CB) mechanism and were used as a basis for the VCP chemistry updates in the new CB7r2 mechanism.

Table 1-1. VOC species added to CB mechanism to better represent VCP emissions

Species[(a)]	Description
IBTA	2-methylpropane (isobutane)
HPAR	Large alkanes, based on n-dodecane
IPOH	Isopropanol
NPOH	1-Propanol

Species[a]	Description
EDOH	1,2-ethanediol (ethylene glycol)
PDOH	1,2-propanediol (propylene glycol)
ROH	Larger alcohols (C4+)
DEE	Diethyl ether
DME	Dimethyl ether
ETHR	Larger ethers (C4+, excluding diethyl ether)
MEFM	Methyl formate
MEAC	Methyl acetate
ETFM	Ethyl formate
ETAC	Ethyl acetate
ESTR	Larger esters (C4+, excluding ethyl acetate)
SXD5	Siloxanes represented by decamethylcyclopentasiloxane (D5)

[a]Species are grouped in the order alkanes, alcohols, ethers, esters and siloxanes.

1.2.2 CAMx aerosol schemes

Models use diverse approaches to simulate SOA but the two most common approaches are the two-product scheme and volatility basis set (VBS) scheme. Both are generally based on the gas-particle partitioning theory of Pankow (1994). When SOA precursors are oxidized in the gas phase by the OH radical, ozone (O_3), or NO radical, gas-phase products (with varying volatility) are used to represent all oxidation products that can potentially condense to form SOA. The two-product scheme assumes there are two gas-phase products (with high and low volatility, respectively) while the VBS scheme includes additional condensable gases that are systematically organized by volatility (i.e., saturation concentration, C*).

Aerosol chemistry in CAMx is handled through the CF3 scheme, which treats aerosol mass distribution as coarse (C) and fine (F) modes and includes options to treat inorganic and SOA chemistry. The SOAP3 SOA scheme in CAMx includes a "complex" and "simple" option. The complex option is a modified two-product model, where gas-phase precursors are oxidized to condensable gases (CGs) that can condense to SOA. SOAP3 modifies the two-product scheme by adding a third product, which is considered non-volatile and always condenses to SOA. Anthropogenic VOC (AVOC; benzene, toluene, xylene), IVOC (CAMx species IVOA) and semi-volatile organic compounds (SVOC; CAMx species SVOA) are oxidized by radicals to yield condensable products (ACG1 and ACG2), which partition to oxidized organic aerosol (AOA1 and AOA2) according to their saturation pressures (C*). ACG2/AOA2 is more volatile (i.e., larger C*) than ACG1/AOA1. Oxidized anthropogenic VOC, IVOA, and SVOA can also yield a non-volatile aerosol (AOA0). Biogenic VOC (BVOC; isoprene, monoterpene, α-pinene, and sesquiterpenes) similarly form condensable products (BCG1 and BCG2) when oxidized which partition to oxidized organic aerosol (BOA1 and BOA2) or BVOC can form non-volatile aerosol (BOA0). The SOAP3 simple option forms only non-volatile SOA from VOC/IVOC/SVOC oxidation reactions. SOAP3 SOA parameters for both the complex and simple schemes are provided in the CAMx User's Guide (Ramboll, 2024b).

2.0 CB7r2 gas phase mechanism updates

The CB7r1 chemical mechanism was updated to CB7r2 by integrating the VCP mechanism developed by Yarwood and Tuite (2024) and making other updates (listed in Table 2-1) that are summarized as follows:

- Maintaining the core mechanism (Updates 1-4) leading to a small decrease (~1%) in the OH + NO_2 rate constant, a small increase (~3%) in formaldehyde photolysis to radical species, and a substantial increase (doubling) of larger aldehyde (ALDX) photolysis to radical species.
- Introducing photolysis of multifunctional organic nitrates (NTR2) to NO_2 (Update 5) to support an improved treatment of NTR2 fate being implemented in CAMx for AQRP project 24-004.
- Revised photolysis reactions for biogenic degradation products (TRPD and ISPD; Updates 7 & 8).
- Fully integrating the VCP chemical mechanism of Yarwood and Tuite (2024) into CB7r2 (Updates 6, 12 and 13).
- Deleting 3 reactions with low importance (Updates 14 & 15) which allowed introducing 3 new reactions for Updates 5 & 6 at logical places.
- Introduced a new species EH2 to represent emitted hydrogen separate from background hydrogen (Update 9), which is analogous to how existing species ECH4 and CH4 represent methane emissions separate from background methane.
- Updated iodine chemistry by considering activation of aerosol-phase iodine oxides (IXOY) by H_2O_2 (Update 10) and redefining the iodine nitrate (INO3) photolysis frequency (Update 11).

Table 2-1. Numbered list of CB7r2 mechanism updates with descriptions

No.	Description[(a)]
1	Changed the rate constants for HONO formation (CB7r2 reaction 38, abbreviated as R38) and PNA formation/destruction (R45/R46) from IUPAC to NASA (2019) values based on measurements and recommendations of Rolletter et al. (2025). Also reviewed the rate constant for OH + NO_2 (R41) and decided to continue using the NASA (2019) value.
2	Corrected a typo in the rate constant expression for OH + NO_2 (R41) from NASA (2019) to use a reference temperature of 298K rather than 300K which decreased the rate constant by ~1% at 298K and 1 atm.
3	Updated the quantum yields used to calculate the photolysis frequency (J) of formaldehyde to radical products [R101; J(HCHOr)] to account for photophysical oxidation based on measurements by Welsh et al. (2023). Specifically, the quantum yields from IUPAC data sheet P1 are increased at wavelengths longer than 330 nm using Figure 5 of Welsh et al. (2023) which increased J(HCHOr) by ~3%.
4	Updated the cross-sections and quantum yields used to calculate the photolysis frequency of larger aldehydes [R109; J(ALDXr)] to the average of IUPAC values for propionaldehyde (Data Sheet P3) and i-butyraldehyde (Data Sheet P24) which doubled J(ALDXr) compared to the previous assumption using only the propionaldehyde values.

No.	Description[a]
5	Introduced photolysis of multifunctional organic nitrates (NTR2) to NO_2 (R96) in competition with the existing pseudo gas-phase hydrolysis of NTR2 to HNO_3 (R97). Hydrolysis of NTR2 is expected to dominate photolysis for many conditions. CAMx models NTR2 hydrolysis by assuming partitioning to organic aerosol (Rollins et al., 2013) followed by particle-phase hydrolysis with a 6 h lifetime (Liu et al., 2012) which is likely too slow (Zhao et al., 2023). The current NTR2 hydrolysis lifetime in CAMx of shorter than 1 day compares to a typical photolysis lifetime of longer than 1 week. However, NTR2 hydrolysis could slow dramatically when organic aerosols enter a glassy phase-state under cold and/or dry conditions (Maclean et al., 2021). Modeling organic aerosol phase-state is being implemented in CAMx for AQRP project 24-004.
6	Introduced species DPAR to eliminate negative product coefficients for PAR from some reactions. For example, propene is represented as OLE + PAR and CB mechanism reactions of OLE (R142 to R144) traditionally included a product "− PAR" to balance carbon in the reaction. This practice made some modelers uncomfortable. CB7r2 replaces negative PAR yields with positive DPAR yields and then DPAR destroys PAR quantitatively in R131 (DPAR + PAR =). To remove the potential for R131 driving the PAR concentration negative, R132 (DPAR =) prevents DPAR from accumulating if the PAR concentration becomes small. This change in mechanism structure has no impact on model results for normal simulation conditions. DPAR is produced by reactions R109, R121, R122, R133, R136, R142, R143 and R144. In R109, ALDX photolysis now produces 1 ALD2 rather than 0.5 ALD2 and C-balance is maintained in R109 by also producing 1 DPAR.
7	Revised the reaction scheme for lumped terpene products (TPRD) and increased the photolysis frequency of TPRD (R214) to 0.71*J(ALDX) from 0.42*J(ROOH), a factor of 10 increase. The updated photolysis frequency is implemented as J(TPRD) = 4.6*J(ROOH) to insulate J(TPRD) from any future change to J(ALDX).
8	Updated the isoprene (ISOP) reaction scheme by resolving hydroxyacetone (HACT) production from lumped isoprene products (ISPD) in R185 and isoprene epoxydiols (EPOX) in R192-R194. Revised the photolysis frequency of ISPD in R187 to J(ISPD) = J(MEPX). Redefining J(ISPD) improves the derivation of R187 by condensing the Caltech Isoprene Mechanism (Wennberg et al., 2018) and R187 was re-derived.
9	Introduced a new species EH2 to represent OH-reaction of emitted hydrogen (R240) separate from background hydrogen (species H2 in R49). CAMx specifies a fixed concentration of 0.6 ppm for H2 which prevented hydrogen emissions from being modeled. EH2 is analogous to species ECH4 added previously to represent OH-reaction of methane emissions (R127) separate from background methane (R128) which is fixed at 1.85 ppm in CAMx.
10	Added activation of aerosol-phase iodine oxides (IXOY) by H_2O_2, following Reza et al. (2024). The mechanisms that convert gas-phase iodine to IXOY are uncertain and CB7r2 reverts to using a gas-phase reaction (R256: I2O2 + O3 = IXOY) used in CB6r4 and CB6r5 and consistent with Reza et al. (2024) rather than the pseudo gas-phase reaction (I2O2 = IXOY) used in CB7r1. CB7r2 introduces R257 (IXOY + H2O2 = I2) which activates aerosol-phase iodine oxides to gas-phase reactive iodine, potentially enhancing the impact of iodine emissions. The rate constant for R257 is set to produce an IXOY activation lifetime of 0.5 days to 5 days (consistent with Reza et al., 2024) for H_2O_2 in the range 2 to 0.2 ppb as observed by the Atmospheric Tomography Mission (AToM) aircraft flights over the Atlantic and Pacific Oceans (Allen et al., 2022).
11	Specified the iodine nitrate (INO3) photolysis frequency [R255; J(INO3)] as J(INO3) = J(N2O5)*470 rather than J(INO3) = J(FORMm)*463 to insulate J(INO3) from any future change in J(FORMm). The change to J(INO3) is minor (less than 15% depending on zenith angle) with no change on average.

No.	Description[a]
12	Fully integrated the VCP chemical mechanism of Yarwood and Tuite (2024) into CB7r2: a) Added 16 VOC species (Table 1-1) that can be used to better speciate VOC emissions. However, CB7r2 can also be used without emitting these species. b) Re-derived the PAR reaction scheme (including ROR and KET) to account for i-butane (IBTA) and heavy alkanes (HPAR) being represented separately. c) Revised the treatment of autoxidation developed for HPAR (using species AUTX) to also represent autoxidation of alkoxy radicals from PAR (species ROR). Larger alcohols (ROH) and esters (ESTR) also produce alkoxy radicals (represented by ROR) that undergo autoxidation via AUTX. d) Updated the reactions of lumped hydroxyperoxyketones (HKET) produced by autoxidation to consider that HKET is produced by PAR as well as HPAR. HKET and AUTX are both 6C species. e) KET remains a 1C species in CB7r2 and uses the new DPAR species (see #6) which differs from the KET scheme in Yarwood and Tuite (2024) where KET is a 4C species. f) Increased the OH-reaction rate constants of KET and ROOH (R122 and R92) to better agree with rate constants for related C4 and C5 compounds in the Master Chemical Mechanism (MCM) version 3.3.1 (https://mcm.york.ac.uk/MCM). g) Reduced the ozone forming tendency of lumped siloxanes (SXD5) based on information provided during the peer-review on Yarwood and Tuite (2024), which is publicly accessible. We multiplied the yields of FORM and FACD in R228 by 0.5. The atmospheric reactions of siloxanes are uncertain.
13	Revised the reactions of XO2H, XO2 and XO2N with HO2 (R84, R87 and R90) by deleting a 10% OH yield because HKET produced by autoxidation reactions now provides an OH source under low NO conditions.
14	Deleted reaction MEO2 + C2O3 because generally unimportant compared to MEO2 reactions with NO, HO2, and RO2 (representing the sum of RO_2 radicals) which dominate over C2O3.
15	Deleted 2 reactions and species XPRP that allowed the organic nitrate yield from propane (PRPA) reactions to depend on temperature and pressure because the variation was minor. In CB7r2, PRPA has a static organic nitrate yield (represented by XO2N) in R130 of 3%, like the MCM.

[a]NASA (2019) means Burkholder et al. (2020) available at https://jpldataeval.jpl.nasa.gov/download.html and IUPAC means Mellouki et al (2021) with the latest IUPAC data sheets available at https://iupac.aeris-data.fr/.

A complete listing of the CB7r2 mechanism is provided in Appendix A together with species definitions and representative photolysis frequencies.

2.1 Ozone Reactivity (MIR) Factors for CB7r2

Initial testing of CB7r2 using a multi-day CAMx 2-box model scenario for Los Angeles found that CB7r2 produced slightly more ozone than CB7r1 but less than both SAPRC07 and RACM2 (Figure 2-1). Using this Los Angeles scenario, we computed maximum incremental reactivity (MIR) factors for VOC species in CB7r2 and CB7r1 as reported in Table 2-2. These MIR factors are needed to implement ozone source apportionment (OSAT) for CB7r2 in CAMx (discussed in Section 5.0). The MIR calculation uses the decoupled direct method (DDM) in CAMx and therefore performing the MIR calculation confirmed that DDM is working correctly for CB7r2.

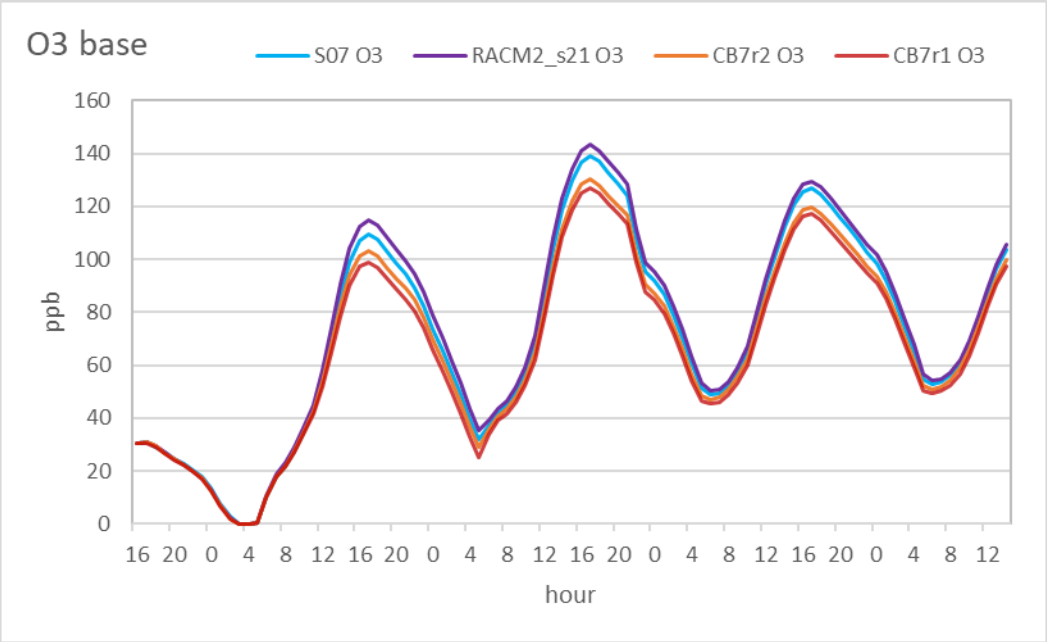

Figure 2-1. Time series of O_3 from initial testing of CB7r2, compared against three other chemical mechanisms, using a multi-day CAMx 2-box model scenario for Los Angeles.

Table 2-2. Ozone forming tendency under VOC-limited conditions as indicated by maximum incremental reactivity (MIR) factor (moles O_3/mole VOC).

Species[(a)]	CB7r1	CB7r2	Change[(b)]
ETHA	0.162	0.166	3%
PAR	0.391	0.382	-2%
PRPA	0.415	0.439	6%
IBTA		1.35	
HPAR		2.96	
ETH	3.93	4.02	2%
OLE	8.11	8.46	4%
IOLE	14.2	14.6	3%
BENZ	1.24	1.11	-10%
TOL	6.97	6.84	-2%
XYL	17.0	16.8	-1%
ETHY	0.427	0.433	1%
MEOH	0.367	0.378	3%
IPOH		0.993	
ETOH	1.38	1.42	3%
PDOH		3.03	
EDOH		3.20	
NPOH		3.34	
ROH		3.45	
DME		0.59	
DEE		4.24	

Species[a]	**CB7r1**	**CB7r2**	**Change[b]**
ETHR		4.46	
FORM	3.94	3.98	1%
GLYD	4.51	4.56	1%
ALD2	4.97	5.02	1%
ALDX	7.09	8.03	13%
GLY	10.9	10.8	-1%
MGLY	17.6	17.5	0%
ACET	0.517	0.562	9%
KET	1.64	2.02	23%
HKET		4.64	
HACT	6.04	6.12	1%
MEFM		0.084	
MEAC		0.146	
ETFM		0.290	
ESTR		1.28	
ETAC		3.45	
SXD5		0.766	
ISOP	10.5	9.7	-7%
SQT	8.32	9.79	18%
APIN	9.69	9.51	-2%
TERP	11.3	11.1	-2%

[a]Species are grouped in the order alkanes, alkenes, aromatics, alkynes, alcohols, ethers, aldehydes, ketones, esters, siloxanes and biogenic alkenes.

[b]Change is (CB7r2/CB7r1)-1 shown as a percentage.

3.0 CF3 SOA scheme updates

To develop a new CAMx aerosol scheme that incorporates VCP species and is compatible with CB7r2, we used a variety of data sources, including EPA's VCPy dataset and recent scientific literature. Utilizing these data sources, we developed a methodology aimed at:

1. Defining a set of VCP model species compatible with the CAMx CB7r2_CF3 scheme to efficiently represent SOA production from VCP emissions.
2. Assigning representative SOA yields to each VCP model species in the CB7r2_CF3 scheme.

To derive SOA yields for the newly added CF3 model species, we searched for published yield data that are formatted for use with a VBS SOA scheme. For newly added model species we developed a mapping scheme from emitted compounds to model species as shown in Appendix B and discussed below. For discussion purposes, we refer to SOA yields calculated under standard conditions of 298 K and OA concentration (C_{OA}) = 10 μg/m^3, unless otherwise specified.

3.1 VCPy dataset

The 2021 VCPy dataset[1] presents comprehensive U.S. wide emissions data of VCP compounds along with supplementary information that includes estimated potential yields of SOA. VCPy identifies VOCs using their SPECIATE database[2] identification number (SPECIATE ID) where most SPECIATE IDs refer to a unique compound (e.g., n-undecane) but some are compound mixtures (e.g., branched C12 alkanes). For simplicity, we refer to all SPECIATE IDs as compounds.

We identified the U.S. wide "Top 100" compounds ranked by emission mass, which collectively represent 94.3% of total emissions mass and 90.6% of total SOA formation potential. These top-ranked compounds are categorized by VCPy into seven distinct groups (Table 3-1): n-alkanes (comprised of 19 compounds), branched alkanes (13), cyclic alkanes (14), alkenes (4), oxygenated compounds (38), aromatics (8), and halocarbons (4).

Table 3-1. Summary information for the "Top 100" VCP compounds in the VCPy 2021 US-wide emission inventory

Group (# of compounds)	Emissions (kg/person/yr)	% of Emissions	% of SOA	Min. SOA yield (g/g)	Max. SOA yield (g/g)
Alkene (4)	0.09	1.25	10.95	0.176	0.595
Aromatic (8)	0.34	4.71	22.73	0.055	0.353
b-alkane (13)	0.66	8.98	8.55	0	0.373
c-alkane (14)	0.29	3.92	14.30	0.039	0.550
n-alkane (19)	1.02	13.90	15.51	0	0.321
Halocarbon (4)	0.27	3.75	0.00	0	0
Oxygenated (38)	4.23	57.72	18.57	0	0.373

[1] https://github.com/USEPA/VCPy/blob/main/output/emissions_by_subpuc/2021/TOTAL_summary_2021.csv, accessed on February 5, 2025

[2] https://www.epa.gov/air-emissions-modeling/speciate, accessed on March 12, 2025

SOA formation from several compounds and compound classes present in the Top 100 can be represented by pre-existing model species within the CF3 scheme, e.g., aromatics and terpenes. We used the Top 100 compounds to develop VCP model species and anticipate that these species can be extrapolated to other VCPs without introducing major uncertainty because the Top 100 dominate both emissions mass and SOA-potential and include a variety of compound types.

3.2 Potential limitations of measured SOA yields

SOA yields parameterized for atmospheric models are typically derived from experiments conducted in smog chambers or oxidation flow reactors (OFRs). However, it is important to understand that many smog chamber experiments have limited applicability in replicating atmospheric conditions because they were conducted using higher SOA precursor concentrations than are typical of the atmosphere, as discussed in detail by Kenagy et al. (2024). For instance, many chamber experiments are conducted with very high NOx concentrations that likely suppress important autoxidation reactions (see below) that coexist with NOx-reactions in the atmosphere (Praske et al., 2018).

OFRs offer several advantages compared to conventional smog chamber experiments by simulating atmospheric oxidation processes rapidly and enabling precise control of important reaction parameters (e.g. temperature, humidity, and concentrations of OH, NO and HO_2) (Sbai et al. 2024). For example, OFRs can simulate prolonged atmospheric aging by controlling OH exposure (Hartikainen et al. 2020). Nevertheless, the elevated NO and/or HO_2 concentrations inherent to OFRs result in significantly shorter lifetimes for organic peroxy (RO_2) radicals compared to atmospheric conditions that almost certainly suppress autoxidation reactions and alter the profiles and types of products generated (Ahlberg et al., 2019; Li et al. 2023).

3.3 Autoxidation chemistry and highly oxidized molecules (HOMs)

Autoxidation is an important reaction process for many RO_2 radicals in the atmosphere (Crounse et al., 2013). A typical RO_2 autoxidation reaction involves an intramolecular hydrogen shift that adds a hydroperoxyl group (-OOH) and also forms a new RO_2 radical that may further autoxidize. Autoxidation can occur rapidly (within seconds) to add hydroperoxyl groups and generate highly oxidized molecules (HOMs) with very low vapor pressures that subsequently produce aerosols (Crounse et al., 2013). Rapid autoxidation reactions can out-compete RO_2 radical reactions with either NO or HO_2 which are traditionally considered to dominate under high or low NO conditions, respectively (Wennberg, 2023). The omission of autoxidation from most SOA schemes utilized by current large-scale atmospheric models may partly explain why models fail to reproduce the observed variability in atmospheric OA (Kenagy et al. 2024).

3.4 Literature review of SOA yield data

Following analysis of the VCPy dataset and a literature review of SOA precursors, we defined three new CF3 model species (IVC1, IVC2, HPAR) and updated SOA yield data for the existing IVOA species. VBS yield parameters and SOA yields are given in Table 3-2 and further details are provided in the sections below.

Table 3-2. VBS yield parameters for new CF3 model species and the resulting SOA yield at 298 K and C_{OA} = 10 µg/m³

Model species	C*						SOA yield (g/g)	Reference
	0.1	1	10	10^2	10^3	10^4		
IVC2	0.0737	0.0050	0.1867	0.3409	/	/	0.202	Sasidharan et al. (2023)
IVC1	0.0369	0.0025	0.0934	0.1705	/	/	0.101	Half of IVC2
IVOA	0	0.111	0.523	0	0	/	0.362	Manavi and Pandis (2022)
HPAR	0	0.056	0.262	0	0	/	0.182	Half of IVOA

3.4.1 Oxygenated VCP

Oxygenated VCPs are the largest category of the Top 100 and we further classified them into the following sub-groups: glycol ethers (6 compounds), glycols (2), esters (10), siloxanes (4), ketones (4), alcohols (8), and others (4).

3.4.1.1 Glycol ethers

The six glycol ethers present in the Top 100 (Table 3-3) have assigned SOA yields in VCPy ranging from 0.022 g/g (ethylene glycol monobutyl ether) to 0.074 g/g (diethylene glycol monobutyl ether), collectively contributing 1.78% to the total SOA formation potential. Humes et al. (2022) reported negligible SOA yields (<0.01 g/g) for glycol ethers in their OFR experiments. Conversely, Sasidharan et al. (2023) reported much higher yields based on chamber experiments. Yu et al. (2023) studied the atmospheric oxidation of the glycol ether 2-ethoxyethanol in detail and showed that SOA forming pathways primarily result from autoxidation reactions. It is likely that the OFR experiments conducted by Humes et al. (2022) suppressed autoxidation processes and therefore also suppressed SOA formation, explaining why they measured negligible SOA formation from glycol ethers. In contrast, Sasidharan et al. (2023) based their findings on chamber experiments performed by Li et al. (2018) using the large UCR chamber operated at atmospherically relevant NOx concentrations which would allow autoxidation to occur. Therefore, for glycol ethers we rely on SOA yield data reported by Sasidharan et al. supplemented by qualitative information presented by Li et al. (2018) and analyzed further in Li and Cocker (2018).

Table 3-3. Glycol ethers present in the VCPy Top 100 compounds

VCPy Name (Common alternative)	SI Name and Formula	Structure	Contains $HO-CH_2-CH_2-O-CH_2-$ functional group?
Diethylene Glycol Monobutyl Ether	2-(2-Butoxyethoxy) ethanol $C_8H_{18}O_3$	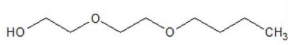	Yes
Glycol Ether Dpnb	1-(2-Butoxy-1-Methylethoxy)-2-Propanol $C_{10}H_{22}O_3$	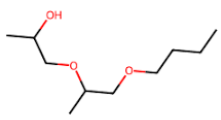	No

VCPy Name (Common alternative)	**SI Name and Formula**	**Structure**	**Contains HO-CH_2-CH_2-O-CH_2- functional group?**
Diethylene Glycol Monoethyl Ether (Carbitol)	2-(2-Ethoxyethoxy) ethanol $C_6H_{14}O_3$	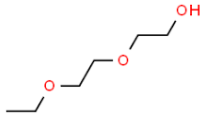	Yes
Dipropylene Glycol Monomethyl Ether	(2-Methoxymethylethoxy) -1-propanol and one isomer $C_7H_{16}O_3$	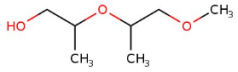	No
Propylene Glycol Butyl Ether	1-Butoxy-2-Propanol $C_7H_{16}O_2$	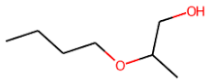	No
Ethylene Glycol Monobutyl Ether	2-Butoxyethanol $C_6H_{14}O_2$	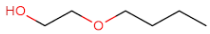	Yes

Table 3-4 summarizes SOA yields reported by Li et al. (2018) for various VCP compounds. These data are qualitatively useful for indicating whether compounds have higher or lower SOA yield, but they are not directly applicable to model development due to the significant variability in SOA loading (C_{OA}) across experiments. Li and Cocker (2018) analyzed data from Li et al. (2018) and concluded that the presence of the HO-CH2-CH2-O-CH2- functional group is critical for promoting SOA formation from glycol ethers. This finding is consistent with the autoxidation chemistry revealed by Yu et al. (2023) for 2-ethoxyethanol which also contains the HO-CH2-CH2-O-CH2- functional group. Sasidharan et al. (2023) also reported SOA yields of 0.21 g/g for carbitol (2-(2-ethoxyethoxy)ethanol) and 0.19 g/g for butyl carbitol (2-(2-butoxyethoxy)ethanol), both of which contain the HO-CH2-CH2-O-CH2- functional group. For other glycol ethers, Sasidharan et al. (2023) suggest using the SOA yield for diethylene glycol (0.015 g/g at C_{OA}=10 μg/m3) as a lower bound estimate and propylene glycol as an upper bound estimate (0.091 g/g at C_{OA} = 10 μg/m³). Diethylene glycol (HO-CH2-CH2-O-CH2-CH2-OH) contains the HO-CH2-CH2-O-CH2- functional group but has low SOA yield presumably because its small size (C4) produces more volatile products than from carbitol and butyl carbitol.

Table 3-4. VCP compound SOA yields reported by Li et al. (2018)

Compound	**Structure**	**H_2O_2 Added[(a)]**	**C_{OA} (μg m^{-3})**	**Yield[(b)]**
Benzyl Alcohol	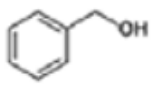	Y	152.9	0.56
		N	43.2	0.41
n-Heptadecane		Y	109.5	0.33
		N	103.6	0.38

Compound	**Structure**	**H_2O_2 Added[(a)]**	**C_{OA} (µg m^{-3})**	**Yield[(b)]**
Diethylene Glycol Butyl Ether (DEGBE)	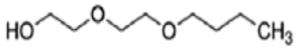	Y	91.5	0.28
		N	47.8	0.16
Dipropylene Glycol Methyl Ether Acetate (DPGMEA)	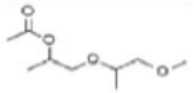	Y	80.3	0.27
		N	6	0.02
n-Tridecane		Y	82.2	0.22
		N	14.7	0.08
Diethylene Glycol Ethyl Ether (DEGEE)	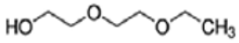	Y	34.9	0.1
		N	23	0.07
Propylene Glycol	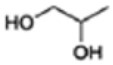	Y	5.6	0.07
		N	0.16	0
Dimethyl Glutarate (DBE-5)	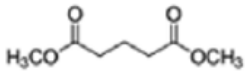	Y	7.7	0.04
		N	9.7	0.06
Diethylene Glycol	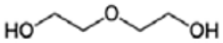	N	2.6	0.01
Texanol	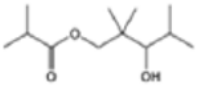	N	1.1	0.01
Glyceryl Triacetate	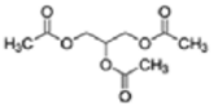	N	0.6	0

[a] NOx and background VOC were added to all experiments and some experiments also added H_2O_2 to generate OH radicals.

[b] The maximum SOA yield (g/g) which occurred at the OA concentration given as C_{OA}.

We introduce two new surrogate species to the CF3 scheme, namely IVC1 and IVC2, with SOA yields (Table 3-2) selected to represent glycol ethers that either lack (assigned to IVC1) or possess (assigned to IVC2) an HO-CH2-CH2-O-CH2- functional group. Small glycol ethers (<C6) would be assigned zero SOA yield based on the example of diethylene glycol (discussed above) however none are present in the Top 100. The SOA yield parameters in VBS format for IVC2 are derived from the average of carbitol and butyl carbitol as reported by Sasidharan et al. (2023), resulting in SOA yields of 0.202 g/g with C_{OA} = 10 µg/m^3. The SOA yield parameters for IVC1 are designated as half that of IVC2, resulting in SOA yields of 0.101 g/g with C_{OA} = 10 µg/m^3.

3.4.1.2 Glycols

In the VCPy dataset, ethylene glycol and propylene glycol (together accounting for 5.7% of total VCP emissions) are both assigned zero SOA yield. However, Sasidharan et al. (2023) reported a

non-negligible yield (0.091 g/g at C_{OA} = 10 µg/m³) for propylene glycol and recommended explicit treatment due to its PAN formation potential and SOA relevance. Therefore, we can represent SOA formation from propylene glycol using IVC1 (yield 0.101 g/g) within the CF3 scheme while assigning zero SOA yield to ethylene glycol. Propylene glycol is already an explicit species (PDOH) in CB7r2 but we chose to represent its SOA formation using IVC1 to reduce the number of SOA precursors treated within the CF3 scheme. Therefore, propylene glycol will be mapped to PDOH + IVC1 in emissions processing for the CB7r2_CF3 scheme.

3.4.1.3 Esters

The VCPy dataset assigns SOA yields to esters, with values ranging from less than 0.05 g/g to 0.373 g/g (misc. esters). Texanol is the most emitted ester and is assigned an SOA yield of 0.165 g/g by VCPy but this is inconsistent with the findings of Sasidharan et al. (2023) who reported a significantly lower SOA yield (0.019 g/g at C_{OA} = 10 µg/m^3) based on the experiments of Li et al. (2018) reported in Table 3-4. Sasidharan et al. suggest using the Texanol SOA yield as a lower bound for esters, although we expect small esters (e.g. methyl acetate) could have even smaller SOA yield. We assigned zero SOA yield for Texanol and esters with SOA yields less than 0.05 g/g in VCPy. We treat large esters, such as alkyl (C16-C18) methyl esters, as if they are alkanes with the same number of carbons which is consistent with their treatment in VCPy. The identity of Top 100 compound "misc. esters" is unclear so we conservatively assign it to CF3 model species IVOA which has a relatively high SOA yield, as discussed below.

3.4.1.4 Siloxanes

Siloxanes are widely used in both consumer and industrial products and decamethylcyclopentasiloxane (D5) is frequently considered as a tracer for emissions originating from consumer products. The four siloxanes present in the Top 100 are each assigned an SOA yield of 0.145 g/g by VCPy. However, the recent study by Kang et al. (2023) found a substantially lower SOA yield for D5 based on experiments with a potential aerosol mass oxidation flow reactor (PAM-OFR) along with a kinetic box model. Utilizing a standard-VBS parameterization (six bins with volatility ranging from 0.1 to 10^5 µg/m^3) without accounting for aging, Kang et al. (2023) determined an SOA yield of 0.067 g/g for D5 + OH at C_{OA} = 10 µg/m^3. If both gas-phase (k_{gas+OH}=2.18 x 10^{-12} cm^3/molec/s) and particle-phase ($k_{particle+OH}$=1.99 x 10^{-12} cm^3/molec/s) aging were considered, the SOA yield after one-day aging at an OH concentration of 3x10^6 molec/cm^3 decreased slightly to 0.058 g/g. CB7r2 uses model species SXD5 to represent siloxanes, based on D5 as a surrogate, and we represent SOA formation from siloxanes using IVC1 (yield 0.101 g/g) within the CF3 scheme. Although the SOA yield reported by Kang et al. (2023) is lower than the IVC1 yield, we decided not to introduce a separate SOA precursor for siloxanes for efficiency purposes in CF3, and believe 0.101 g/g is a reasonable estimate considering the range of SOA yields reported in Kang et al. (2023) and VCPy.

3.4.1.5 Other oxygenated VCPs

Top 100 compound benzyl alcohol is assigned an SOA yield of 0.0504 g/g in VCPy which is significantly lower than the yield reported by Sasidharan et al. (2023) of 0.217 g/g at C_{OA} = 10 µg/m³. The Sasidharan et al. (2023) yield is consistent with previous observations suggesting high yields (35–104%) although these yields were derived from calculations conducted at higher OA loadings (100–600 µg/m³) as reported by Charan et al. (2020) and Li et al. (2018). We rely on the

yield of 0.217 g/g from Sasidharan et al. and map benzyl alcohol to IVC2 which has a yield of 0.202 g/g at C_{OA} = 10 µg/m³.

3.4.2 Alkane VCPs

The carbon numbers of alkanes included in the Top 100 range from 3 (propane) to 15 (C15 Cycloalkanes) and the SOA yields assigned by VCPy range from 0 (usually with less than 5 carbon numbers) to 0.55 g/g (C15 Cycloalkanes). There is a positive relationship between the carbon number and SOA yields and for alkanes with the same carbon number, SOA yields from cyclic isomers are highest, followed by linear isomers, and then branched isomers.

The VCP chemical mechanism developed by Yarwood and Tuite (2024) maps large alkanes (>C8) to model species PAR, HPAR and/or IVOA using a scheme that conserves carbon. For example, HPAR has 12 carbons and therefore C12 alkanes are mapped to HPAR, whereas IVOA has 15 carbons and C15 alkanes are mapped to IVOA. We retain the Yarwood and Tuite (2024) mapping scheme for C10+ alkanes and update the mapping scheme for C7-C9 alkanes to produce more SOA. The SOA yields for PAR, HPAR and IVOA are designed to work with the updated mapping scheme to produce alkane SOA yields that are similar to VCPy.

IVOA is assigned an SOA yield of 0.362 g/g at C_{OA} = 10 µg/m³ based on n-pentadecane ($C_{15}H_{32}$) from Manavi and Pandis (2022). HPAR is assigned an SOA yield of half IVOA, i.e., 0.181 g/g at C_{OA} = 10 µg/m³ (Table 3-2) which produces satisfactory agreement with the VCPy SOA yields for C7 to C12 alkanes that are represented by HPAR. The SOA yield for PAR is zero. Table 3-5 shows the CB7r2_CF3 mapping scheme for C7 to C15 alkanes to PAR, HPAR and IVOA together with the resulting SOA yield at C_{OA} = 10 µg/m³. Figure 3-1 compares these CB7r2_CF3 SOA yields to VCPy SOA yields by C# and shows satisfactory agreement, given the relatively large ranges of the VCPy SOA yields (represented by bars).

Table 3-5. Recommended mappings for C7 to C15 alkanes.

Alkane	PAR (=1 Carbon)	HPAR (=12 Carbon)	IVOA (=15 Carbon)	Total Carbon[(a)]	SOA yield (g/g)
C7 alkane	5.5	0.125		7	0.02
C8 alkane	5	0.25		8	0.05
C9 alkane	4.5	0.375		9	0.07
C10 alkane	4	0.5		10	0.09
C11 alkane	2	0.75		11	0.14
C12 alkane	0	1		12	0.18
C13 alkane		0.67	0.33	13	0.24
C14 alkane		0.33	0.67	14	0.30
C15 alkane		0	1	15	0.36

[a] PAR+HPAR+IVOA

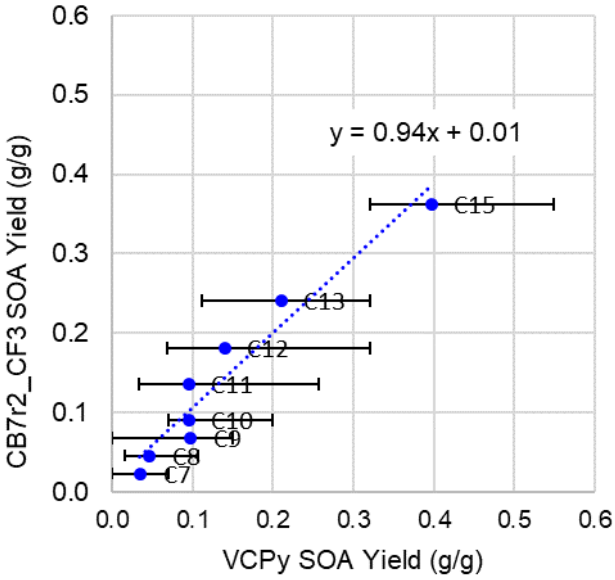

Figure 3-1. Comparison of C7 to C15 alkane SOA yields for the CB7r2_CF3 scheme and VCPy, with VCPy yields shown as average value (symbol) and range (bars).

3.5 NO-dependence of SOA yields

SOA yields can depend on NO concentration because NO strongly influences the fate of RO_2 radicals. Carefully designed chamber experiments can quantify yields for high and low NO conditions (Sarrafzadeh et al., 2016; Wildt et al., 2014). In general, higher yields are expected at low NO because the condensable products from RO_2 autoxidation and/or RO_2 + HO_2 reactions (peroxides) are less volatile than the condensable products from RO_2 + NO reactions (nitrates). In the SOAP3 SOA scheme the yields for aromatic (BENZ, TOL, XYL), terpene (APIN, TERP) and sesquiterpene (SQT) precursors are set 30% larger for low NO conditions than high NO conditions based on chamber experiments for terpenes (Sarrafzadeh et al., 2016) extrapolated to the other compounds.

We found little experimental data to show how NO concentration influences SOA yields for the oxygenated and alkane species discussed above. For the oxygenated compounds, Sasidharan et al. (2023) relied on chamber experiments of Li et al. (2018) which Sasidharan et al. concluded were representative of high NO conditions. However, many of the experiments performed by Li et al. (2018) produced substantial ozone concentrations which suggests that the experiments transitioned from high to low NO conditions with a consequent shift in RO_2 radical fate from NO-reaction to autoxidation/HO_2-reaction. Thus, it is difficult to determine whether the yield data provided by Sasidharan et al. (2023) represent high or low NO conditions. Charan et al. (2020) studied SOA formation from benzyl alcohol and found ~30% higher yield at low NO compared to high NO (see their Figure 9). However, for oxygenated SOA precursors (IVC1, IVC2) we applied the same SOA yields for high and low NO conditions due to limited evidence for any NO effect.

The SOA yields for C7 and larger alkanes derived above are based on Manavi and Pandis (2022) who derived alkane SOA yields only for high NO conditions. They also derived SOA yields for

aromatic and polycyclic aromatic hydrocarbon (PAH) SOA precursors for both high and low NO conditions with the low NO yields being ~30% larger (see their Figures 10 and 11) which supports the SOAP3 assumption of 30% larger SOA yields from aromatics at low NO conditions. PAH precursors are mapped to IVOA for SOAP3. For the alkane SOA precursors (HPAR and IVOA) we applied 30% larger SOA yields at low NO conditions.

3.6 Discussion

We mapped the Top 100 VCP compounds to the CB7r2_CF3 scheme as shown in Appendix B and derived the SOA yields using the CB7r2_CF3 scheme for comparison with the yields assigned in VCPy. The emission-weighted average SOA yield for the Top 100 compounds is 0.061 g/g using VCPy yields and 0.057 g/g using CF3 yields. Figure 3-2 presents the relative contributions of compound classes to emission-weighted SOA formation potential using VCPy and CF3 yields. The contribution of oxygenated VCPs is nearly the same, the contributions of aromatics and alkenes are somewhat smaller using CF3 yields, and the total alkane contribution is somewhat larger using CF3 yields. For sub-classes of alkanes the differences become larger, with the relative contribution of b-alkanes doubled with CF3 yields whereas c-alkanes show the opposite trend. However, we consider the overall agreement to be reasonable considering that the CB7r2_CF3 scheme uses many fewer unique yield parameters than VCPy, and that there are uncertainties in the VCPy yield estimates.

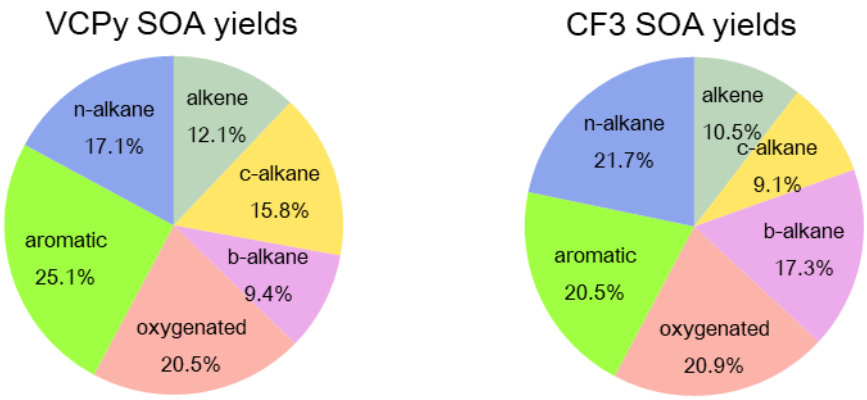

Figure 3-2. Relative contributions of compound classes to emission-weighted SOA formation potential for the Top 100 compounds using VCPy SOA yields (left) and CF3 SOA yields (right).

4.0 Emission speciation mapping updates

Speciation mapping refers to translating the detailed VOC compounds present in VOC speciation profiles to the VOC model species used by condensed chemical mechanisms such as CB7r2. The TCEQ's existing speciation mapping for CB7r1 was updated for CB7r2 by adding the 16 emitted gas phase species from the VCP mechanism (Table 1-1), along with 2 new SOA precursor species (IVC1 and IVC2) that are introduced in the updated CAMx CF3 SOA scheme. We provided the TCEQ with an Excel workbook (Deliverable_4.2_CB7r2_CF3_speciation_mapping_17Jun2025.xlsx) containing updated mappings and notes indicating which mappings were added, modified, or retained as is. We followed the rules below to make the new assignments for CB7r2_CF3.

1. Assigned explicit VCP species and lumped siloxanes (SXD5).
2. Assigned lumped oxygenates with the priority ETHR>ROH>ESTR, except species mapped as NVOL (logC*<2.5) remain NVOL. Large (C8+) esters were mapped like alkanes (see below), subtracting 1 Carbon for the C(O) functional group.
3. Updated KET to a 4C species by reducing PAR.
4. Assigned HPAR with consequent updates to PAR, UNR, and IVOC. The prior strategy of assigning the quaternary carbon in paraffins to UNR is retired as part of this new mapping.
5. Updated prior IVOA mappings to TERP/SQT as needed for terpenes and sesquiterpenes.
6. Mapped large (C7+) alkanes following Table 3-5, except species mapped as NVOL remain NVOL.
7. Mapped large (C7+) terminal alkenes following Table 4-1, except >C24 alkanes mapped as NVOL remain NVOL.
8. Mapped IVC1 and IVC2:
    a. Retained existing mappings (e.g., to PAR, ETHR, etc.) when assigning mappings to IVC1 or IVC2, except when changing an existing IVOA mapping to either IVC1 or IVC2.
    b. For compounds mapped to ETHR:
        i. Simple ethers (one functional group) were **not** mapped to IVC1 or IVC2.
        ii. Complex ethers with <=C4 were **not** mapped to IVC1 or IVC2.
        iii. C6+ ethylene glycols containing an HO-CH_2-CH_2-O-CH_2- functional group were mapped to IVC2.
        iv. Complex ethers with C6+ and log(C*)<=4 were mapped to IVC2
        v. Complex ethers with C6+ and log(C*)> 4 were mapped to IVC1.
    c. Compounds mapped to ROH or ESTR were **not** mapped to IVC1 or IVC2

Table 4-1. Recommended mappings for C7 to C15 terminal alkenes.

1-Alkene	PAR (=1 Carbon)	OLE (=2 Carbon)	HPAR (=12 Carbon)	Total Carbon[(a)]
C7 alkene	3.5	1	0.125	7
C8 alkene	3	1	0.25	8
C9 alkene	2.5	1	0.375	9
C10 alkene	2	1	0.5	10
C11 alkene	1	1	0.666	11
C12 alkene	1	1	0.75	12
C13 alkene	1	1	0.833	13
C14 alkene	1	1	0.917	14
C15 alkene	1	1	1	15

[a] PAR+OLE+HPAR

5.0 CAMx probing tool updates

CAMx includes several probing tools that must be implemented specifically for each gas-phase chemical mechanism. Some probing tool updates are automated by the Chemical Mechanism Compiler (CMC) which also creates code needed by the CAMx gas-phase chemistry solvers, whereas other probing tools are updated manually. CB7r2 is implemented as an update to CAMx version 7.3 and replaces CB7r1. The updated CAMx code which incorporates CB7r2, CF3 updates, and probing tool updates is referred to as CAMx version v7.32-CB7r2.

- The decoupled direct method (DDM) was updated for CB7r2 using the CMC and confirmed working because we used DDM to compute MIR factors for CB7r2 as shown in Table 2-2.
- Chemical Process Analysis (CPA) was updated for CB7r2 using the CMC and tested in CAMx 2-box model runs (described in Section 6.0). All mechanisms now produce a consistent set of CPA parameters, as listed in Table 5-1, to facilitate using CPA for mechanism comparison. CPA was confirmed working by ensuring all output CPA parameters have valid values and by cross-comparing related parameters. For example, parameters PH2O2_PHN3, LNoQ, and OPE for the Dallas-Fort Worth (DFW) simulation with CB7r2 are shown in Figure 5-1. Both PH2O2_PHN3 and LNoQ diagnose whether the instantaneous ozone production is limited by availability of NOx or VOC. They are computed independently and both diagnose that ozone production transitions from VOC-limited to NOx-limited at ~9 am. OPE diagnoses the instantaneous ozone production efficiency (OPE) and it climbs from low values in the early morning to afternoon values (12 to 14) that are consistent with efficient ozone production from NOx under NOx-limited conditions.
- We updated the ozone source apportionment (OSAT) manually for CB7r2 and tested the updates in CAMx 2-box model runs (Section 6.0). The OSAT update required the MIR factors for CB7r2 (Table 2-2) together with OH-rate constants and carbon numbers for the species listed in Table 2-2, which are provided in Appendix A. The Anthropogenic Precursor Culpability Assessment (APCA) probing tool, which is a special configuration of OSAT, was updated as part of these changes.
- We updated the particulate matter source apportionment (PSAT) manually for the CB7r2 and CF3 SOA scheme updates. Two new SOA precursors, IVC1 and IVC2, are included in the updated CAMx SOA scheme to better differentiate VCP and IVOC species. IVC1 and IVC2 were implemented in PSAT like IVOA but have different SOA yields (Table 3-2). The gas phase species HPAR also produces SOA. The following PSAT reactive tracers were updated to include contribution from IVC1, IVC2, and HPAR – IVOA aerosol precursor (IVA), condensable gases from anthropogenic precursors (AG1 and AG2), and anthropogenic particulate non-volatile organic aerosol (PA0). PSAT updates were tested using CAMx 2-box model runs (Section 6.0).

Table 5-1. Chemical Process Analysis (CPA) parameters for all mechanisms.

CPA Parameter	Description	Unit
J_NO2	NO_2 photolysis frequency	hr^{-1}
J_O3O1D	O_3 to $O^1(D)$ atom photolysis frequency	hr^{-1}
J_HCHOr	HCHO (formaldehyde) to radical products photolysis frequency	hr^{-1}

CPA Parameter	Description	Unit
PO3_net	Net O_3 production rate	ppb hr^{-1}
PO3_VOCsns	Net O_3 production rate under VOC-limited conditions (PH2O2_PHN3 < 0.35)	ppb hr^{-1}
PO3_NOxsns	Net O_3 production rate under NOx-limited conditions (PH2O2_PHN3 > 0.35)	ppb hr^{-1}
PH2O2_PHN3	Ratio of production rates of H_2O_2 to HNO_3	ratio
O3_dest	O_3 destruction rate estimated using the OSAT method	ppb hr^{-1}
PNO_net	Net NO production rate	ppb hr^{-1}
PNO2_net	Net NO_2 production rate	ppb hr^{-1}
PNOx_net	Net NOx production rate	ppb hr^{-1}
OH_prod	Total OH production rate including conversion from other radicals	ppb hr^{-1}
newOH_O1D	OH production from $O^1(D)$ + H_2O reaction	ppb hr^{-1}
newOH_O3	OH production from O_3 + alkene reactions	ppb hr^{-1}
newOH_phot	OH production directly from photolysis reactions, excluding from PNA	ppb hr^{-1}
OH_new	New OH production rate, i.e., newOH_O1D + newOH_O3 + newOH_phot	ppb hr^{-1}
newOH_HONO	OH production from HONO photolysis	ppb hr^{-1}
newOH_HPLD	OH production from isoprene-derived hydroxyperoxyaldehyde (HPALD) photolysis	ppb hr^{-1}
OH_loss	Total OH loss rate, also called "OH reactivity"	ppb hr^{-1}
OHwH2	OH reaction rate with H_2	ppb hr^{-1}
OHwEH2	OH reaction rate with emitted H_2	ppb hr^{-1}
OHwCO	OH reaction rate with CO	ppb hr^{-1}
OHwCH4	OH reaction rate with CH_4	ppb hr^{-1}
OHwECH4	OH reaction rate with emitted CH_4	ppb hr^{-1}
OHwISOP	OH reaction rate with isoprene	ppb hr^{-1}
OHwTERPS	OH reaction rate with all terpenes and sesquiterpenes	ppb hr^{-1}
OHwHRVOC	OH reaction rate with HRVOC, i.e., anthropogenic alkenes	ppb hr^{-1}
OHwArom	OH reaction rate with aromatic hydrocarbons	ppb hr^{-1}
OHwETHY	OH reaction rate with ethyne (acetylene)	ppb hr^{-1}
OHwAlkane	OH reaction rate with all alkanes	ppb hr^{-1}
OHwHCHO	OH reaction rate with HCHO	ppb hr^{-1}
OHwROH	OH reaction rate with all alcohols	ppb hr^{-1}
OHwOVOC	OH reaction rate with all oxygenated VOC (including alcohols, excluding predominantly secondary, e.g., methacrolein)	ppb hr^{-1}
OHwVOC	OH reaction rate with all VOC (excluding predominantly secondary, e.g., methacrolein)	ppb hr^{-1}
HCHO_prod	HCHO production rate	ppb hr^{-1}
nwHCHO_HRV	HCHO production rate from HRVOCs at first generation (unreliable for RACM2)	ppb hr^{-1}
nwHCHO_ISP	HCHO production rate from isoprene at first generation (unreliable for RACM2)	ppb hr^{-1}
HO2_prod	Total HO_2 production rate including conversion from other radicals and excluding from PNA	ppb hr^{-1}
newHO2_O3	HO_2 production from O_3 + alkene reactions	ppb hr^{-1}

CPA Parameter	Description	Unit
newHO2_pht	HO_2 production directly from photolysis, excluding from PNA	ppb hr^{-1}
HO2_new	New HO_2 production rate, i.e. newHO2_O3 + newHO2_pht	ppb hr^{-1}
nwHO2_HCHO	New HO_2 production from HCHO photolysis	ppb hr^{-1}
HO2_loss	Total HO_2 loss rate	ppb hr^{-1}
HO2wHO2	HO_2 loss by self-reaction	ppb hr^{-1}
HOx_CL	HOx chain length computed as (OH_loss + HO2_loss / (OH_new + HO2_new)	ratio
NO3_prod	Total NO_3 production rate	ppb hr^{-1}
N2O5toNO3	NO_3 production rate from N_2O_5 decomposition and photolysis	ppb hr^{-1}
NO3_loss	NO_3 loss by reaction with all species	ppb hr^{-1}
NO3toN2O5	NO_3 conversion rate to N_2O_5	ppb hr^{-1}
RO2_loss	Total RO_2 loss rate	ppb hr^{-1}
RO2wNO	RO_2 loss by NO-reaction	ppb hr^{-1}
RO2wHO2	RO_2 loss by HO_2-reaction	ppb hr^{-1}
RO2wNO3	RO_2 loss by NO_3-reaction	ppb hr^{-1}
RO2wRO2	RO_2 loss by self-reaction (challenging for RACM2)	ppb hr^{-1}
ON_prod	Total production rate of organic nitrate (ON) species	ppb hr^{-1}
ON_dest	Total destruction rate of ON species	ppb hr^{-1}
HNO3_prod	Total production rate of HNO_3	ppb hr^{-1}
NO2wOH	Production rate of HNO_3 from OH + NO_2 reaction(s)	ppb hr^{-1}
N2O5wH2O	Production rate of HNO_3 from N_2O_5 hydrolysis	ppb hr^{-1}
NOXrcyHNO3	NOx production rate from HNO_3 (NOx recycling)	ppb hr^{-1}
NOXrcyNTR	NOx production rate from ONs (NOx recycling)	ppb hr^{-1}
PAN_prdNet	Net production rate of peroxyacylnitrate (PAN) species	ppb hr^{-1}
NO3wVOC	NO_3 reaction rate with all VOC (excluding predominantly secondary, e.g., methacrolein)	ppb hr^{-1}
NOz_prod	Net production rate of NOz species, i.e., NO2wOH + NO3wVOC + N2O5wH2O + PAN_prdNet + ON_prod - ON_dest	ppb hr^{-1}
OPE	Ozone Production Efficiency (OPE), i.e., PO3/NOz_prod	ratio
LNoQ	LN/Q metric for ozone sensitivity, i.e., NOz_prod / HOx_new (constrained between 0 and 100)	ratio
I_prod[(a)]	Total I-atom production rate	ppb hr^{-1}
I_O3dest[(a)]	Net ozone destruction rate by I-atom (estimated from IO conversion to I)	ppb hr^{-1}

[(a)]CB6r5h also provides CPA parameters for Cl-atom and Br-atom reactions that are analogous to the parameters I_prod and I_O3dest.

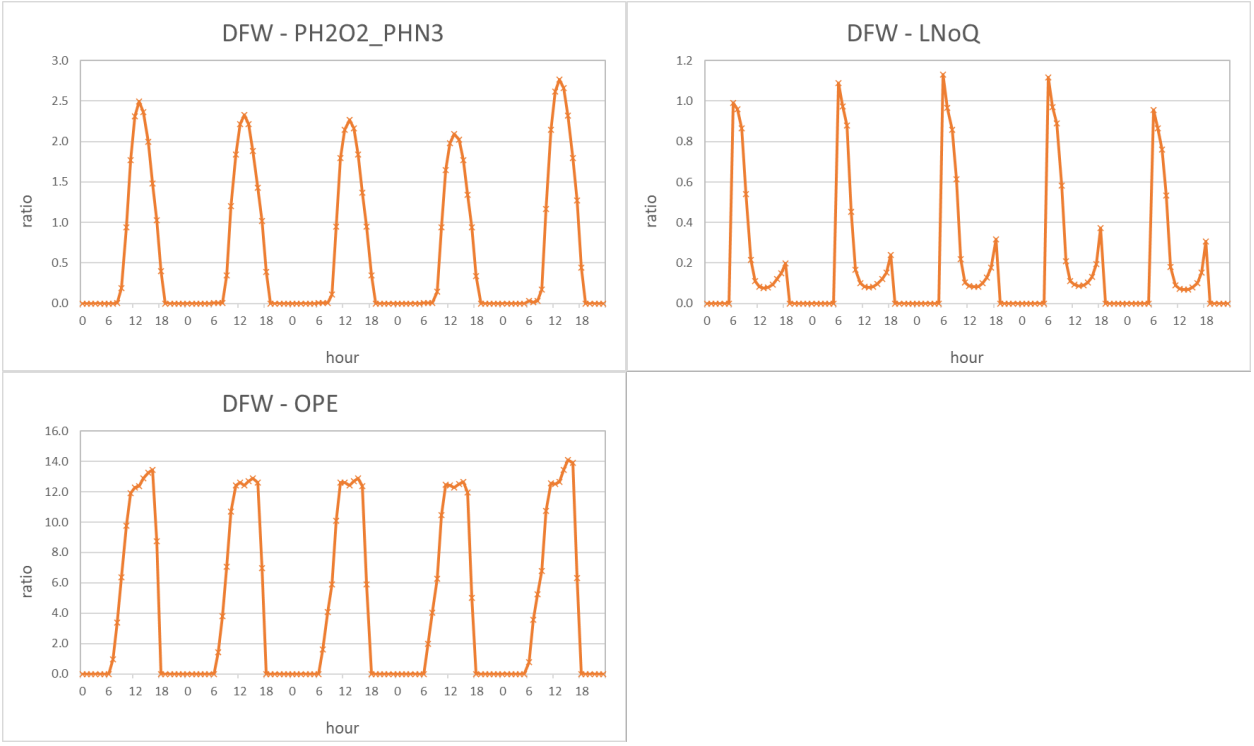

Figure 5-1. Example CPA parameters (PH202_PHN3, LNoQ, and OPE) from the Dallas-Fort Worth (DFW) 2-box model simulation with CB7r2 used to ensure proper implementation of CPA probing tool updates.

6.0 CAMx 2-box model tests

The simplicity of box models makes them useful to investigate atmospheric chemistry and test new chemical mechanisms and model updates. We therefore tested the new CAMx updates (v7.32-CB7r2), including the implementation of the new CB7r2 gas-phase mechanism and CB7r2_CF3 aerosol scheme, and related updates to CAMx probing tools, using 2-box model applications for three Texas location: Dallas-Fort Worth (DFW), San Antonio (SAN), and Tyler (TYL) in Northeast Texas. The 2-box model inputs and setup were developed from existing model scenarios developed in previous TCEQ projects to compare chemical mechanisms for ozone (Ramboll, 2023) and to test new SOA schemes (Ramboll, 2024a).

6.1 2-box model scenarios

CAMx 2-box model runs are simulations with emissions and meteorology that represent a limited area. The modeling domains for the CAMx model used in this study are each 3 x 3 x 2 grid cells (in the x, y, and z dimensions). The center grid cells of each domain, i.e. (2,2,1) and (2,2,2), form a 1-D column of 2 "boxes" with layer 1 representing the planetary boundary layer (PBL) and layer 2 representing a residual layer between the PBL and the CAMx top. The PBL depth varies in time, whereas the top of layer 2 is constant at 3,000 m. Horizontal wind speeds in layer 1 are set to zero, preventing horizontal exchange between grid cells and ensuring boundary conditions (BCs) in neighboring cells are not used to compute concentrations. In layer 2, there is a constant horizontal wind speed to purge the layer with a 12-hour lifetime to limit the accumulation of pollutants over time.

Input data for the 2-box model scenarios were extracted from 3D CAMx simulations from the TCEQ's 2019 modeling platform. Data from the 3D simulations were averaged over the grid cells within representative areas for each model location (DFW, SAN, TYL) to provide the initial conditions, meteorology (temperature, humidity, PBL height), and emissions (gridded and point) used in the 2-box model. Surface emissions of primary PM species were not included in the original model input from previous projects (Ramboll, 2023; 2024a) but have since been added to TCEQ's modelling platform. Emissions inputs for the 2-box model have been updated accordingly.

Additional details on the box model scenarios and development of model input are described in Ramboll (2023).

6.2 Emissions of new VCP species

6.2.1 Adding VCP Species to Area Source Emissions

TCEQ provided emission data for the box models with CB6 speciation that lacks the VCP precursor species added in CB7r2. We added VCP precursors to the box model emission files using scaling factors derived from ambient speciated VOC measurements (Chen et al., 2024). This method was sufficient for us to complete CB7r2 testing using the 2-box models. However, TCEQ will likely obtain different VCP emission estimates when area source emission files are re-processed for CB7r2 using the updated speciation profiles described in Section 4.0. Comparing these independently derived VCP emission estimates will be useful.

6.2.2 Mapping Factors to Convert Area Source Emissions from CB7r1 to CB7r2 with VCP Species

Chen et al. (2024) investigated the impact of VCP emissions on ozone in Los Angeles using a box model. They developed speciated VOC emission rates from ambient VOC measurements and reported them as observed emission ratios, i.e., ratio of VOC species emission rate to CO emission rate. For VOC compounds that do not have VCP source types (e.g., alkenes), the observed emission ratios were derived from ambient measurements during the CalNex 2010 field campaign (de Gouw et al., 2017). For VOC species that have VCP source types (whether measured during CalNex or not), the VCP source contribution to emission ratios were calculated using the VCP emission inventory proposed by McDonald et al. (2018) and reported in Chen et al. (2024) Table S1 under column VCP-ER.

We analyzed the speciated VCP emission rates of Chen et al. (2024) by mapping each of their 548 reported VOC species to CB7r2 model species. Figure 6-1 shows the resulting CB7r2 speciation of VCP emissions on a relative basis as percent Carbon. CB7r2 species definitions are provided in Appendix A. Many of the CB7r2 species shown in Figure 6-1 are present in CB7r1 (e.g., PAR, ETOH, ACET) but others are newly added in CB7r2 (e.g., HPAR, IPOH, PDOH) or for the update to CF3 (i.e., IVC1 and IVC2). We assumed that newly added CB7r2 species would likely have been represented as PAR in CB7r1 and computed a set of mapping factors for converting VCP emissions speciated as CB7r1 PAR to CB7r2 (Table 6-1). The model species have varying carbon numbers and the mapping factors were developed to conserve carbon. These factors can be applied to the VCP emissions category. Since the TCEQ model ready emissions that we provide to box models do not have a separate VCP category we applied the factors to the area category, which likely contain the majority of VCP emissions. Making these assumptions allowed us to conduct reasonable model testing.

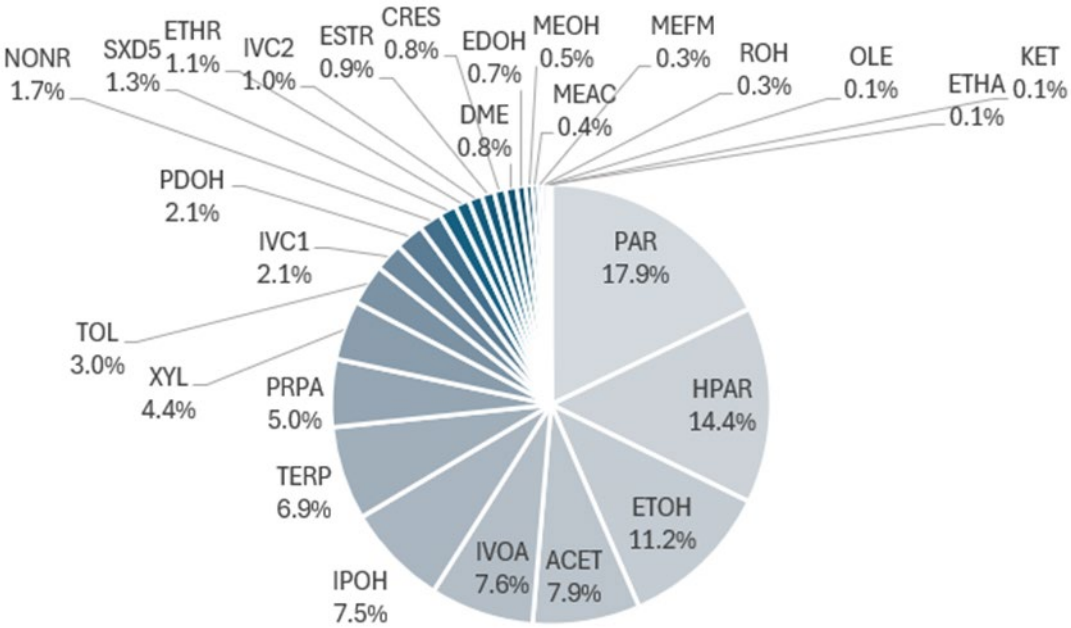

Figure 6-1. Speciated VCP emission rates from Chen et al. (2024) mapped to CB7r2 model species and shown on a relative basis as percent Carbon.

Table 6-1. Mapping factors to convert VCP emissions speciated as CB7r1 PAR to CB7r2 for model testing.

CB7r2 Model Species	Carbon No.	Mapping Factor
PAR	1	0.5819
IPOH	3	0.0258
HPAR	12	0.0124
PDOH	3	0.0072
IVOA	15	0.0052
DME	2	0.0043
EDOH	2	0.0034
IVC1	6.5	0.0033
ETHR	4	0.0027
ESTR	4	0.0024
MEFM	2	0.0017
MEAC	3	0.0014
IVC2	7.5	0.0014
SXD5	10	0.0013
ROH	4	0.0008
NPOH	3	0.0001

6.3 Results from 2-box model scenarios

Box model tests for all three locations were performed using the CB7r1 mechanism and the newly updated CB7r2. The CB7r1 runs were conducted with CAMx v7.30 (Ramboll, 2024b) and the CB7r2 runs were conducted with the updated CAMx version (v7.32-CB7r2). We conducted CB7r2 runs with and without emissions of new VCP species to assess their impact on model results. Model runs were performed with the COMPLX and SIMPLE SOA schemes, and the 'NoEvap' option for primary PM was employed for all runs. We focus on comparisons of total SOA and O_3 which are relevant to TCEQ's SIP modeling.

6.3.1 Total SOA

Figure 6-2 through Figure 6-4 show timeseries of total SOA concentration at each location for each mechanism and SOA scheme configuration. Daily average SOA concentration for model days 2 through 4 are provided in Table 6-2. Model day 1 is excluded from the table since it is considered spin-up.

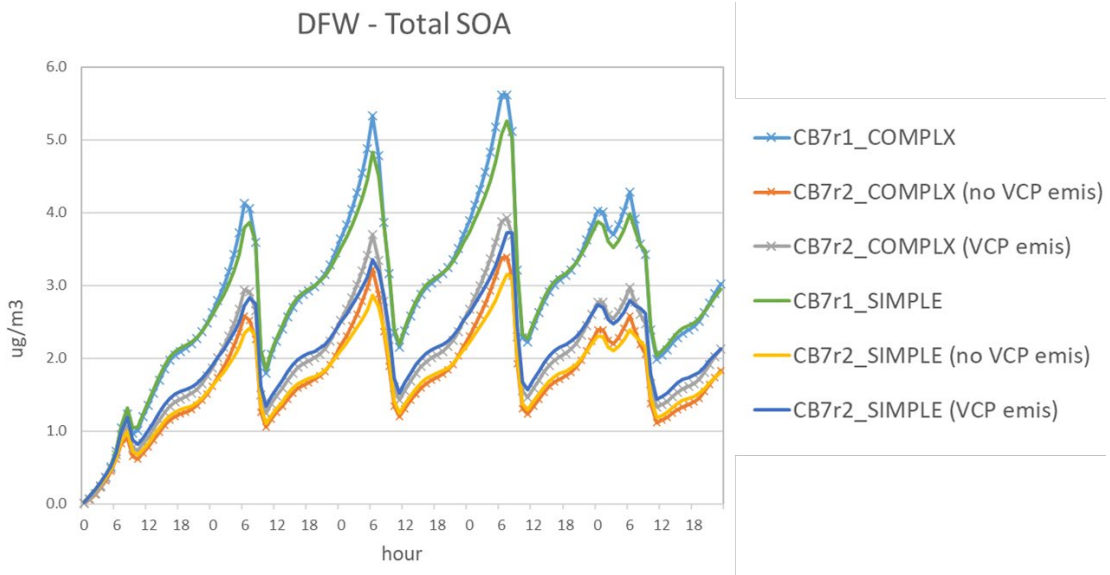

Figure 6-2. Time series of total SOA from DFW box model tests using various chemical mechanisms and CAMx SOA options.

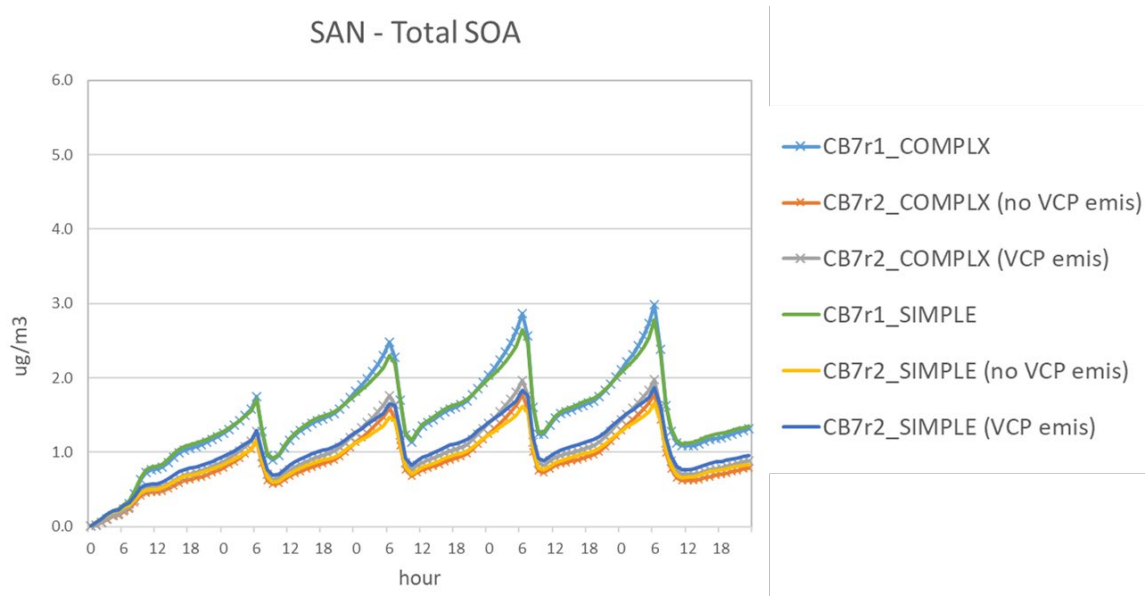

Figure 6-3. Time series of total SOA from SAN box model tests using various chemical mechanisms and CAMx SOA options.

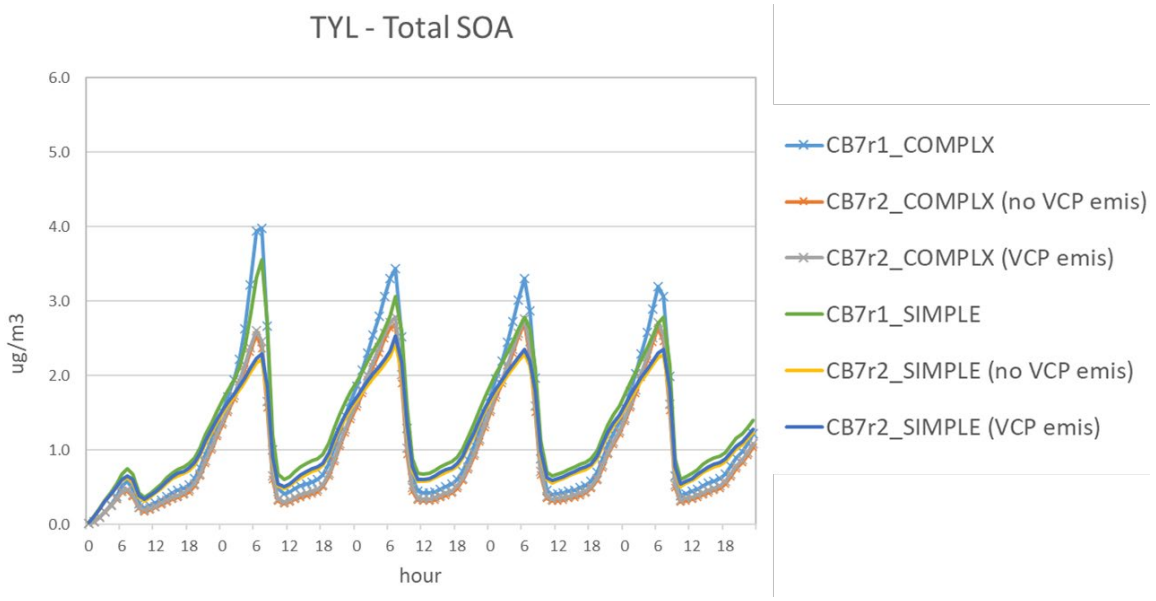

Figure 6-4. Time series of total SOA from TYL box model tests using various chemical mechanisms and CAMx SOA options.

Table 6-2. Daily average total SOA (ug/m^3).

	CB7r2 COMPLX (no VCP emis)	CB7r2 SIMPLE (no VCP emis)	CB7r2 COMPLX (VCP emis)	CB7r2 SIMPLE (VCP emis)	CB7r1 COMPLX	CB7r1 SIMPLE
DFW						
Day 2	1.76	1.75	2.05	2.08	2.95	2.90
Day 3	2.03	2.00	2.38	2.38	3.48	3.39
Day 4	2.15	2.11	2.51	2.51	3.68	3.58
Day 5	1.78	1.78	2.09	2.12	3.02	2.97
Average	1.93	1.91	2.26	2.27	3.28	3.21
SAN						
Day 2	0.84	0.87	0.93	0.99	1.36	1.37
Day 3	1.05	1.05	1.18	1.21	1.74	1.72
Day 4	1.12	1.12	1.25	1.28	1.87	1.85
Day 5	0.98	0.99	1.10	1.13	1.63	1.62
Average	1.00	1.01	1.11	1.15	1.65	1.64
TYL						
Day 2	1.10	1.23	1.14	1.27	1.49	1.57
Day 3	1.18	1.31	1.23	1.36	1.46	1.56
Day 4	1.13	1.27	1.17	1.31	1.35	1.48
Day 5	1.09	1.24	1.14	1.28	1.32	1.44
Average	1.12	1.26	1.17	1.31	1.40	1.51

Notes: COMPLX and SIMPLE refer to CAMx SOA options; All model runs are performed with the 'NoEvap' option for primary aerosol; 'VCP emis' are the runs with emissions of new VCP species added.

At all locations, CB7r1 produces the most SOA and CB7r2 without VCP emissions produces the least. The larger SOA concentrations in the CB7r1 runs are due to changes made to SOA yields in the COMPLX and SIMPLE schemes. In CAMx v7.30, the IVOA yields in the SIMPLE scheme are 1.00 under both high and low NO conditions. These were reduced to 0.362 (high-NO) and 0.471 (low NO) in CAMx v7.32-CB7r2 (Table 3-2) based on recently published SOA yield data (Manavi and Pandis, 2022) for the types of compounds represented by IVOA. The decreased yields lead to lower SOA production, particularly at DFW and SAN where IVOA is the dominant SOA precursor.

Figure 6-5 through Figure 6-7 show the relative contribution of precursor species to total SOA for the various model runs, as well as the emission-weighted SOA potential of each precursor. SOA potential is calculated by multiplying the average daily emissions by the SIMPLE scheme molar SOA yield. IVOA contributes 50% or more to the total SOA potential for all model scenarios at DFW (Figure 6-5) and SAN (Figure 6-6), but there is a notable decrease in SOA potential from IVOA and its contribution between the CB7r1 and CB7r2 runs. At TYL (Figure 6-7), there is greater contribution from biogenic SOA precursors (ISOP, TERP, APIN, SESQ). The change in IVOA yield therefore has a smaller impact on SOA concentrations, particularly during the day when biogenic emissions are high.

The addition of new VCP species emissions to the CB7r2 runs increase SOA due to additional emitted SOA precursors (IVC1, IVC2, and HPAR), and increased IVOA emissions when PAR is re-speciated (Table 6-1). Table 6-4 shows the percent increase in daily average SOA concentration due to the new emissions, which varies between 10-16% at DFW and SAN and 3-4% at TYL. The contribution of these new species to total SOA, shown in Figure 6-5 through Figure 6-7, increases SOA potential by 65-80 mole/day at DFW, 25-30 mole/day at SAN, and 6-8 mole/day at TYL. The lower values in each range are for high NO conditions and the upper values are for low NO conditions. Since sources of VCPs are primarily anthropogenic, it is expected that the new VCP emissions will have a greater impact in urban areas.

SOA concentrations are highest at DFW, followed by TYL and then SAN. There is a similar diurnal profile at each location, with SOA increasing throughout the day and overnight and a sharp decline in the early morning around 6:00 am when the PBL depth starts to increase. At DFW and SAN, the SIMPLE and COMPLX SOA schemes predict similar amounts of SOA, but the two diverge slightly as SOA concentrations increase overnight (Hr 00-07) and the COMPLX scheme produces more SOA. At TYL, The COMPLX scheme similarly produces more SOA overnight, but it produces less than the SIMPLE scheme during the day, which is likely due to the increased importance of biogenic SOA precursors at TYL.

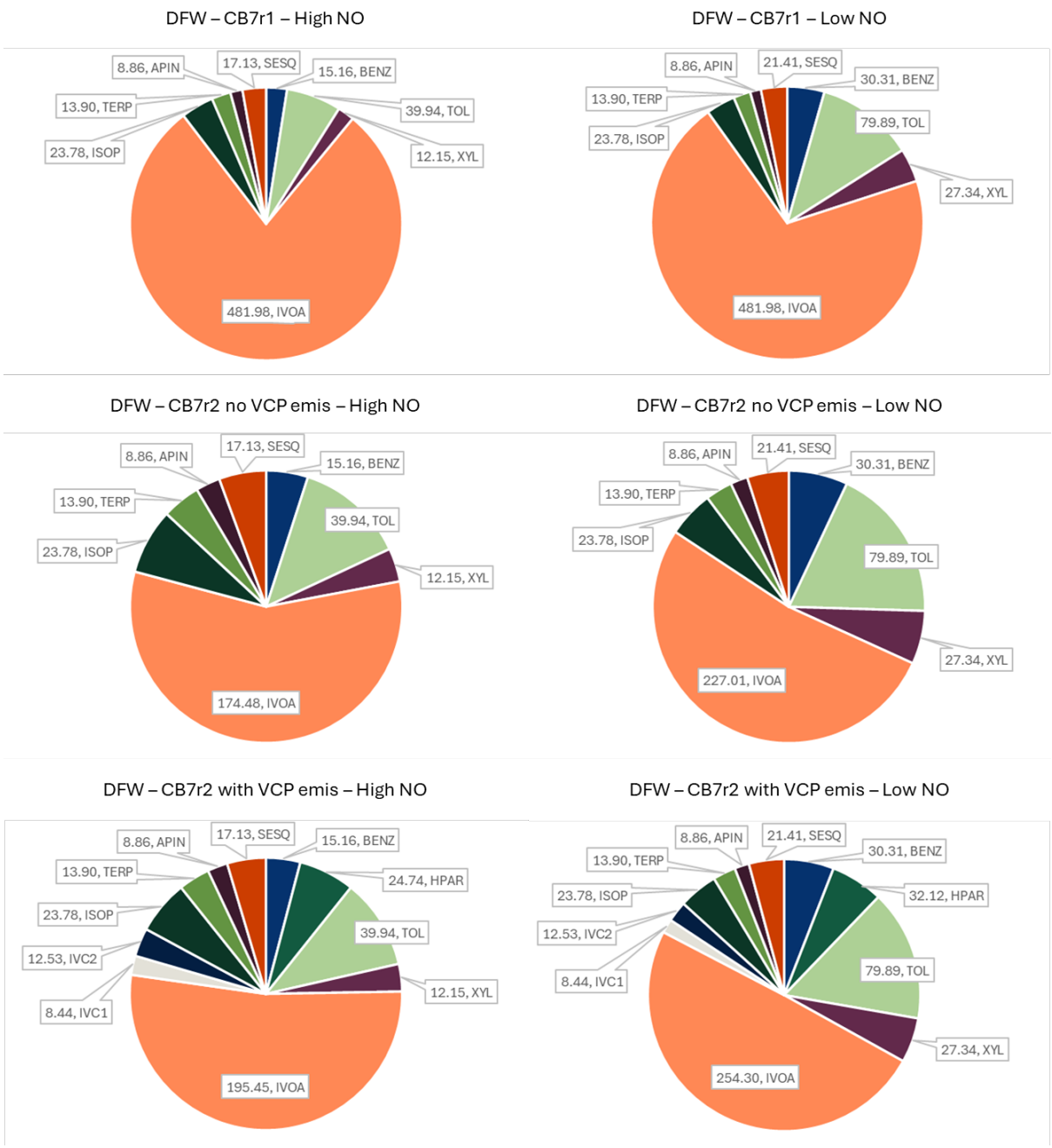

Figure 6-5. Emission-weighted SOA potential (mole/day) of precursor species and their relative contribution to total SOA potential under high and low NO conditions at DFW.

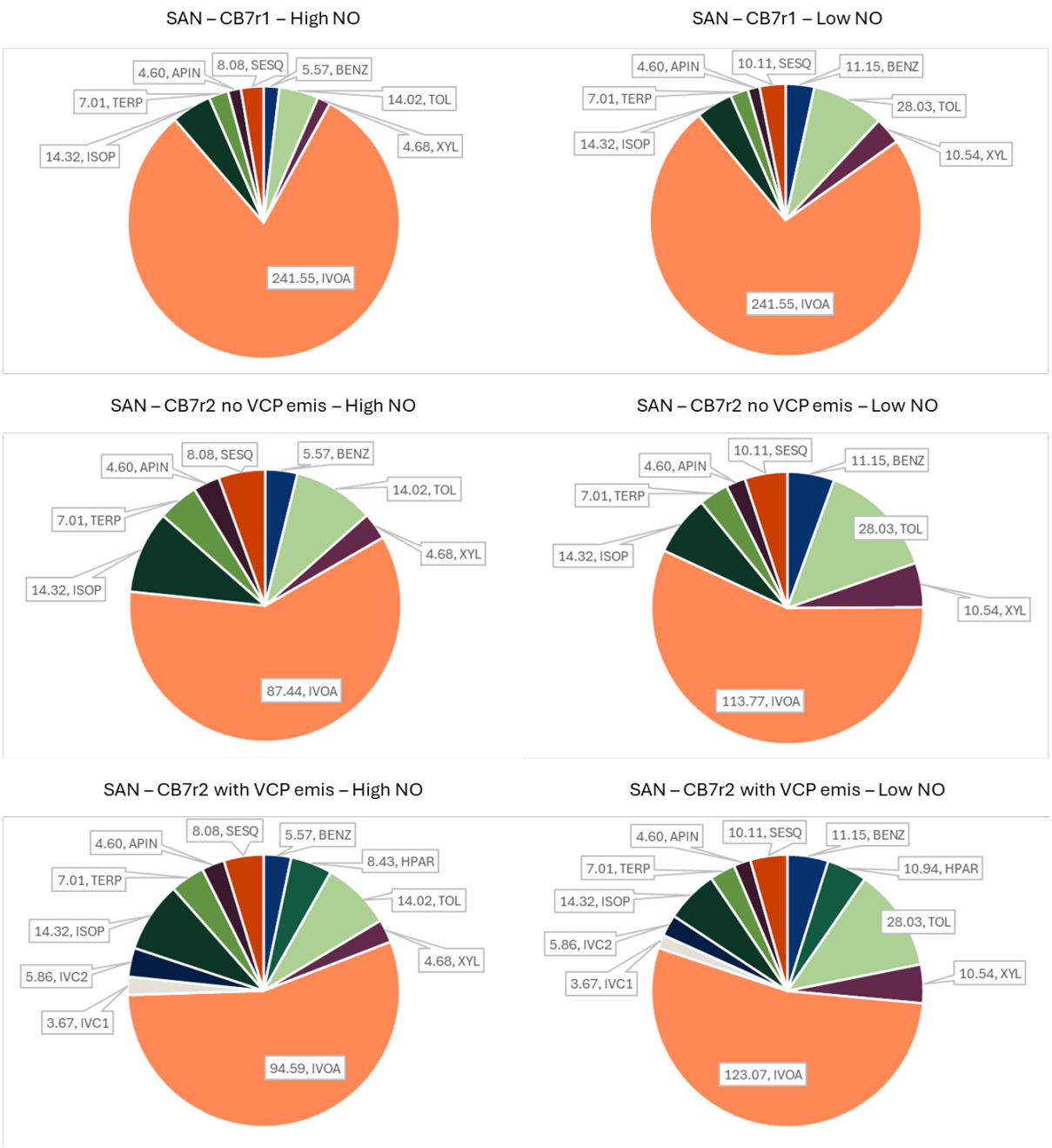

Figure 6-6. Emission-weighted SOA potential (mole/day) of precursor species and their relative contribution to total SOA potential under high and low NO conditions at SAN.

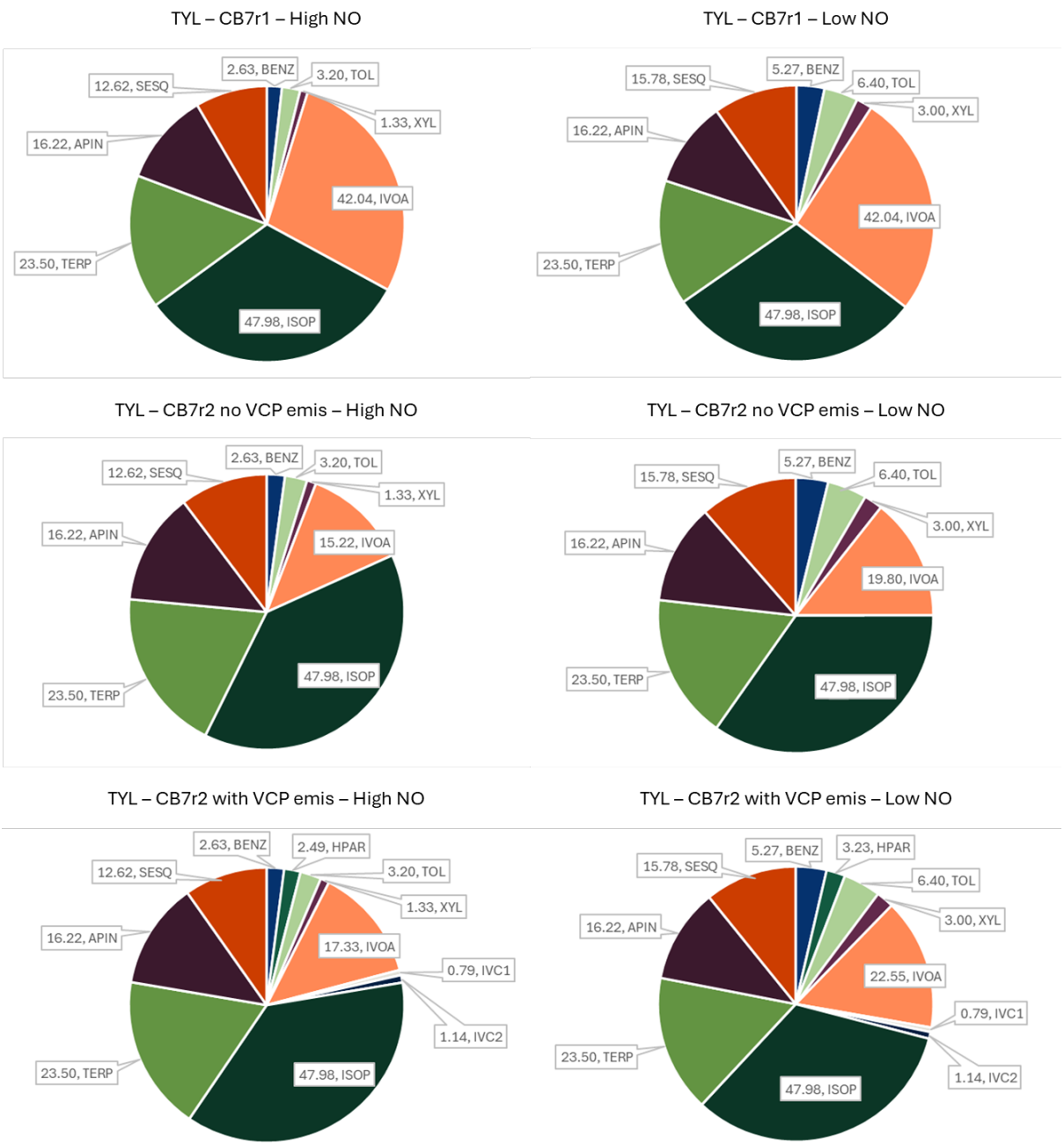

Figure 6-7. Emission-weighted SOA potential (mole/day) of precursor species and their relative contribution to total SOA potential under high and low NO conditions at TYL.

6.3.2 Ozone

Daily maximum 1-hour O_3 concentration for model days 2 through 4 are provided in Table 6-3. There is little difference in O_3 concentration between the model runs for a given location and the 4-day average values vary by less than 1 ppb. The addition of new VCP species emissions has a minor impact on O_3, with hourly concentration changes less than 0.5%. Table 6-4 shows the percent change in daily maximum 1-hour O_3 concentration due to the new emissions.

Table 6-3. Daily 1-hour max O_3 (ppb).

	CB7r2 COMPLX (no VCP emis)	CB7r2 SIMPLE (no VCP emis)	CB7r2 COMPLX (VCP emis)	CB7r2 SIMPLE (VCP emis)	CB7r1 COMPLX	CB7r1 SIMPLE
DFW						
Day 2	96.22	96.21	95.91	95.89	95.34	95.33
Day 3	97.37	97.36	96.99	96.98	96.41	96.41
Day 4	98.74	98.73	98.33	98.32	97.74	97.73
Day 5	92.35	92.34	92.02	92.01	91.47	91.47
Average	96.17	96.16	95.81	95.80	95.24	95.24
SAN						
Day 2	71.11	71.11	71.05	71.04	70.67	70.66
Day 3	73.44	73.44	73.35	73.35	72.98	72.97
Day 4	73.80	73.79	73.69	73.68	73.28	73.28
Day 5	68.02	68.02	67.93	67.93	67.46	67.46
Average	71.59	71.59	71.51	71.50	71.10	71.10
TYL						
Day 2	59.68	59.67	59.68	59.67	59.60	59.60
Day 3	60.26	60.25	60.26	60.25	60.14	60.14
Day 4	59.04	59.02	59.04	59.03	58.92	58.92
Day 5	60.48	60.46	60.48	60.46	60.35	60.35
Average	59.87	59.85	59.87	59.85	59.75	59.75

Notes: COMPLX and SIMPLE refer to CAMx SOA options; All model runs are performed with the 'NoEvap' option for primary aerosol; 'VCP emis' are the runs with emissions of new VCP species added.

Table 6-4. Change in daily average SOA and daily 1-hour max O_3, averaged over model days 2-4, due to addition of new VCP species in CB7r2.

Day	Daily avg total SOA (COMPLX)	Daily avg total SOA (SIMPLE)	Daily 1-hour max O_3 (COMPLX)	Daily 1-hour max O_3 (SIMPLE)
DFW				
Day 2	14.2%	15.8%	-0.3%	-0.3%
Day 3	14.4%	16.1%	-0.4%	-0.4%
Day 4	14.4%	16.0%	-0.4%	-0.4%
Day 5	14.6%	16.0%	-0.4%	-0.4%
Average	14.4%	16.0%	-0.4%	-0.4%
SAN				
Day 2	10.4%	12.1%	-0.1%	-0.1%
Day 3	10.7%	12.6%	-0.1%	-0.1%
Day 4	10.7%	12.6%	-0.1%	-0.1%
Day 5	10.7%	12.4%	-0.1%	-0.1%
Average	10.6%	12.4%	-0.1%	-0.1%
TYL				
Day 2	3.8%	3.4%	<0.1%	<0.1%

Day	Daily avg total SOA (COMPLX)	Daily avg total SOA (SIMPLE)	Daily 1-hour max O_3 (COMPLX)	Daily 1-hour max O_3 (SIMPLE)
Day 3	4.0%	3.5%	<0.1%	<0.1%
Day 4	3.5%	3.0%	<0.1%	<0.1%
Day 5	3.7%	3.2%	<0.1%	<0.1%
Average	3.8%	3.3%	<0.1%	<0.1%

Notes: COMPLX and SIMPLE refer to CAMx SOA options; All model runs are performed with the 'NoEvap' option for primary aerosol

6.3.3 PSAT tests

The Texas 2-box model scenarios were used to test proper implementation of the probing tool updates described in Section 5.0. In this section, we focus on the PSAT results rather than OSAT since the CB7r2 updates caused little change to ozone concentrations compared to CB7r1 (Table 6-3 and Table 6-4). We configured PSAT to apportion PM to the following emission sectors provided by the TCEQ:

1. Biogenic (bio)
2. On-road mobile sources (onroad)
3. Off-road mobile sources from EPA's Nonroad model (nonroad)
4. Other off-road mobile sources (offroad)
5. Oil and gas production sources (oilgas)
6. Areas sources (area)
7. Low level point sources (loptus)
8. Electric generating units (egu)
9. Non-egu point sources (neguus)

Note that there are no EGU sources within the domain for the TYL model scenario so the egu PSAT category is excluded from the TYL runs. Figure 6-8 through Figure 6-10 show the daily average relative contribution of emission source categories to the total SOA concentration for each modeled location. At DFW and SAN, area sources dominate, contributing greater than 60%, followed by biogenic sources. SOA at TYL is largely dominated by biogenic sources (<80%). The contributions from biogenic versus anthropogenic emissions at each location roughly align with the relative contribution of biogenic (ISOP, TERP, APIN, SESQ) versus anthropogenic (IVOA, BENZ, TOL, XYL, IVC1, IVC2, HPAR) precursors to the SOA potential shown in Figure 6-5 through Figure 6-7. The SOA scheme has only a minor impact on the relative contributions. As noted in the previous section, emissions of new VCP species were added only to the area source category, which causes a slight increase in the relative contribution of area sources to total SOA.

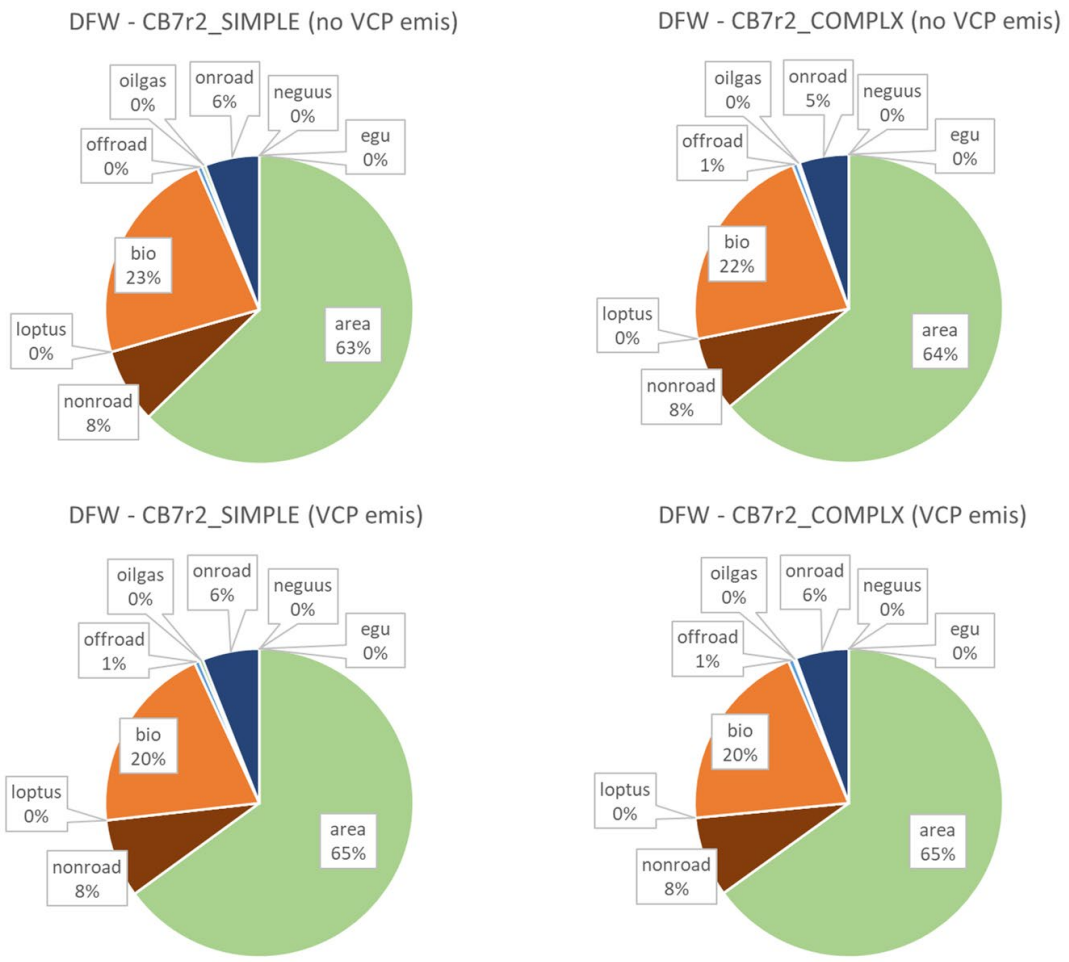

Figure 6-8. Contribution of emission source categories to total SOA from CAMx PSAT model runs for DFW.

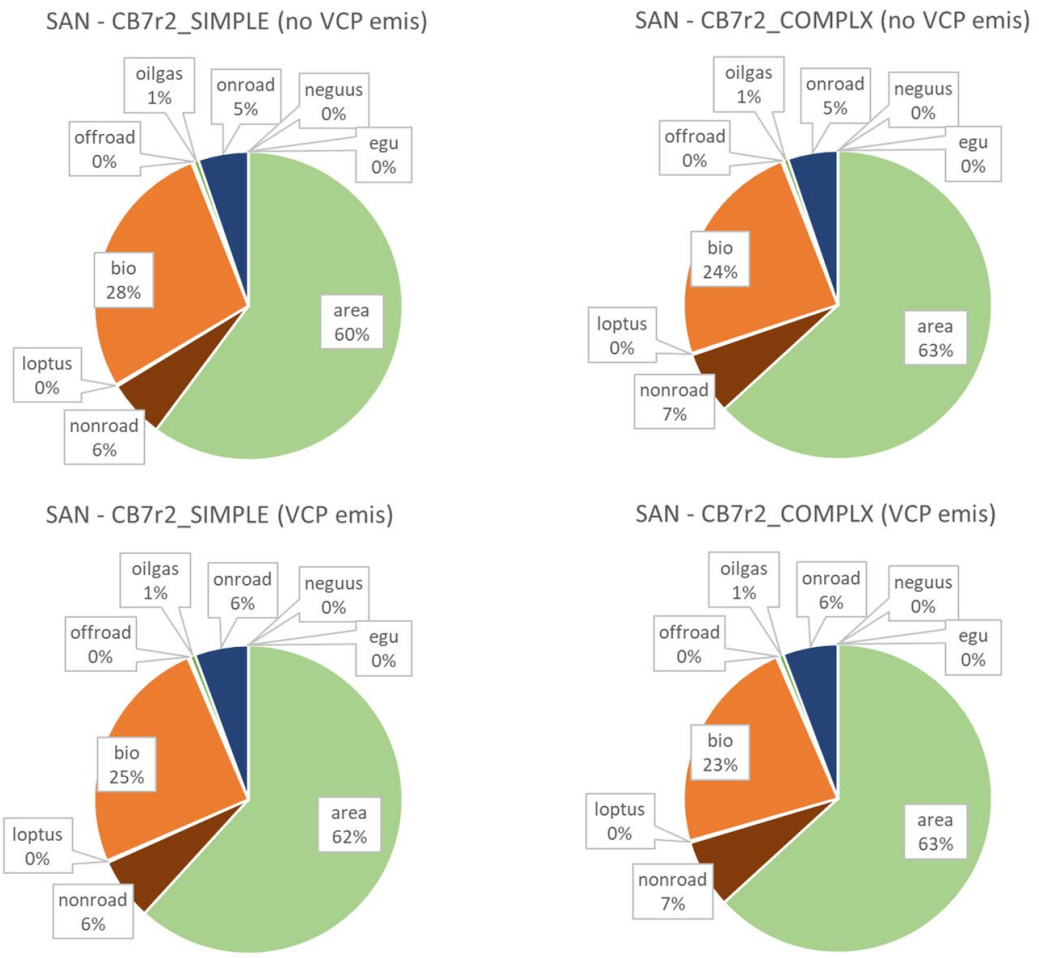

Figure 6-9. Contribution of emission source categories to total SOA from CAMx PSAT model runs for SAN.

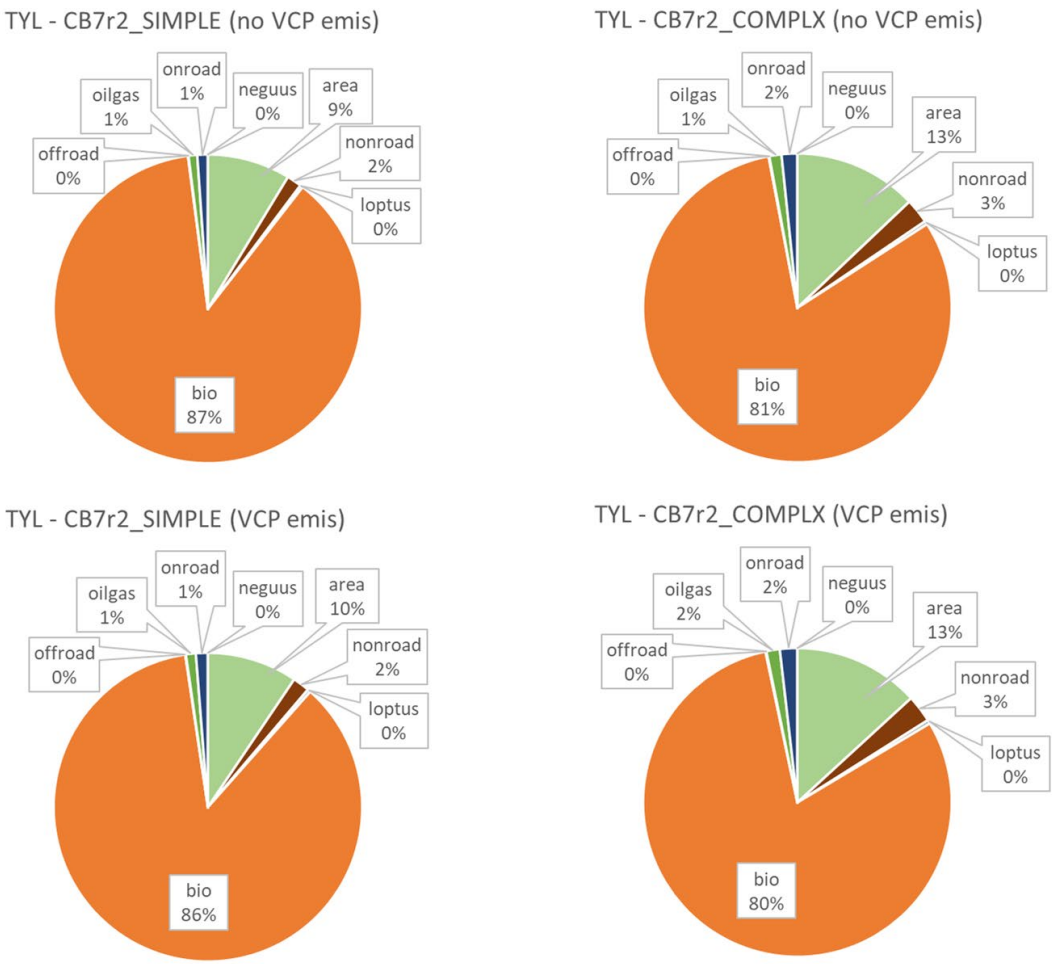

Figure 6-10. Contribution of emission source categories to total SOA from CAMx PSAT model runs for TYL.

7.0 Summary and Recommendations

CAMx was updated to include VCP chemistry and to better represent SOA production from VCPs and IVOA. Updates were made to the gas-phase chemical mechanism (CB7r2), aerosol scheme (CF3 SIMPLE and CF3 COMPLEX), and the related CAMx probing tools (PSAT, OSAT, DDM, CPA). The emission speciation mapping was also updated to include the new species added to CB7r2 and CF3. CAMx 2-box model runs were conducted to test proper implementation of these updates and evaluate their potential impact on total SOA.

Model results using the updated version of CAMx (v7.32-CB7r2) were compared to CAMx v7.30 with CB7r1. The CAMx updates implemented in this project lead to an overall decrease in SOA concentration, primarily due to the updated SOA yields for IVOA in CF3. IVOA is an important SOA precursor so decreasing it's yield from the previous value of 1.0 to 0.362 under high-NO conditions and 0.471 under low NO conditions, causes a significant decrease in SOA production. Although additional SOA precursors, including IV1, IVC2, and HPAR, were added to CF3 to better represent SOA formation from VCPs, the decrease in the IVOA yield by more than one half dominates the SOA impact. The previous assumption that all species assigned to IVOA have unit SOA yield was too simple, especially when coupled to emissions mapping strategies that map compounds to IVOA based solely on their vapor pressure without consideration of SOA-forming potential.

Better representing VCP species was found to increase SOA concentrations in the 2-box model testing due to increased emissions of SOA precursors (IVC1, IVC2, HPAR, IVOA). However, the emissions used in the 2-box model scenarios were based on VOC measurement data from Chen et al., 2024 and will differ from those generated using the updated speciation mapping for CB7r2. We recommend that TCEQ generate new emissions files using the CB7r2 speciation mapping to compare against the estimates used in this study. While CB7r2 and CAMxv7.32-CB7r2 can be used without VCP emissions, correctly speciated emissions are needed to better understand how VCPs impact SOA and ozone. When updated emissions files become available for TCEQ's 3D CAMx modeling they can be readily re-processed for the 2-box model scenarios. When 3D CAMx model runs become available they can be analyzed to understand how CB7r2 and CAMx v7.31-CB7r2 impact model performance against observations.

The CAMx updates made in this project are intended to improve TCEQ's ability to accurately model PM, especially for urban areas where SOA from anthropogenic emissions can make important contributions to $PM_{2.5}$ air quality. Additional updates to CB7r2 and CF3 may further improve the accuracy and should be considered.

- Improved treatment of VOC autoxidation. Autoxidation is an important process that can create highly oxidized molecules which produce aerosols. A limited representation of autoxidation was introduced in CB7r2 using species AUTX (Update 12, Table 2-1). Other mechanisms, including SAPRC22 (Carter, 2023), have a more complex treatment of autoxidation but it is unclear if this leads to better PM prediction. Comparison between CB7r2 and SAPRC22 using CAMx 2-box model scenarios would help us better understand autoxidation's role in PM formation.

- Improved representation of wildfire VOCs. Important oxygenated VOCs (such as phenols, cresols, and furans) that are emitted from wildfires and contribute to SOA formation are not well represented in CB7r2. Ramboll is currently planning to update CB7r2 with new VOC species and their relevant oxidation reactions to better characterize the gas-phase chemistry of wildfire smoke. This work can be expanded with updates to CF3, similar to those performed in this project, which add new precursor species to better represent SOA formation from wildfire smoke.

8.0 References

Ahlberg, E., Eriksson, A., Brune, W.H., Roldin, P. and Svenningsson, B., 2019. Effect of salt seed particle surface area, composition and phase on secondary organic aerosol mass yields in oxidation flow reactors. Atmospheric Chemistry and Physics, 19(4), pp.2701-2712.

Allen, H.M., Crounse, J.D., Kim, M.J., Teng, A.P., Ray, E.A., McKain, K., Sweeney, C. and Wennberg, P.O., 2022. H2O2 and CH3OOH (MHP) in the remote atmosphere: 1. Global distribution and regional influences. Journal of Geophysical Research: Atmospheres, 127(6), p.e2021JD035701.

Burkholder, J.B., Sander, S.P., Abbatt, J.P.D., Barker, J.R., Cappa, C., Crounse, J.D., Dibble, T.S., Huie, R.E., Kolb, C.E., Kurylo, M.J. and Orkin, V.L., 2020. Chemical kinetics and photochemical data for use in atmospheric studies; evaluation number 19. Pasadena, CA: Jet Propulsion Laboratory, National Aeronautics and Space Administration.

Carter, W.P., 2010. Development of the SAPRC-07 chemical mechanism. Atmospheric Environment, 44(40), pp.5324-5335.

Carter, W.P., 2023. Documentation of the SAPRC-22 Mechanism. Report to the California Air Resources Board, Contract No. 21AQP011, https://intra.engr.ucr.edu/~carter/SAPRC/22/S22doc.pdf.

Charan, S.M., Buenconsejo, R.S. and Seinfeld, J.H., 2020. Secondary organic aerosol yields from the oxidation of benzyl alcohol. Atmospheric Chemistry and Physics, 20(21), pp.13167-13190.

Chen, T., Gilman, J., Kim, S.-W., Lefer, B., Washenfelder, R., Young, C. J., Rappenglueck, B., Stevens, P. S., Veres, P. R., Xue, L. and de Gouw, J., 2024. Modeling the Impacts of Volatile Chemical Product Emissions on Atmospheric Photochemistry and Ozone Formation in Los Angeles. Journal of Geophysical Research: Atmospheres, 129, e2024JD040743. doi: 10.1029/ 2024JD040743.

Crounse, J. D., Nielsen, L. B., Jørgensen, S., Kjaergaard, H. G., & Wennberg, P. O., 2013. Autoxidation of organic compounds in the atmosphere. The Journal of Physical Chemistry Letters, 4(20), 3513-3520.

de Gouw, J.D., Gilman, J.B., Kim, S.W., Lerner, B.M., Isaacman-VanWertz, G., McDonald, B.C., Warneke, C., Kuster, W.C., Lefer, B.L., Griffith, S.M. and Dusanter, S., 2017. Chemistry of volatile organic compounds in the Los Angeles basin: Nighttime removal of alkenes and determination of emission ratios. Journal of Geophysical Research: Atmospheres, 122(21), pp.11-843.

Hartikainen, A., Tiitta, P., Ihalainen, M., Yli-Pirilä, P., Orasche, J., Czech, H., Kortelainen, M., Lamberg, H., Suhonen, H., Koponen, H. and Hao, L., 2020. Photochemical transformation of residential wood combustion emissions: dependence of organic aerosol composition on OH exposure. Atmospheric Chemistry and Physics, 20(11), pp.6357-6378.

Humes, M.B., Wang, M., Kim, S., Machesky, J.E., Gentner, D.R., Robinson, A.L., Donahue, N.M. and Presto, A.A., 2022. Limited secondary organic aerosol production from acyclic

oxygenated volatile chemical products. Environmental Science & Technology, 56(8), pp.4806-4815.

Kang, H.G., Chen, Y., Park, Y., Berkemeier, T. and Kim, H., 2023. Volatile oxidation products and secondary organosiloxane aerosol from D 5+ OH at varying OH exposures. Atmospheric Chemistry and Physics, 23(22), pp.14307-14323.

Kenagy, H.S., Heald, C.L., Tahsini, N., Goss, M.B. and Kroll, J.H., 2024. Can we achieve atmospheric chemical environments in the laboratory? An integrated model-measurement approach to chamber SOA studies. Science Advances, 10(37), p.eado1482.

Li, L. and Cocker III, D.R., 2018. Molecular structure impacts on secondary organic aerosol formation from glycol ethers. Atmospheric Environment, 180, pp.206-215.

Li, W., Li, L., Chen, C.L., Kacarab, M., Peng, W., Price, D., Xu, J. and Cocker III, D.R., 2018. Potential of select intermediate-volatility organic compounds and consumer products for secondary organic aerosol and ozone formation under relevant urban conditions. Atmospheric environment, 178, pp.109-117.

Li, Z., Buchholz, A., Barreira, L.M., Ylisirniö, A., Hao, L., Pullinen, I., Schobesberger, S. and Virtanen, A., 2023. Isothermal evaporation of α-pinene secondary organic aerosol particles formed under low NOx and high NOx conditions. Atmospheric Chemistry and Physics, 23(1), pp.203-220.

Liu, S., Shilling, J.E., Song, C., Hiranuma, N., Zaveri, R.A. and Russell, L.M., 2012. Hydrolysis of organonitrate functional groups in aerosol particles. Aerosol Science and Technology, 46(12), pp.1359-1369.

Maclean, A.M., Li, Y., Crescenzo, G.V., Smith, N.R., Karydis, V.A., Tsimpidi, A.P., Butenhoff, C.L., Faiola, C.L., Lelieveld, J., Nizkorodov, S.A. and Shiraiwa, M., 2021. Global distribution of the phase state and mixing times within secondary organic aerosol particles in the troposphere based on room-temperature viscosity measurements. ACS Earth and Space Chemistry, 5(12), pp.3458-3473.

Manavi, S.E. and Pandis, S.N., 2022. A lumped species approach for the simulation of secondary organic aerosol production from intermediate-volatility organic compounds (IVOCs): application to road transport in PMCAMx-iv (v1. 0). Geoscientific Model Development, 15(20), pp.7731-7749.

McDonald, B.C., De Gouw, J.A., Gilman, J.B., Jathar, S.H., Akherati, A., Cappa, C.D., Jimenez, J.L., Lee-Taylor, J., Hayes, P.L., McKeen, S.A. and Cui, Y.Y., 2018. Volatile chemical products emerging as largest petrochemical source of urban organic emissions. Science, 359(6377), pp.760-764.

Mellouki, A., Ammann, M., Cox, R.A., Crowley, J.N., Herrmann, H., Jenkin, M.E., McNeill, V.F., Troe, J. and Wallington, T.J., 2021. Evaluated kinetic and photochemical data for atmospheric chemistry: volume VIII–gas-phase reactions of organic species with four, or more, carbon atoms (≥ C 4). Atmospheric Chemistry and Physics, 21(6), pp.4797-4808.

Pankow, J. F., 1994. An absorption model of the gas/aerosol partitioning involved in the formation of secondary organic aerosol. Atmospheric Environment, 28(2), 189-193.

Praske, E., Otkjær, R.V., Crounse, J.D., Hethcox, J.C., Stoltz, B.M., Kjaergaard, H.G. and Wennberg, P.O., 2018. Atmospheric autoxidation is increasingly important in urban and suburban North America. Proceedings of the National Academy of Sciences, 115(1), pp.64-69.

Ramboll, 2023. Comparing ozone precursor responses and volatile organic compound (VOC) reactivity of Cabon Bond version 7 revision 1 (CB7r1) to other mechanisms. Report prepared for TCEQ Work Order 582-23-42327-033, June 2023.

Ramboll, 2024a. Secondary Organic Aerosol (SOA) Update in CAMx. Report prepared for TCEQ Work Order 582-23-45978-06, June 2024.

Ramboll, 2024b. CAMx User's Guide, Version 7.30. Retrieved from https://www.camx.com/.

Reza, M., Iezzi, L., Finkenzeller, H., Roose, A., Ammann, M. and Volkamer, R., 2024. Iodine Activation from Iodate Reduction in Aqueous Films via Photocatalyzed and Dark Reactions. ACS Earth and Space Chemistry, 8(12), pp.2495-2508.

Rolletter, M., Hofzumahaus, A., Novelli, A., Wahner, A. and Fuchs, H., 2025. Kinetics of the reactions of OH with CO, NO, and NO2 and of HO2 with NO2 in air at 1 atm pressure, room temperature, and tropospheric water vapour concentrations. Atmospheric Chemistry and Physics, 25(6), pp.3481-3502.

Rollins, A.W., Pusede, S., Wooldridge, P., Min, K.-E., Gentner, D.R., Goldstein, A.H., Liu, S., Day, D.A., Russell, L.M., Rubitschun, C.L., Surratt, J.D., Cohen, R.C. 2013. Gas/particle partitioning of total alkyl nitrates observed with TD-LIF in Bakersfield. J. Geophys. Res. Atmos., 118, 6651–6662, doi:10.1002/jgrd.50522.

Sarrafzadeh, M., Wildt, J., Pullinen, I., Springer, M., Kleist, E., Tillmann, R., Schmitt, S.H., Wu, C., Mentel, T.F., Zhao, D. and Hastie, D.R., 2016. Impact of NO x and OH on secondary organic aerosol formation from β-pinene photooxidation. Atmospheric chemistry and physics, 16(17), pp.11237-11248.

Sasidharan, S., He, Y., Akherati, A., Li, Q., Li, W., Cocker, D., McDonald, B.C., Coggon, M.M., Seltzer, K.M., Pye, H.O. and Pierce, J.R., 2023. Secondary organic aerosol formation from volatile chemical product emissions: Model parameters and contributions to anthropogenic aerosol. Environmental Science & Technology, 57(32), pp.11891-11902.

Sbai, S.E., Mejjad, N., Mabrouki, J., 2024. Oxidation Flow Reactor for Simulating and Accelerating Atmospheric Secondary Aerosol Formation. In: Mabrouki, J., Mourade, A. (eds) Technical and Technological Solutions Towards a Sustainable Society and Circular Economy. World Sustainability Series. Springer, Cham. https://doi.org/10.1007/978-3-031-56292-1_43

Welsh, B.A., Corrigan, M.E., Assaf, E., Nauta, K., Sebastianelli, P., Jordan, M.J., Fittschen, C. and Kable, S.H., 2023. Photophysical oxidation of HCHO produces HO2 radicals. Nature Chemistry, 15(10), pp.1350-1357.

Wennberg, P.O., Bates, K.H., Crounse, J.D., Dodson, L.G., McVay, R.C., Mertens, L.A., Nguyen, T.B., Praske, E., Schwantes, R.H., Smarte, M.D. and St Clair, J.M., 2018. Gas-phase reactions of isoprene and its major oxidation products. Chemical reviews, 118(7), pp.3337-3390.

Wennberg, P.O., 2023. Let's Abandon the "High NOx" and "Low NOx" Terminology. ACS ES&T Air, 1(1), pp.3-4.

Wildt, J., Mentel, T.F., Kiendler-Scharr, A., Hoffmann, T., Andres, S., Ehn, M., Kleist, E., Müsgen, P., Rohrer, F., Rudich, Y. and Springer, M., 2014. Suppression of new particle formation from monoterpene oxidation by NOx. Atmospheric chemistry and physics, 14(6), pp.2789-2804.

Yarwood, G. and Tuite, K., 2024. Representing Ozone Formation from Volatile Chemical Products (VCP) in Carbon Bond (CB) Chemical Mechanisms. Atmosphere, 15(2), 178. https://doi.org/10.3390/atmos15020178

Yu, H., Møller, K.H., Buenconsejo, R.S., Crounse, J.D., Kjaergaard, H.G. and Wennberg, P.O., 2023. Atmospheric Photo-Oxidation of 2-Ethoxyethanol: Autoxidation Chemistry of Glycol Ethers. The Journal of Physical Chemistry A, 127(45), pp.9564-9579.

Zhao, Q., Xie, H.B., Ma, F., Nie, W., Yan, C., Huang, D., Elm, J. and Chen, J., 2023. Mechanism-based structure-activity relationship investigation on hydrolysis kinetics of atmospheric organic nitrates. npj Climate and Atmospheric Science, 6(1), p.192.

Appendix A

Details of the CB7r2 mechanism

Appendix A Details of the CB7r2 mechanism

Table A-1. Reactions and rate constant expressions for the CB7r2 mechanism. See Table A-2 for species names. k298 is the rate constant at 298 K and 1 atmosphere using units in cm^3 $molecule^{-1}$ and s^{-1}. For photolysis reactions k298 shows the photolysis frequency (J) at a solar zenith angle of 60° (see Table A-4)and the rate constant expression for primary photolysis reactions refer to the TUV data file (see Table A-3).

Number	Reactants and Products	Rate Constant Expression	k_{298}
1	NO2 = NO + O	Photolysis: NO2.PHF	$6.30x10^{-3}$
2	O2 + O + M = O3 + M	$k = 6.00x10^{-34}$ $(T/300)^{-2.6}$	$6.11x10^{-34}$
3	NO + O3 = NO2	$k = 2.07x10^{-12}$ exp(−1400/T)	$1.89x10^{-14}$
4	NO + O = NO2	Falloff: F=0.85; n=0.84 $k(0) = 1.00x10^{-31}$ $(T/300)^{-1.6}$ $k(inf) = 5.00x10^{-11}$ $(T/300)^{-0.3}$	$2.26x10^{-12}$
5	NO2 + O = NO	$k = 5.10x10^{-12}$ exp(198/T)	$9.91x10^{-12}$
6	NO2 + O = NO3	Falloff: F=0.6; n=1 $k(0) = 1.30x10^{-31}$ $(T/300)^{-1.5}$ $k(inf) = 2.30x10^{-11}$ $(T/300)^{0.24}$	$2.11x10^{-12}$
7	O3 + O =	$k = 8.00x10^{-12}$ exp(−2060/T)	$7.96x10^{-15}$
8	O3 = O	Photolysis: O3O3P.PHF	$3.33x10^{-4}$
9	O3 = O1D	Photolysis: O3O1D.PHF	$8.78x10^{-6}$
10	O1D + M = O + M	$k = 2.23x10^{-11}$ exp(115/T)	$3.28x10^{-11}$
11	O1D + H2O = 2 OH	$k = 2.14x10^{-10}$	$2.14x10^{-10}$
12	O3 + OH = HO2	$k = 1.70x10^{-12}$ exp(−940/T)	$7.25x10^{-14}$
13	O3 + HO2 = OH	$k = 2.03x10^{-16}$ $(T/300)^{4.57}$ exp(693/T)	$2.01x10^{-15}$
14	OH + O = HO2	$k = 2.40x10^{-11}$ exp(110/T)	$3.47x10^{-11}$
15	HO2 + O = OH	$k = 3.00x10^{-11}$ exp(200/T)	$5.87x10^{-11}$
16	OH + OH = O	$k = 6.20x10^{-14}$ $(T/298)^{2.6}$ exp(945/T)	$1.48x10^{-12}$
17	OH + OH = H2O2	Falloff: F=0.42; n=1.23 $k(0) = 9.00x10^{-31}$ $(T/300)^{-3.2}$ $k(inf) = 3.90x10^{-11}$ $(T/300)^{-0.47}$	$6.21x10^{-12}$
18	OH + HO2 =	$k = 4.80x10^{-11}$ exp(250/T)	$1.11x10^{-10}$
19	HO2 + HO2 = H2O2	k = k1 + k2 [M] $k1 = 2.20x10^{-13}$ exp(600/T) $k2 = 1.90x10^{-33}$ exp(980/T)	$2.90x10^{-12}$
20	HO2 + HO2 + H2O = H2O2	k = k1 + k2 [M] $k1 = 3.08x10^{-34}$ exp(2800/T) $k2 = 2.66x10^{-54}$ exp(3180/T)	$6.53x10^{-30}$
21	H2O2 = 2 OH	Photolysis: H2O2.PHF	$3.78x10^{-6}$
22	H2O2 + OH = HO2	$k = 1.80x10^{-12}$	$1.80x10^{-12}$
23	H2O2 + O = OH + HO2	$k = 1.40x10^{-12}$ exp(−2000/T)	$1.70x10^{-15}$
24	NO + NO + O2 = 2 NO2	$k = 4.25x10^{-39}$ exp(664/T)	$3.95x10^{-38}$
25	NO + HO2 = OH + NO2	$k = 3.45x10^{-12}$ exp(270/T)	$8.54x10^{-12}$
26	NO2 + O3 = NO3	$k = 1.40x10^{-13}$ exp(−2470/T)	$3.52x10^{-17}$
27	NO3 = NO2 + O	Photolysis: NO3_NO2.PHF	$1.56x10^{-1}$
28	NO3 = NO	Photolysis: NO3_NO.PHF	$1.98x10^{-2}$
29	NO3 + NO = 2 NO2	$k = 1.80x10^{-11}$ exp(110/T)	$2.60x10^{-11}$

Number	Reactants and Products	Rate Constant Expression	k_{298}
30	NO3 + NO2 = NO + NO2	k = 4.35×10^{-14} exp(−1335/T)	4.93×10^{-16}
31	NO3 + OH = HO2 + NO2	k = 2.00×10^{-11}	2.00×10^{-11}
32	NO3 + HO2 = OH + NO2	k = 4.00×10^{-12}	4.00×10^{-12}
33	NO3 + NO3 = 2 NO2	k = 8.50×10^{-13} exp(−2450/T)	2.28×10^{-16}
34	NO3 + NO2 = N2O5	Falloff: F=0.35; n=1.33 k(0) = 3.60×10^{-30} $(T/300)^{-4.1}$ k(inf) = 1.90×10^{-12} $(T/300)^{0.2}$	1.24×10^{-12}
35	N2O5 = NO3 + NO2	Falloff: F=0.35; n=1.33 k(0) = 1.30×10^{-3} $(T/300)^{-3.5}$ exp(−11000/T) k(inf) = $9.70\times10^{+14}$ $(T/300)^{0.1}$ exp(−11080/T)	4.46×10^{-2}
36	N2O5 = NO2 + NO3	Photolysis: N2O5.PHF	2.52×10^{-5}
37	N2O5 + H2O = 2 HNO3	k = 1.00×10^{-22}	1.00×10^{-22}
38	NO + OH = HONO	Falloff: F=0.6; n=1 k(0) = 7.10×10^{-31} $(T/298)^{-2.6}$ k(inf) = 3.60×10^{-11} $(T/298)^{-0.1}$	7.39×10^{-12}
39	HONO = NO + OH	Photolysis: HONO.PHF	1.04×10^{-3}
40	HONO + OH = NO2	k = 2.50×10^{-12} exp(260/T)	5.98×10^{-12}
41	NO2 + OH = HNO3	Falloff: F=0.6; n=1 k(0) = 1.80×10^{-30} $(T/298)^{-3}$ k(inf) = 2.80×10^{-11}	1.06×10^{-11}
42	NO2 + OH + H2O = HNO3 + H2O	k = 1.10×10^{-30}	1.10×10^{-30}
43	HNO3 + OH = NO3	k = k1 + k3 [M] / (1 + k3 [M] / k2) k1 = 2.40×10^{-14} exp(460/T) k2 = 2.70×10^{-17} exp(2199/T) k3 = 6.50×10^{-34} exp(1335/T)	1.54×10^{-13}
44	HNO3 = OH + NO2	Photolysis: HNO3.PHF	2.54×10^{-7}
45	NO2 + HO2 = PNA	Falloff: F=0.6; n=1 k(0) = 1.90×10^{-31} $(T/298)^{-3.4}$ k(inf) = 4.00×10^{-12} $(T/298)^{-0.3}$	1.30×10^{-12}
46	PNA = HO2 + NO2	k = k(ref)/K k(ref) = k(45) K = 2.10×10^{-27} exp(10900/T)	8.04×10^{-2}
47	PNA = 0.59 HO2 + 0.59 NO2 + 0.41 OH + 0.41 NO3	Photolysis: PNA.PHF	2.36×10^{-6}
48	PNA + OH = NO2	k = 3.20×10^{-13} exp(690/T)	3.24×10^{-12}
49	H2 + OH = HO2	k = 7.70×10^{-12} exp(−2100/T)	6.70×10^{-15}
50	CO + OH = HO2	k = k1 + k2 [M] k1 = 1.44×10^{-13} k2 = 3.43×10^{-33}	2.28×10^{-13}
51	SO2 + OH = SULF + HO2	Falloff: F=0.53; n=1.1 k(0) = 2.80×10^{-31} $(T/300)^{-2.6}$ k(inf) = 2.00×10^{-12}	9.35×10^{-13}
52	SO2 = SULF	k = 0	0
53	DMS + OH = SO2 + FORM + MEO2	k = 1.12×10^{-11} exp(−250/T)	4.84×10^{-12}
54	DMS + OH + O2 = SULF + MEO2	k = 1.28×10^{-37} exp(4480/T)	4.33×10^{-31}
55	DMS + NO3 = SO2 + FORM + MEO2 + HNO3	k = 1.90×10^{-13} exp(520/T)	1.09×10^{-12}

Number	Reactants and Products	Rate Constant Expression	k_{298}
56	C2O3 + NO = NO2 + MEO2 + RO2	k = 7.50×10^{-12} exp(290/T)	1.98×10^{-11}
57	C2O3 + NO2 = PAN	Falloff: F=0.3; n=1.41 k(0) = 3.61×10^{-28} $(T/300)^{-6.87}$ k(inf) = 1.24×10^{-11} $(T/300)^{-1.105}$	9.86×10^{-12}
58	PAN = NO2 + C2O3	Falloff: F=0.3; n=1.41 k(0) = 1.10×10^{-5} exp(−10100/T) k(inf) = $1.90 \times 10^{+17}$ exp(−14100/T)	4.31×10^{-4}
59	PAN = 0.6 NO2 + 0.6 C2O3 + 0.4 NO3 + 0.4 MEO2 + 0.4 RO2	Photolysis: PAN.PHF	3.47×10^{-7}
60	C2O3 + HO2 = 0.37 PACD + 0.13 AACD + 0.13 O3 + 0.5 OH + 0.5 MEO2 + 0.5 RO2	k = 3.14×10^{-12} exp(580/T)	2.20×10^{-11}
61	C2O3 + RO2 = 0.3 AACD + 0.7 MEO2 + 1.7 RO2	k = 4.40×10^{-13} exp(1070/T)	1.60×10^{-11}
62	C2O3 + C2O3 = 2 MEO2 + 2 RO2	k = 2.90×10^{-12} exp(500/T)	1.55×10^{-11}
63	CXO3 + NO = NO2 + 0.5 ALD2 + XO2H + RO2	k = 6.70×10^{-12} exp(340/T)	2.10×10^{-11}
64	CXO3 + NO2 = PANX	k = k(ref)/K k(ref) = k(57) K = 1.19	8.28×10^{-12}
65	PANX = NO2 + CXO3	k = k(ref)/K k(ref) = k(58) K = 1.19	3.62×10^{-4}
66	PANX + OH = 0.5 ALD2 + NO2	k = 3.00×10^{-12}	3.00×10^{-12}
67	CXO3 + HO2 = 0.19 PACD + 0.06 AACD + 0.25 ALD2 + 0.06 O3 + 0.25 OH + 0.25 HO2	k = k(ref)/K k(ref) = k(60) K = 1.0	2.20×10^{-11}
68	CXO3 + RO2 = 0.3 AACD + 0.7 ALD2 + 0.7 XO2H + 1.7 RO2	k = k(ref)/K k(ref) = k(61) K = 1.0	1.60×10^{-11}
69	OPO3 + NO = NO2 + 0.5 GLY + 0.5 CO + 0.8 HO2 + 0.2 CXO3	k = k(ref)/K k(ref) = k(63) K = 1.0	2.10×10^{-11}
70	OPO3 + NO2 = OPAN	k = k(ref)/K k(ref) = k(64) K = 1.0	8.28×10^{-12}
71	OPAN = OPO3 + NO2	k = k(ref)/K k(ref) = k(65) K = 1.0	3.62×10^{-4}
72	OPAN + OH = 0.5 NO2 + 0.5 NTR2 + 0.5 GLY + CO	k = 3.60×10^{-11}	3.60×10^{-11}
73	OPO3 + HO2 = 0.37 PACD + 0.13 AACD + 0.13 O3 + 0.5 OH + 0.5 MEO2 + 0.5 RO2	k = k(ref)/K k(ref) = k(60) K = 1.0	2.20×10^{-11}
74	OPO3 + RO2 = 0.3 AACD + 0.35 GLY + 0.4 XO2H 0.35 CO + 0.14 CXO3 + 1.4 RO2	k = k(ref)/K k(ref) = k(61) K = 1.0	1.60×10^{-11}
75	RO2 + NO = NO	k = 2.70×10^{-12} exp(360/T)	9.04×10^{-12}
76	RO2 + HO2 = HO2	k = 1.93×10^{-13} exp(1300/T)	1.52×10^{-11}

Number	Reactants and Products	Rate Constant Expression	k_{298}
77	RO2 + RO2 =	k = 1.55×10^{-13} exp(350/T)	5.00×10^{-13}
78	MEO2 + NO = FORM + HO2 + NO2	k = 2.30×10^{-12} exp(360/T)	7.70×10^{-12}
79	MEO2 + HO2 = 0.9 MEPX + 0.1 FORM	k = 3.80×10^{-13} exp(780/T)	5.21×10^{-12}
80	MEO2 + RO2 = 0.685 FORM + 0.315 MEOH + 0.37 HO2 + RO2	k = k(ref)/K k(ref) = k(77) K = 1.0	5.00×10^{-13}
81	MEPX + OH = 0.6 MEO2 + 0.6 RO2 + 0.4 FORM + 0.4 OH	k = 5.30×10^{-12} exp(190/T)	1.00×10^{-11}
82	MEPX = MEO2 + RO2 + OH	Photolysis: MEPX.PHF	2.68×10^{-6}
83	XO2H + NO = NO2 + HO2	k = k(ref)/K k(ref) = k(75) K = 1.0	9.04×10^{-12}
84	XO2H + HO2 = ROOH	k = k(ref)/K k(ref) = k(76) K = 1.0	1.52×10^{-11}
85	XO2H + RO2 = RO2	k = k(ref)/K k(ref) = k(77) K = 1.0	5.00×10^{-13}
86	XO2 + NO = NO2	k = k(ref)/K k(ref) = k(75) K = 1.0	9.04×10^{-12}
87	XO2 + HO2 = ROOH	k = k(ref)/K k(ref) = k(76) K = 1.0	1.52×10^{-11}
88	XO2 + RO2 = RO2	k = k(ref)/K k(ref) = k(77) K = 1.0	5.00×10^{-13}
89	XO2N + NO = 0.5 NTR1 + 0.5 NTR2	k = k(ref)/K k(ref) = k(75) K = 1.0	9.04×10^{-12}
90	XO2N + HO2 = ROOH	k = k(ref)/K k(ref) = k(76) K = 1.0	1.52×10^{-11}
91	XO2N + RO2 = RO2	k = k(ref)/K k(ref) = k(77) K = 1.0	5.00×10^{-13}
92	ROOH + OH = 0.56 XO2H + 0.04 XO2N + 0.6 RO2 + 0.4 OH	k = 9.00×10^{-12} exp(190/T)	1.70×10^{-11}
93	ROOH = HO2 + OH	Photolysis: J(ROOH) = J(MEPX)x1.0	2.68×10^{-6}
94	NTR1 + OH = NO2	k = 2.00×10^{-12}	2.00×10^{-12}
95	NTR1 = NO2	Photolysis: NTR.PHF	1.06×10^{-6}
96	NTR2 = NO2	Photolysis: J(NTR2) = J(NTR1)x1.0	1.06×10^{-6}
97	NTR2 = HNO3	k = 2.30×10^{-5}	2.30×10^{-5}
98	MEOH + OH = FORM + HO2	k = 2.85×10^{-12} exp(−345/T)	8.95×10^{-13}
99	ETOH + OH = 0.95 ALD2 + 0.9 HO2 + 0.1 XO2H + 0.1 RO2 + 0.078 FORM + 0.011 GLYD	k = 3.00×10^{-12} exp(20/T)	3.21×10^{-12}
100	FORM + OH = HO2 + CO	k = 5.40×10^{-12} exp(135/T)	8.49×10^{-12}

Number	Reactants and Products	Rate Constant Expression	k_{298}
101	FORM = 2 HO2 + CO	Photolysis: FORM_R72.PHF	1.75×10^{-5}
102	FORM = CO + H2	Photolysis: FORM_Mr5.PHF	2.69×10^{-5}
103	FORM + NO3 = HNO3 + HO2 + CO	$k = 5.50 \times 10^{-16}$	5.50×10^{-16}
104	ALD2 + OH = C2O3	$k = 4.70 \times 10^{-12} \exp(345/T)$	1.50×10^{-11}
105	ALD2 + NO3 = C2O3 + HNO3	$k = 1.40 \times 10^{-12} \exp(-1860/T)$	2.73×10^{-15}
106	ALD2 = MEO2 + RO2 + CO + HO2	Photolysis: ALD2_Rr5.PHF	1.96×10^{-6}
107	ALDX + OH = CXO3	$k = 4.90 \times 10^{-12} \exp(405/T)$	1.91×10^{-11}
108	ALDX + NO3 = CXO3 + HNO3	$k = 6.30 \times 10^{-15}$	6.30×10^{-15}
109	ALDX = ALD2 + CO + HO2 + XO2H + DPAR + RO2	Photolysis: ALDX_R72.PHF	1.54×10^{-5}
110	GLYD + OH = 0.2 GLY + 0.2 HO2 + 0.8 C2O3	$k = 8.00 \times 10^{-12}$	8.00×10^{-12}
111	GLYD = 0.74 FORM + 0.89 CO + 1.4 HO2 + 0.15 MEOH + 0.19 OH + 0.11 GLY + 0.11 XO2H + 0.11 RO2	Photolysis: GLYDr5.PHF	2.76×10^{-6}
112	GLYD + NO3 = HNO3 + C2O3	k = k(ref)/K k(ref) = k(105) K = 1.0	2.73×10^{-15}
113	GLY + OH = 1.8 CO + 0.2 XO2 + 0.2 RO2 + HO2	$k = 3.10 \times 10^{-12} \exp(340/T)$	9.70×10^{-12}
114	GLY = 2 HO2 + 2 CO	Photolysis: GLY_Rr5.PHF	7.95×10^{-5}
115	GLY + NO3 = HNO3 + 1.5 CO + 0.5 XO2 + 0.5 RO2 + HO2	$k = 4.00 \times 10^{-16}$	4.00×10^{-16}
116	MGLY = C2O3 + HO2 + CO	Photolysis: MGLY.PHF	1.46×10^{-4}
117	MGLY + NO3 = HNO3 + C2O3 + XO2 + RO2	$k = 5.00 \times 10^{-16}$	5.00×10^{-16}
118	MGLY + OH = C2O3 + CO	$k = 1.90 \times 10^{-12} \exp(575/T)$	1.31×10^{-11}
119	ACET = 0.38 CO + 1.38 MEO2 + 1.38 RO2 + 0.62 C2O3	Photolysis: ACET.PHF	2.27×10^{-7}
120	ACET + OH = FORM + C2O3 + XO2 + RO2	$k = 1.41 \times 10^{-12} \exp(-620.6/T)$	1.76×10^{-13}
121	KET = 0.64 ALD2 + 0.32 ALDX + 0.64 C2O3 + 0.32 CXO3 + 0.96 XO2H + 0.04 XO2N + 3.0 DPAR + RO2	Photolysis: KET.PHF	2.08×10^{-7}
122	KET + OH = 0.63 ALD2 + 0.31 ALDX + 0.63 C2O3 + 0.31 CXO3 + 0.94 XO2 + 0.06 XO2N + 3.0 DPAR + RO2	$k = 2.70 \times 10^{-12} \exp(^{-90}/T)$	2.00×10^{-12}
123	HACT + OH = MGLY + HO2	$k = 2.00 \times 10^{-12} \exp(320/T)$	5.85×10^{-12}
124	FACD + OH = HO2	$k = 4.50 \times 10^{-13}$	4.50×10^{-13}
125	AACD + OH = MEO2 + RO2	$k = 4.00 \times 10^{-14} \exp(850/T)$	6.93×10^{-13}
126	PACD + OH = C2O3	$k = 5.30 \times 10^{-12} \exp(190/T)$	1.00×10^{-11}
127	CH4 + OH = MEO2 + RO2	$k = 1.85 \times 10^{-12} \exp(-1690/T)$	6.37×10^{-15}
128	ECH4 + OH = MEO2 + RO2	$k = 1.85 \times 10^{-12} \exp(-1690/T)$	6.37×10^{-15}
129	ETHA + OH = 0.991 ALD2 + 0.991 XO2H + 0.009 XO2N + RO2	$k = 6.90 \times 10^{-12} \exp(-1000/T)$	2.41×10^{-13}

Number	Reactants and Products	Rate Constant Expression	k_{298}
130	PRPA + OH = 0.71 ACET + 0.26 ALDX + 0.26 PAR + 0.97 XO2H + 0.03 XO2N + RO2	$k = 7.60x10^{-12} \exp(-585/T)$	$1.07x10^{-12}$
131	DPAR + PAR =	$k = 1.00x10^{-9}$	$1.00x10^{-9}$
132	DPAR =	$k = 1.00x10^{-1}$	$1.00x10^{-1}$
133	OH + PAR = XPAR + 3 DPAR	$k = 3.09x10^{-13} (T/300)^2 \exp(300/T)$	$8.34x10^{-13}$
134	XPAR = XO2N + RO2	Falloff: F=0.41; n=1 $k(0) = 4.80x10^{-20}$ $k(inf) = 4.30x10^{-1} (T/298)^{-8}$	$1.49x10^{-1}$
135	XPAR = ROR + XO2	k = 1.0	1.0
136	ROR = 0.14 ACET + 0.04 FORM + 0.46 ALD2 + 0.19 ALDX + 0.57 HO2 + 0.3 XO2H + 0.05 XO2N + 0.5 AUTX + 0.95 DPAR + 0.85 RO2	k = k1 + k2 [M] $k1 = 2.70x10^{+12} \exp(-5000/T)$ $k2 = 7.00x10^{-15} \exp(-250/T)$	$2.14x10^{+5}$
137	ROR + O2 = KET + 3. PAR + HO2	$k = 2.00x10^{-14} \exp(-250/T)$	$8.64x10^{-15}$
138	ETHY + OH = 0.7 GLY + 0.7 OH + 0.3 FACD + 0.3 CO + 0.3 HO2	Falloff: F=0.37; n=1.3 $k(0) = 5.00x10^{-30} (T/300)^{-1.5}$ $k(inf) = 1.00x10^{-12}$	$7.52x10^{-13}$
139	ETH + OH = 1.56 FORM + 0.22 GLYD + XO2H + RO2	Falloff: F=0.48; n=1.15 $k(0) = 8.60x10^{-29} (T/300)^{-3.1}$ $k(inf) = 9.00x10^{-12} (T/300)^{-0.85}$	$7.84x10^{-12}$
140	ETH + O3 = FORM + 0.35 CO + 0.42 FACD + 0.17 OH + 0.27 HO2	$k = 6.82x10^{-15} \exp(-2500/T)$	$1.55x10^{-18}$
141	ETH + NO3 = 0.5 NO2 + 0.5 NTR1 + 1.125 FORM + 0.5 XO2H + 0.5 XO2 + RO2	$k = 3.30x10^{-12} \exp(-2880/T)$	$2.10x10^{-16}$
142	OLE + OH = 0.781 FORM + 0.488 ALD2 + 0.488 ALDX + 0.976 XO2H + 0.195 XO2 + 0.024 XO2N + 0.73 DPAR + 1.195 RO2	Falloff: F=0.5; n=1.13 $k(0) = 8.00x10^{-27} (T/300)^{-3.5}$ $k(inf) = 3.00x10^{-11} (T/300)^{-1}$	$2.86x10^{-11}$
143	OLE + O3 = 0.295 ALD2 + 0.555 FORM + 0.27 ALDX + 0.378 CO + 0.075 GLY + 0.075 MGLY + 0.09 FACD + 0.13 AACD + 0.04 H2O2 + 0.334 OH + 0.08 HO2 + 0.15 XO2H + 0.79 DPAR + 0.15 RO2	$k = 5.50x10^{-15} \exp(-1880/T)$	$1.00x10^{-17}$
144	OLE + NO3 = 0.5 NO2 + 0.5 NTR1 + 0.5 FORM + 0.25 ALD2 + 0.375 ALDX + 0.48 XO2 + 0.48 XO2H + 0.04 XO2N + DPAR + RO2	$k = 4.60x10^{-13} \exp(-1155/T)$	$9.54x10^{-15}$
145	IOLE + OH = 1.3 ALD2 + 0.7 ALDX + 2 PAR + XO2H + RO2	$k = 1.05x10^{-11} \exp(519/T)$	$5.99x10^{-11}$
146	IOLE + O3 = 0.732 ALD2 + 0.442 ALDX + 0.128 FORM + 0.245 CO + 0.24 GLY + 0.06 MGLY + 0.29 PAR + 0.08 AACD + 0.08 H2O2 + 0.5 OH + 0.3 XO2H + 0.3 RO2	$k = 4.70x10^{-15} \exp(-1013/T)$	$1.57x10^{-16}$

Number	Reactants and Products	Rate Constant Expression	k_{298}
147	IOLE + NO3 = 0.5 NO2 + 0.5 NTR1 + 0.5 ALD2 + 0.625 ALDX + PAR + 0.48 XO2 + 0.48 XO2H + 0.04 XO2N + RO2	$k = 3.70x10^{-13}$	$3.70x10^{-13}$
148	BENZ + OH = 0.53 CRES + 0.118 OPEN + 0.118 OH + 0.53 HO2 + 0.352 BZO2 + 0.352 RO2	$k = 2.30x10^{-12} \exp(-190/T)$	$1.22x10^{-12}$
149	BZO2 + NO = 0.918 NO2 + 0.082 NTR2 + 0.918 GLY + 0.918 OPEN + 0.918 HO2	k = k(ref)/K k(ref) = k(75) K = 1.0	$9.04x10^{-12}$
150	BZO2 + HO2 = ARPX	k = k(ref)/K k(ref) = k(76) $K = 8.55x10^{-1}$	$1.77x10^{-11}$
151	BZO2 + RO2 = GLY + OPEN + HO2 + RO2	k = k(ref)/K k(ref) = k(77) K = 1.0	$5.00x10^{-13}$
152	TOL + OH = 0.18 CRES + 0.1 OPEN + 0.1 OH + 0.18 HO2 + 0.65 TO2 + 0.07 XO2H + 0.72 RO2	$k = 1.80x10^{-12} \exp(340/T)$	$5.63x10^{-12}$
153	TO2 + NO = 0.86 NO2 + 0.14 NTR2 + 0.417 GLY + 0.443 MGLY + 0.66 OPEN + 0.2 XOPN + 0.86 HO2	k = k(ref)/K k(ref) = k(75) K = 1.0	$9.04x10^{-12}$
154	TO2 + HO2 = ARPX	k = k(ref)/K k(ref) = k(76) $K = 8.13x10^{-1}$	$1.86x10^{-11}$
155	TO2 + RO2 = 0.48 GLY + 0.52 MGLY + 0.77 OPEN + 0.23 XOPN + HO2 + RO2	k = k(ref)/K k(ref) = k(77) K = 1.0	$5.00x10^{-13}$
156	XYL + OH = 0.155 CRES + 0.244 XOPN + 0.244 OH + 0.155 HO2 + 0.544 XLO2 + 0.058 XO2H + 0.602 RO2	$k = 1.85x10^{-11}$	$1.85x10^{-11}$
157	XLO2 + NO = 0.86 NO2 + 0.14 NTR2 + 0.221 GLY + 0.675 MGLY + 0.3 OPEN + 0.56 XOPN + 0.86 HO2	k = k(ref)/K k(ref) = k(75) K = 1.0	$9.04x10^{-12}$
158	XLO2 + HO2 = ARPX	k = k(ref)/K k(ref) = k(76) $K = 7.83x10^{-1}$	$1.94x10^{-11}$
159	XLO2 + RO2 = 0.26 GLY + 0.77 MGLY + 0.35 OPEN + 0.65 XOPN + HO2 + RO2	k = k(ref)/K k(ref) = k(77) K = 1.0	$5.00x10^{-13}$
160	OPEN = OPO3 + HO2 + CO	Photolysis: J(OPEN) = J(NO2)x0.03	$1.89x10^{-4}$
161	OPEN + OH = 0.6 OPO3 + 0.4 GLY + 0.4 XO2H + 0.4 RO2	$k = 4.40x10^{-11}$	$4.40x10^{-11}$
162	OPEN + O3 = 1.4 GLY + 0.24 MGLY + 0.5 OH + 0.12 C2O3 + 0.08 FORM + 0.02 ALD2 + 1.98 CO + 0.56 HO2	$k = 5.40x10^{-17} \exp(-500/T)$	$1.01x10^{-17}$
163	OPEN + NO3 = OPO3 + HNO3	$k = 3.80x10^{-12}$	$3.80x10^{-12}$

Number	Reactants and Products	Rate Constant Expression	k_{298}
164	XOPN = 0.4 GLY + XO2H + 0.7 HO2 + 0.7 CO + 0.3 C2O3 + RO2	Photolysis: J(XOPN) = J(NO2)x0.08	5.04×10^{-4}
165	XOPN + OH = MGLY + 0.4 GLY + 2 XO2H + 2 RO2	$k = 9.00 \times 10^{-11}$	9.00×10^{-11}
166	XOPN + O3 = 1.2 MGLY + 0.5 OH + 0.6 C2O3 + 0.1 ALD2 + 0.5 CO + 0.3 XO2H + 0.3 RO2	$k = 1.08 \times 10^{-16} \exp(-500/T)$	2.02×10^{-17}
167	XOPN + NO3 = 0.5 NO2 + 0.5 NTR2 + 0.25 OPEN + 0.25 MGLY + 0.45 XO2H + 0.45 XO2 + 0.1 XO2N + RO2	$k = 3.00 \times 10^{-12}$	3.00×10^{-12}
168	CRES + OH = 0.7 CAT1 + 0.7 HO2 + 0.3 CRO	$k = 1.70 \times 10^{-12} \exp(950/T)$	4.12×10^{-11}
169	CRES + NO3 = 0.5 HNO3 + 0.5 CRON + 0.5 CRO	$k = 1.40 \times 10^{-11}$	1.40×10^{-11}
170	CRO + NO2 = CRON	$k = 2.10 \times 10^{-12}$	2.10×10^{-12}
171	CRO + HO2 = CRES	$k = 5.50 \times 10^{-12}$	5.50×10^{-12}
172	CRON + OH = NTR2 + 0.5 CRO	$k = 1.53 \times 10^{-12}$	1.53×10^{-12}
173	CRON + NO3 = HNO3 + NTR2 + 0.5 CRO	$k = 3.80 \times 10^{-12}$	3.80×10^{-12}
174	CRON = HONO + 0.5 CRO	Photolysis: J(CRON) = J(NO2)x0.015	9.45×10^{-5}
175	CAT1 + OH = 0.5 CRO	$k = 5.00 \times 10^{-11}$	5.00×10^{-11}
176	CAT1 + NO3 = 0.5 CRO + HNO3	$k = 1.70 \times 10^{-10}$	1.70×10^{-10}
177	ARPX + OH = 0.5 OH + 0.2 BZO2 + 0.15 TO2 + 0.15 XLO2 + 0.5 RO2	$k = 8.00 \times 10^{-11}$	8.00×10^{-11}
178	ISOP + OH = ISO2 + RO2	$k = 2.70 \times 10^{-11} \exp(390/T)$	9.99×10^{-11}
179	ISO2 + NO = 0.9 NO2 + 0.1 INTR + 0.9 FORM + 0.9 ISPD + 0.9 HO2	k = k(ref)/K k(ref) = k(75) K = 1.0	9.04×10^{-12}
180	ISO2 + HO2 = 0.94 ISPX + 0.06 FORM + 0.06 ISPD + 0.06 OH + 0.06 HO2	k = k(ref)/K k(ref) = k(76) $K = 9.13 \times 10^{-1}$	1.66×10^{-11}
181	ISO2 + RO2 = ISPD + RO2	k = k(ref)/K k(ref) = k(77) K = 1.0	5.00×10^{-13}
182	ISO2 = 0.4 HPLD + 0.1 ISPD + 0.1 GLY + 0.1 GLYD + CO + 1.7 OH + 0.35 HO2	$k = 3.30 \times 10^{+9} \exp(-8300/T)$	2.64×10^{-3}
183	ISOP + O3 = 0.8 FORM + 0.5 ISPD + 0.58 FACD + 0.5 CO + 0.28 OH + 0.5 HO2 + 0.4 MEO2 + 0.4 RO2	$k = 1.03 \times 10^{-14} \exp(-1995/T)$	1.27×10^{-17}
184	ISOP + NO3 = 0.25 NO2 + 0.75 NTR2 + 0.25 FORM + 0.25 ISPD + 0.25 OH + 0.25 XO2 + 0.25 RO2	$k = 2.95 \times 10^{-12} \exp(-450/T)$	6.52×10^{-13}
185	ISPD + OH = 0.28 MGLY + 0.14 HACT + 0.2 GLYD + 0.1 FORM + CO + 0.1 OH + 0.1 HO2 + 0.1 OPO3 + 0.4 C2O3	$k = 7.00 \times 10^{-12} \exp(430/T)$	2.96×10^{-11}

Number	Reactants and Products	Rate Constant Expression	k_{298}
186	ISPD + NO3 = 0.9 NTR2 + 0.1 HNO3 + 0.1 CO + 0.1 C2O3	$k = 3.94x10^{-14} exp(475/T)$	$1.94x10^{-13}$
187	ISPD = 0.5 FORM + 0.35 OLE + 0.35 PAR + 0.95 CO + 0.15 OPO3 + 0.4 C2O3 + 0.1 MEO2 + 0.55 HO2 + 0.1 RO2	Photolysis: J(ISPD) = J(MEPX)x1.0	$2.68x10^{-6}$
188	ISPX + OH = 0.6 EPOX + 0.2 MGLY + 0.2 FORM + 0.2 ROOH + OH + 0.5 HO2	$k = 2.80x10^{-11} exp(370/T)$	$9.69x10^{-11}$
189	HPLD = 0.6 HPLD + 0.3 ISPD + 1.65 OH + 0.2 HO2 + 0.8 CO	Photolysis: J(HPLD) = J(NO2)x0.07	$4.41x10^{-4}$
190	HPLD + OH = ISPD + 0.2 FORM + 0.5 CO + 1.1 OH	$k = 1.17x10^{-11} exp(450/T)$	$5.30x10^{-11}$
191	EPOX + OH = 0.2 ISPD + 0.2 HO2 + 0.8 EPX2 + 0.8 RO2	$k = 5.43x10^{-11} exp(-450/T)$	$1.20x10^{-11}$
192	EPX2 + NO = 0.98 NO2 + 0.02 NTR2 + 0.7 MGLY + 0.2 HACT + 0.7 GLYD + 0.2 GLY + 0.2 CO + 0.7 OH + HO2	k = k(ref)/K k(ref) = k(75) K = 1.0	$9.04x10^{-12}$
193	EPX2 + HO2 = 0.2 ISPD + 0.3 MGLY + 0.15 HACT + 0.1 GLY + 0.2 GLYD + 1.5 FORM + ROOH + 0.2 CO + 1.7 OH + HO2	k = k(ref)/K k(ref) = k(76) $K = 9.13x10^{-1}$	$1.66x10^{-11}$
194	EPX2 + RO2 = 0.6 MGLY + 0.1 HACT + 0.5 GLY + 0.5 FORM + 0.3 GLYD + 0.2 CO + 0.85 OH + HO2 + RO2	k = k(ref)/K k(ref) = k(77) K = 1.0	$5.00x10^{-13}$
195	INTR + OH = 0.45 NO2 + 0.45 NTR2 + 0.1 INTR + 0.4 ISPD + 0.1 EPOX	$k = 1.00x10^{-11} exp(300/T)$	$2.74x10^{-11}$
196	APIN + OH = APO2 + 0.11 AUTX	$k = 1.34x10^{-11} exp(410/T)$	$5.30x10^{-11}$
197	APO2 + NO = 0.77 NO2 + 0.23 NTR2 + 0.55 TPRD + 0.21 FORM + 0.09 ACET + 0.77 HO2	k = k(ref)/K k(ref) = k(75) K = 1.0	$9.04x10^{-12}$
198	APO2 + HO2 = 0.65 ROOH + 0.29 TPRD + 0.08 FORM + 0.06 ACET + 0.48 HO2 + 0.35 OH	k = k(ref)/K k(ref) = k(76) $K = 7.21x10^{-1}$	$2.10x10^{-11}$
199	APO2 + RO2 = 0.13 ROOH + 0.77 TPRD + 0.06 ACET + 0.5 HO2 + RO2	k = k(ref)/K k(ref) = k(77) K = 1.0	$5.00x10^{-13}$
200	APIN + O3 = 0.35 TPRD + 0.27 FORM + 0.22 H2O2 + 0.17 CO + 0.77 OH + 0.17 HO2 + 0.27 CXO3 + 0.33 XO2 + 0.33 RO2	$k = 8.05x10^{-16} exp(-640/T)$	$9.40x10^{-17}$
201	APIN + NO3 = 0.76 NO2 + 0.24 NTR2 + 0.68 TPRD + 0.42 OH	$k = 1.20x10^{-12} exp(490/T)$	$6.21x10^{-12}$
202	TERP + OH = TPO2	$k = 3.20x10^{-11} exp(390/T)$	$1.18x10^{-10}$

Number	Reactants and Products	Rate Constant Expression	k_{298}
203	TPO2 + NO = 0.75 NO2 + 0.25 NTR2 + 0.49 TPRD + 0.45 FORM + 0.1 ACET + 0.39 PAR + 0.13 KET + 0.75 HO2	k = k(ref)/K k(ref) = k(75) K = 1.0	9.04×10^{-12}
204	TPO2 + HO2 = 0.94 ROOH + 0.04 TPRD + 0.04 FORM + 0.01 ACET + 0.06 HO2 + 0.06 OH	k = k(ref)/K k(ref) = k(76) K = 7.21×10^{-1}	2.10×10^{-11}
205	TPO2 + RO2 = 0.7 TPRD + 0.31 FORM + 0.05 ACET + 0.51 PAR + 0.17 KET + 0.5 HO2 + RO2	k = k(ref)/K k(ref) = k(77) K = 1.0	5.00×10^{-13}
206	TERP + O3 = 0.74 TPRD + 0.63 FORM + 0.04 ACET + 0.03 HACT + 0.05 FACD + 0.27 H2O2 + 0.44 OH + 0.09 HO2 + 0.08 C2O3 + 0.26 CXO3 + 0.07 XO2 + 0.07 RO2	$k = 4.24 \times 10^{-15} \exp(-1030/T)$	1.34×10^{-16}
207	TERP + NO3 = 0.35 NO2 + 0.65 NTR2 + 0.31 TPRD + 0.09 ACET + 0.29 OH + 0.2 HO2	$k = 6.15 \times 10^{-12}$	6.15×10^{-12}
208	SQT + OH = 0.6 TPRD + 0.6 XO2H + 0.4 XO2N + RO2	$k = 2.00 \times 10^{-10}$	2.00×10^{-10}
209	SQT + O3 = 0.58 TPRD + 0.08 FORM + 0.17 H2O2 + 0.57 OH + 0.08 HO2	$k = 1.20 \times 10^{-14}$	1.20×10^{-14}
210	SQT + NO3 = 0.58 NO2 + 0.42 NTR2 + 0.39 TPRD + 0.3 OH	$k = 1.90 \times 10^{-11}$	1.90×10^{-11}
211	TPRD + OH = FORM + 0.5 ACET + 0.5 CO + 0.8 HO2 + 0.3 C2O3 + 1.1 XO2 + 0.4 XO2N + 1.5 RO2	$k = 1.35 \times 10^{-11} \exp(400/T)$	5.17×10^{-11}
212	TPRD + NO3 = 0.87 HNO3 + 0.08 NO2 + 0.05 NTR2 + 0.3 FORM + 0.1 CO + 0.1 HO2 + 0.6 CXO3	$k = 1.00 \times 10^{-13}$	1.00×10^{-13}
213	TPRD + O3 = 0.5 FORM + 0.2 FACD + 0.1 H2O2 + 0.1 OH + 0.3 MEO2 + 0.3 RO2	$k = 1.10 \times 10^{-17}$	1.10×10^{-17}
214	TPRD = 1.5 FORM + 0.5 ACET + 1.8 CO + 1.8 HO2 + 0.5 C2O3 + 0.3 XO2N + 1.5 XO2 + 1.8 RO2	Photolysis: J(TPRD) = J(MEPX)x4.6	1.23×10^{-5}
215	EDOH + OH = GLYD + HO2	$k = 1.45 \times 10^{-11}$	1.45×10^{-11}
216	PDOH + OH = 0.61 ACET + 0.39 ALDX + 0.39 PAR + HO2	$k = 2.10 \times 10^{-11}$	2.10×10^{-11}
217	IPOH + OH = 0.86 ACET + 0.14 ALD2 + 0.14 FORM + 0.86 HO2 + 0.14 XO2H + 0.14 RO2	$k = 2.60 \times 10^{-12} \exp(200/T)$	5.09×10^{-12}
218	NPOH + OH = 0.55 ALDX + 0.43 ALD2 + 0.55 PAR + 0.43 FORM + 0.48 HO2 + 0.5 XO2H + 0.02 XO2N + 0.52 RO2	$k = 4.60 \times 10^{-12} \exp(70/T)$	5.82×10^{-12}

Number	Reactants and Products	Rate Constant Expression	k_{298}
219	ROH + OH = 0.2 ALDX + 0.4 PAR + 0.77 ROR + 0.2 HO2 + 0.77 XO2 + 0.03 XO2N + 0.8 RO2	$k = 7.00x10^{-12} \exp(60/T)$	$8.56x10^{-12}$
220	DME + OH = 0.99 MEFM + 0.99 XO2H + 0.01 XO2N + RO2	$k = 5.70x10^{-12} \exp(-215/T)$	$2.77x10^{-12}$
221	DEE + OH = 0.8 ETFM + 0.2 ALD2 + 0.04 ETAC + 0.8 MEO2 + 0.9 XO2 + 0.14 XO2H + 0.06 XO2N + 2 RO2	$k = 8.91x10^{-18} (T)^2 \exp(837/T)$	$1.31x10^{-11}$
222	ETHR + OH = 0.62 ESTR + 0.3 ALDX + 0.3 PAR + 0.62 MEO2 + 0.3 XO2H + 0.62 XO2 + 0.08 XO2N + RO2	$k = 8.90x10^{-12} \exp(100/T)$	$1.24x10^{-11}$
223	MEFM + OH = 0.17 FACD + 0.55 CO + 0.45 MEO2 + 0.55 XO2H + 0.005 XO2N + RO2	$k = 9.39x10^{-13} \exp(-461/T)$	$2.00x10^{-13}$
224	MEAC + OH = 0.67 AACD + 0.67 CO + 0.32 MEO2 + 0.67 XO2H + 0.32 XO2 + 0.01 XO2N + 1.32 RO2	$k = 8.54x10^{-19} (T)^2 \exp(455/T)$	$3.49x10^{-13}$
225	ETFM + OH = 0.78 AACD + 0.78 CO + 0.2 ALD2 + 0.98 XO2H + 0.02 XO2N + 1.2 RO2	$k = 5.66x10^{-13} \exp(134/T)$	$8.87x10^{-13}$
226	ETAC + OH = 0.93 AACD + 0.93 C2O3 + 0.93 XO2 + 0.07 XO2N + RO2	$k = 6.92x10^{-19} (T)^2 \exp(986/T)$	$1.68x10^{-12}$
227	ESTR + OH = 0.13 AACD + 0.13 FACD + 0.15 PAR + 0.63 ROR + 0.25 CXO3 + 0.89 XO2 + 0.11 XO2N + RO2	$k = 2.50x10^{-13} \exp(740/T)$	$2.99x10^{-12}$
228	SXD5 + OH = 0.5 FORM + 0.5 FACD + XO2H + RO2	$k = 2.10x10^{-12}$	$2.10x10^{-12}$
229	IBTA + OH = 0.78 ACET + 0.19 ALDX + 0.78 MEO2 + 0.78 XO2 + 0.19 XO2H + 0.03 XO2N + RO2	$k = 5.40x10^{-12} \exp(-285/T)$	$2.08x10^{-12}$
230	HPAR + OH = HPO2 + RO2	$k = 2.54x10^{-11} \exp(-180/T)$	$1.39x10^{-11}$
231	HPO2 + NO = NTR2	k = k(ref)/K k(ref) = k(75) $K = 6.16x10^{+2} \exp(-1540/T)$	$2.57x10^{-12}$
232	HPO2 + NO = NO2 + HO2 + AUTX + RO2	k = k(ref)/K k(ref) = k(75) $K = 1.13x10^{-1} \exp(750/T)$	$6.46x10^{-12}$
233	HPO2 + HO2 = ROOH	k = k(ref)/K k(ref) = k(76) $K = 7.31x10^{-1}$	$2.07x10^{-11}$
234	HPO2 + RO2 = 0.6 HO2 + 0.6 AUTX + 0.6 RO2	k = k(ref)/K k(ref) = k(77) K = 1.0	$5.00x10^{-13}$

Number	Reactants and Products	Rate Constant Expression	k_{298}
235	AUTX + NO = 0.88 NO2 + 0.12 NTR2 + 0.46 HKET + 0.3 KET + 0.12 ALDX + 1.98 PAR	k = k(ref)/K k(ref) = k(75) K = 1.0	9.04×10^{-12}
236	AUTX + HO2 = ROOH	k = k(ref)/K k(ref) = k(76) K = 8.13×10^{-1}	1.86×10^{-11}
237	AUTX = 0.9 HKET + 0.9 XO2 + 0.1 XO2N	k = $2.20\times10^{+8}$ exp(−6200/T)	2.03×10^{-1}
238	HKET + OH = 1.5 KET + 4.5 PAR + OH	k = 6.00×10^{-11}	6.00×10^{-11}
239	HKET = ALDX + 0.25 FORM + 2.7 PAR + 0.5 CXO3 + OH + HO2	Photolysis: J(HKET) = J(MEPX)x1.1	2.95×10^{-6}
240	EH2 + OH = HO2	k = 7.70×10^{-12} exp(−2100/T)	6.70×10^{-15}
241	I2 = 2 I	Photolysis: J(I2) = J(NO3)x0.922	1.44×10^{-1}
242	HOI = I + OH	Photolysis: J(HOI) = J(NO2)x10.1	6.36×10^{-2}
243	I + O3 = IO	k = 2.10×10^{-11} exp(−830/T)	1.30×10^{-12}
244	IO = I + O	Photolysis: J(IO) = J(NO2)x18.7	1.18×10^{-1}
245	IO + IO = 0.4 I + 0.4 OIO + 0.6 I2O2	k = 5.40×10^{-11} exp(180/T)	9.88×10^{-11}
246	IO + HO2 = HOI	k = 1.40×10^{-11} exp(540/T)	8.57×10^{-11}
247	IO + NO = I + NO2	k = 7.15×10^{-12} exp(300/T)	1.96×10^{-11}
248	IO + NO2 = INO3	Falloff: F=0.4; n=1.26 k(0) = 7.70×10^{-31} $(T/300)^{-5}$ k(inf) = 1.60×10^{-11}	3.54×10^{-12}
249	OIO = I	Photolysis: J(OIO) = J(NO3)x0.908	1.41×10^{-1}
250	OIO + OH = 0.5 IXOY	Falloff: F=0.3; n=1.41 k(0) = 1.50×10^{-27} $(T/300)^{-3.93}$ k(inf) = 5.50×10^{-10} exp(46/T)	3.96×10^{-10}
251	OIO + IO = IXOY	k = 1.00×10^{-10}	1.00×10^{-10}
252	OIO + NO = IO + NO2	k = 1.10×10^{-12} exp(542/T)	6.78×10^{-12}
253	I2O2 = I + OIO	k = $1.00\times10^{+1}$	$1.00\times10^{+1}$
254	I2O2 + O3 = IXOY	k = 1.00×10^{-12}	1.00×10^{-12}
255	INO3 = I + NO3	Photolysis: J(INO3) = J(N2O5)x470.0	1.18×10^{-2}
256	INO3 + H2O = HOI + HNO3	k = 2.50×10^{-22}	2.50×10^{-22}
257	IXOY + H2O2 = I2	k = 5.00×10^{-16}	5.00×10^{-16}

Table A-2. CB7r2 species names, descriptions, atom counts and molecular weights.

Species	Description	C	H	O	N	S	I	Si	M.Wt.
APO2	Peroxy radical from OH addition to α-pinene	10	17	3					185.24
AUTX	Operator for hydroxyalkylperoxy radical autoxidation	6	13	2					117.17
BZO2	Peroxy radical from OH addition to benzene	6	7	5					159.12
C2O3	Acetylperoxy radical	2	3	3					75.04
CRO	Alkoxy radical from cresol	7	7	1					107.13

Species	Description	C	H	O	N	S	I	Si	M.Wt.
CXO3	C3 and higher acylperoxy radicals	2	3	3					75.04
DPAR	Operator for PAR destruction (replacing negative PAR product)	1	2.5						14.53
EPX2	Peroxy radical from EPOX reaction with OH	5	9	5					149.12
HO2	Hydroperoxy radical		1	2					33.01
HPO2	Peroxy radical from HPAR reaction with OH	12	25	3					217.33
ISO2	Peroxy radical from OH addition to isoprene	5	9	3					117.12
MEO2	Methylperoxy radical	1	3	2					47.03
O	Oxygen atom in the $O^3(P)$ electronic state			1					16.00
O1D	Oxygen atom in the $O^1(D)$ electronic state			1					16.00
OH	Hydroxyl radical		1	1					17.01
OPO3	Peroxyacyl radical from OPEN and other model species	4	3	4					115.06
RO2	Operator to approximate total peroxy radical concentration			2					32.00
ROR	Secondary alkoxy radical	4	9	1					73.12
TPO2	Peroxy radical from OH addition to TERP	10	17	3					185.24
TO2	Peroxy radical from OH addition to TOL	7	9	5					173.14
XLO2	Peroxy radical from OH addition to XYL	8	11	5					187.17
XO2	NO to NO2 conversion from a peroxy radical			2					32.00
XO2H	NO to NO2 conversion (XO2) accompanied by HO2 production from a peroxy radical			2					32.00
XO2N	NO to organic nitrate conversion from a peroxy radical	4	9	2					89.11
XPAR	Operator to enable T-dependent organic nitrate yield from PAR	4	9	2					89.11
AACD	Acetic acid	2	4	2					60.05
ACET	Acetone	3	6	1					58.08
ALD2	Acetaldehyde	2	4	1					44.05
ALDX	Higher aldehydes (R-C-CHO)	2	3	1					43.05
APIN	α-Pinene	10	16						136.24
ARPX	Aromatic peroxide from BZO2, TO2 and XLO2	6	8	6					176.12
BENZ	Benzene	6	6						78.11
CAT1	Methyl-catechols	7	8	2					124.14
CO	Carbon monoxide	1		1					28.01
CH4	Background methane (see also ECH4)	1	4						16.04
CRES	Cresols	7	8	1					108.14

Species	Description	C	H	O	N	S	I	Si	M.Wt.
CRON	Nitro-cresols	7	7	3	1				153.14
DEE	Diethyl ether	4	10	1					74.12
DME	Dimethyl ether	2	6	1					46.07
DMS	Dimethyl sulfide	2	6			1			62.14
ECH4	Emitted methane (to enable tracking separate from CH4)	1	4						16.04
EDOH	1,2-ethanediol (ethylene glycol)	2	6	2					62.07
EH2	Emitted hydrogen (to enable tracking separate from H2)		2						2.02
EPOX	Epoxide formed from ISPX reaction with OH	5	10	3					118.13
ESTR	Larger esters (C4+, excluding ethyl acetate)	4	8	2					88.11
ETAC	Ethyl acetate	4	8	2					88.11
ETFM	Ethyl formate	3	6	2					74.08
ETH	Ethene	2	4						28.05
ETHA	Ethane	2	6						30.07
ETHR	Larger ethers (C4+, excluding diethyl ether)	4	10	1					74.12
ETHY	Ethyne	2	2						26.04
ETOH	Ethanol	2	6	1					46.07
FACD	Formic acid	1	2	2					46.03
FORM	Formaldehyde	1	2	1					30.03
GLY	Glyoxal	2	2	2					58.04
GLYD	Glycolaldehyde	2	4	2					60.05
H2	Background hydrogen		2						2.02
H2O2	Hydrogen peroxide		2	2					34.01
HACT	Hydroxyacetone	3	6	2					74.08
HKET	Hydroperoxyketones from alkoxy radical autoxidation	6	12	4					148.16
HNO3	Nitric acid		1	3	1				63.01
HONO	Nitrous acid		1	2	1				47.01
HPAR	Large alkanes, based on n-dodecane	12	26						170.34
HPLD	Hydroperoxyaldehyde from ISO2 isomerization	5	8	3					116.12
IBTA	2-methylpropane (isobutane)	4	10						58.12
INTR	Organic nitrates from ISO2 reaction with NO	5	9	4	1				147.13
IOLE	Internal olefin carbon bond (R-C=C-R)	4	8						56.11
IPOH	Isopropanol	3	8	1					60.10
ISOP	Isoprene	5	8						68.12
ISPD	Isoprene product (methacrolein, methyl vinyl ketone, etc.)	4	6	1					70.09
ISPX	Hydroperoxides from ISO2 reaction with HO2	5	10	3					118.13

Species	Description	C	H	O	N	S	I	Si	M.Wt.
KET	Ketone bond in larger ketones (C4+)	1		1					28.01
MEAC	Methyl acetate	3	6	2					74.08
MEFM	Methyl formate	2	4	2					60.05
MEOH	Methanol	1	4	1					32.04
MEPX	Methylhydroperoxide	1	4	2					48.04
MGLY	Methylglyoxal	3	4	2					72.06
N2O5	Dinitrogen pentoxide			5	2				108.01
NO	Nitric oxide			1	1				30.01
NO2	Nitrogen dioxide			2	1				46.01
NO3	Nitrate radical			3	1				62.00
NPOH	1-Propanol	3	8	1					60.10
NTR1	Simple organic nitrates	4	9	3	1				119.12
NTR2	Multi-functional organic nitrates	4	9	4	1				135.12
O3	Ozone			3					48.00
OLE	Terminal olefin carbon bond (R-C=C)	2	4						28.06
OPAN	Other peroxyacyl nitrates (PAN compounds) from OPO3	4	3	6	1				161.07
OPEN	Aromatic ring opening product (unsaturated dicarbonyl)	4	4	2					84.07
PACD	Peroxyacetic and higher peroxycarboxylic acids	2	4	3					76.05
PAN	Peroxyacetyl Nitrate	2	3	5	1				121.05
PANX	Larger alkyl peroxyacyl nitrates (from CXO3)	2	3	5	1				121.05
PAR	Paraffin carbon bond (C-C)	1	2.5						14.53
PDOH	1,2-propanediol (propylene glycol)	3	8	2					76.10
PNA	Peroxynitric acid		1	4	1				79.01
PRPA	Propane	3	8						44.10
ROH	Larger alcohols (C4+)	4	10	1					74.12
ROOH	Higher organic peroxide	4	10	2					90.12
SO2	Sulfur dioxide			2		1			64.06
SULF	Sulfuric acid (gaseous)		2	4		1			98.08
SQT	Sesqiterpenes	15	24						204.36
SXD5	Siloxanes represented by decamethylcyclopentasiloxane (D5)	10	30	5				5	370.62
TERP	Monoterpenes	10	16						136.24
TOL	Toluene and other monoalkyl aromatics	7	8						92.14
TPRD	Terpene product (pinonaldehyde, limonaldehyde, etc.)	8	14	2					142.20
XOPN	Aromatic ring opening product (unsaturated dicarbonyl)	5	6	2					98.10
XYL	Xylene and other polyalkyl aromatics	8	10						106.17
I2	Molecular iodine						2		253.81

Species	Description	C	H	O	N	S	I	Si	M.Wt.
I	Iodine atom						1		126.91
IO	Iodine monoxide			1			1		142.90
OIO	Iodine dioxide			2			1		158.90
I2O2	Diiodine dioxide			2			2		285.81
IXOY	Condensable iodine oxides			3			2		301.81
HOI	Hypoiodous acid		1	1			1		143.91
INO3	Iodine nitrate			3	1		1		188.91

Table A-3. CB7r2 photolysis rate label and data references.

J-Label	Cross Section Data[(a)]	Quantum Yield Data
ACET.PHF	IUPAC Data Sheet P7 (19 Dec 2005)	IUPAC Data Sheet P7 (19 Dec 2005)
ALD2_Rr5.PHF	IUPAC Data Sheet P2 (Jun2013)	IUPAC Data Sheet P2 (Jun2013)
ALDX_R.PHF	IUPAC Data Sheet P3 (May2002)	IUPAC Data Sheet P3 (May2002)
FORM_Mr5.PHF	IUPAC Data Sheet P1 (16Apr2013)	IUPAC Data Sheet P1 (16Apr2013)
FORM_R72.PHF	IUPAC Data Sheet P1 (16Apr2013)	IUPAC Data Sheet P1 (16Apr2013) plus PPO from Welsh et al. (2023) doi: s41557-023-01272-4
GLY_Rr5.PHF	IUPAC Data Sheet P4 (May2013)	IUPAC Data Sheet P4 (May2013)
GLYDr5.PHF	IUPAC Data Sheet P5 (16May2002)	IUPAC Data Sheet P5 (16May2002)
H2O2.PHF	IUPAC Data Sheet PHOx2 (2Oct2001)	IUPAC Data Sheet PHOx2 (2Oct2001)
HNO3.PHF	IUPAC Data Sheet PNOx2 (16Jul2001)	IUPAC Data Sheet PNOx2 (16Jul2001)
HONO.PHF	IUPAC Data Sheet PNOx1 (16Jul2001)	IUPAC Data Sheet PNOx1 (16Jul2001)
KET.PHF	IUPAC Data Sheet P8 (5Dec2005)	IUPAC Data Sheet P7 (acetone; 19 Dec 2005)
MEPX.PHF	IUPAC Data Sheet P12 (16May2002)	IUPAC Data Sheet P12 (16May2002)
MGLY.PHF	IUPAC Data Sheet P6 (16Jan2003)	IUPAC Data Sheet P6 (16Jan2003)
N2O5.PHF	IUPAC Data Sheet PNOx7 (16Jul2001)	IUPAC Data Sheet PNOx7 (16Jul2001)
NO2.PHF	IUPAC Data Sheet PNOx4 (16Jul2001)	IUPAC Data Sheet PNOx4 (16Jul2001)
NO3_NO.PHF	NASA JPL15 Table 4-15 (20Nov2006)	NASA JPL15 Table 4-16 (20Nov2006)
NO3_NO2.PHF	NASA JPL15 Table 4-15 (20Nov2006)	NASA JPL15 Table 4-16 (20Nov2006)
NTR.PHF	IUPAC Data Sheet P17 (i-C3H7ONO2; 16May2002)	IUPAC Data Sheet P17 (i-C3H7ONO2; 16May2002)
O3O1D.PHF	IUPAC Data Sheet POx2 (2Oct2001)	IUPAC Data Sheet POx2 (2Oct2001)
O3O3P.PHF	IUPAC Data Sheet POx2 (2Oct2001)	IUPAC Data Sheet POx2 (2Oct2001)
PAN.PHF	IUPAC Data Sheet P21 (19Dec2005)	IUPAC Data Sheet P21 (19Dec2005)
PNA.PHF	IUPAC Data Sheet PNOx3(16Jul2001)	IUPAC Data Sheet PNOx3(16Jul2001)

[(a)]NASA (2019) means Burkholder et al. (2020) available at https://jpldataeval.jpl.nasa.gov/download.html and IUPAC means Mellouki et al (2021) with the latest IUPAC data sheets available at https://iupac.aeris-data.fr/.

Table A-4. Zenith angle (Z, in degrees) dependence of photolysis frequencies (min^{-1}) for CB7r2 reactions computed by the TUV discrete ordinates radiative transfer scheme (Stamnes et al., 1988) with cross-section and quantum yield data for each reaction recommended by the mechanism developer (See Table A-3). Conditions are 600 m above ground level at mean sea level with surface UV albedo of 0.04, stratospheric ozone column of 0.3 atm cm, and the aerosol profile of Elterman (1968) provided with TUV

Number	Species	Z=0	Z=20	Z=40	Z=60	Z=78	Z=86
1	NO2	$1.01x10^{-02}$	$9.77x10^{-03}$	$8.75x10^{-03}$	$6.30x10^{-03}$	$2.09x10^{-03}$	$5.12x10^{-04}$
8	O3	$4.26x10^{-04}$	$4.19x10^{-04}$	$3.94x10^{-04}$	$3.33x10^{-04}$	$1.79x10^{-04}$	$4.27x10^{-05}$
9	O3	$4.55x10^{-05}$	$3.99x10^{-05}$	$2.54x10^{-05}$	$8.78x10^{-06}$	$9.20x10^{-07}$	$1.52x10^{-07}$
21	H2O2	$8.79x10^{-06}$	$8.26x10^{-06}$	$6.64x10^{-06}$	$3.78x10^{-06}$	$8.81x10^{-07}$	$2.03x10^{-07}$
27	NO3	$1.88x10^{-01}$	$1.86x10^{-01}$	$1.79x10^{-01}$	$1.56x10^{-01}$	$8.22x10^{-02}$	$1.79x10^{-02}$
28	NO3	$2.32x10^{-02}$	$2.31x10^{-02}$	$2.23x10^{-02}$	$1.98x10^{-02}$	$1.12x10^{-02}$	$2.63x10^{-03}$
36	N2O5	$5.54x10^{-05}$	$5.23x10^{-05}$	$4.26x10^{-05}$	$2.52x10^{-05}$	$6.30x10^{-06}$	$1.48x10^{-06}$
39	HONO	$1.74x10^{-03}$	$1.68x10^{-03}$	$1.49x10^{-03}$	$1.04x10^{-03}$	$3.29x10^{-04}$	$8.35x10^{-05}$
44	HNO3	$8.47x10^{-07}$	$7.70x10^{-07}$	$5.57x10^{-07}$	$2.54x10^{-07}$	$4.20x10^{-08}$	$7.98x10^{-09}$
47	PNA	$7.02x10^{-06}$	$6.46x10^{-06}$	$4.84x10^{-06}$	$2.36x10^{-06}$	$4.16x10^{-07}$	$7.73x10^{-08}$
59	PAN	$9.53x10^{-07}$	$8.81x10^{-07}$	$6.72x10^{-07}$	$3.47x10^{-07}$	$7.05x10^{-08}$	$1.52x10^{-08}$
82	MEPX	$6.02x10^{-06}$	$5.68x10^{-06}$	$4.61x10^{-06}$	$2.68x10^{-06}$	$6.52x10^{-07}$	$1.53x10^{-07}$
93	ROOH	$6.02x10^{-06}$	$5.68x10^{-06}$	$4.61x10^{-06}$	$2.68x10^{-06}$	$6.52x10^{-07}$	$1.53x10^{-07}$
95	NTR1	$3.29x10^{-06}$	$3.01x10^{-06}$	$2.22x10^{-06}$	$1.06x10^{-06}$	$1.85x10^{-07}$	$3.60x10^{-08}$
96	NTR2	$3.29x10^{-06}$	$3.01x10^{-06}$	$2.22x10^{-06}$	$1.06x10^{-06}$	$1.85x10^{-07}$	$3.60x10^{-08}$
101	FORM	$4.27x10^{-05}$	$4.00x10^{-05}$	$3.18x10^{-05}$	$1.75x10^{-05}$	$3.72x10^{-06}$	$7.81x10^{-07}$
102	FORM	$5.43x10^{-05}$	$5.18x10^{-05}$	$4.35x10^{-05}$	$2.69x10^{-05}$	$7.06x10^{-06}$	$1.73x10^{-06}$
106	ALD2	$7.29x10^{-06}$	$6.59x10^{-06}$	$4.65x10^{-06}$	$1.96x10^{-06}$	$2.54x10^{-07}$	$3.93x10^{-08}$
109	ALDX	$4.27x10^{-05}$	$3.96x10^{-05}$	$3.03x10^{-05}$	$1.54x10^{-05}$	$2.90x10^{-06}$	$5.67x10^{-07}$
111	GLYD	$9.03x10^{-06}$	$8.24x10^{-06}$	$6.01x10^{-06}$	$2.76x10^{-06}$	$4.40x10^{-07}$	$7.94x10^{-08}$
114	GLY	$1.35x10^{-04}$	$1.30x10^{-04}$	$1.14x10^{-04}$	$7.95x10^{-05}$	$2.57x10^{-05}$	$6.08x10^{-06}$
116	MGLY	$2.36x10^{-04}$	$2.29x10^{-04}$	$2.04x10^{-04}$	$1.46x10^{-04}$	$4.92x10^{-05}$	$1.16x10^{-05}$
119	ACET	$1.16x10^{-06}$	$1.02x10^{-06}$	$6.50x10^{-07}$	$2.27x10^{-07}$	$2.34x10^{-08}$	$3.59x10^{-09}$
121	KET	$1.02x10^{-06}$	$9.02x10^{-07}$	$5.83x10^{-07}$	$2.08x10^{-07}$	$2.25x10^{-08}$	$3.51x10^{-09}$
160	OPEN	$3.02x10^{-04}$	$2.93x10^{-04}$	$2.62x10^{-04}$	$1.89x10^{-04}$	$6.27x10^{-05}$	$1.54x10^{-05}$
164	XOPN	$8.04x10^{-04}$	$7.82x10^{-04}$	$7.00x10^{-04}$	$5.04x10^{-04}$	$1.67x10^{-04}$	$4.09x10^{-05}$
174	CRON	$1.51x10^{-04}$	$1.47x10^{-04}$	$1.31x10^{-04}$	$9.45x10^{-05}$	$3.13x10^{-05}$	$7.68x10^{-06}$
187	ISPD	$6.02x10^{-06}$	$5.68x10^{-06}$	$4.61x10^{-06}$	$2.68x10^{-06}$	$6.52x10^{-07}$	$1.53x10^{-07}$
189	HPLD	$7.04x10^{-04}$	$6.84x10^{-04}$	$6.12x10^{-04}$	$4.41x10^{-04}$	$1.46x10^{-04}$	$3.58x10^{-05}$
214	TPRD	$2.77x10^{-05}$	$2.61x10^{-05}$	$2.12x10^{-05}$	$1.23x10^{-05}$	$3.00x10^{-06}$	$7.06x10^{-07}$
239	HKET	$6.62x10^{-06}$	$6.24x10^{-06}$	$5.07x10^{-06}$	$2.95x10^{-06}$	$7.17x10^{-07}$	$1.69x10^{-07}$
241	I2	$1.73x10^{-01}$	$1.72x10^{-01}$	$1.65x10^{-01}$	$1.44x10^{-01}$	$7.58x10^{-02}$	$1.65x10^{-02}$
242	HOI	$1.02x10^{-01}$	$9.87x10^{-02}$	$8.84x10^{-02}$	$6.36x10^{-02}$	$2.11x10^{-02}$	$5.17x10^{-03}$
244	IO	$1.88x10^{-01}$	$1.83x10^{-01}$	$1.64x10^{-01}$	$1.18x10^{-01}$	$3.91x10^{-02}$	$9.57x10^{-03}$
249	OIO	$1.71x10^{-01}$	$1.69x10^{-01}$	$1.62x10^{-01}$	$1.41x10^{-01}$	$7.46x10^{-02}$	$1.63x10^{-02}$
255	INO3	$2.60x10^{-02}$	$2.46x10^{-02}$	$2.00x10^{-02}$	$1.18x10^{-02}$	$2.96x10^{-03}$	$6.97x10^{-04}$

Appendix B

VCPy Top 100 VCP Compounds

Appendix B VCPy Top 100 VCP Compounds

Table B-1. Mapping the VCPy Top 100 VCP compounds to CB7r2_CF3 model species and SOA yield comparison to VCPy.

Rank	Chemical Name	Group	Emissions (kg/person/year)	VCPy SOA yield (g/g)	CB7r2_CF3 species[(a)]	CB7r2_CF3 SOA yield (g/g)
1	Terpene	alkene	0.045	0.595	TERP	0.481
2	d-Limonene	alkene	0.023	0.595	TERP	0.481
3	Dl-Limonene (Dipentene)	alkene	0.015	0.595	TERP	0.481
4	C10 Internal Alkenes	alkene	0.007	0.176	C10 alkane	0.091
5	Isomers of xylene	aromatic	0.129	0.353	XYL	0.236
6	Ethyl Benzene	aromatic	0.020	0.353	TOL	0.230
7	m-Xylene	aromatic	0.010	0.353	XYL	0.236
8	UNC peaks to CBM xylene	aromatic	0.010	0.353	XYL	0.236
9	Toluene	aromatic	0.132	0.332	TOL	0.230
10	Isomers Of Butylbenzene	aromatic	0.013	0.0791	TOL	0.230
11	Trimethylbenzenes	aromatic	0.008	0.0651	XYL	0.236
12	Styrene	aromatic	0.024	0.0546	XYL	0.236
13	Alkyl (C16-C18) Methyl Esters	b-alkane	0.066	0.373	IVOA	0.343
14	C13 Branched Alkanes	b-alkane	0.048	0.111	C13 alkane	0.241
15	Branched C12 Alkanes	b-alkane	0.102	0.068	C12 alkane	0.181
16	2,2,4,6,6-Pentamethylheptane	b-alkane	0.010	0.068	C12 alkane	0.181
17	Branched C11 alkanes	b-alkane	0.035	0.034	C11 alkane	0.136
18	2-methyldecane	b-alkane	0.016	0.034	C11 alkane	0.136
19	Dimethylnonane	b-alkane	0.008	0.034	C11 alkane	0.136
20	2,4-Dimethyloctane	b-alkane	0.022	0.009	C10 alkane	0.091
21	2,4,5-Trimethylheptane	b-alkane	0.020	0.009	C10 alkane	0.091
22	2-Methylnonane	b-alkane	0.014	0.009	C10 alkane	0.091
23	Isobutane	b-alkane	0.297	0	none	0.000
24	Branched C6 Alkanes	b-alkane	0.011	0	none	0.000

Rank	Chemical Name	Group	Emissions (kg/person/year)	VCPy SOA yield (g/g)	CB7r2_CF3 species[(a)]	CB7r2_CF3 SOA yield (g/g)
25	Branched C9 Alkanes	b-alkane	0.008	0	C9 alkane	0.068
26	C15 Cycloalkanes	c-alkane	0.007	0.55	C15 alkane	0.362
27	C12 Cycloalkanes	c-alkane	0.069	0.321	C12 alkane	0.181
28	C13 Cycloalkanes	c-alkane	0.012	0.321	C13 alkane	0.241
29	C11 Cycloalkanes	c-alkane	0.081	0.257	C11 alkane	0.136
30	Methyl Propylcyclohexanes	c-alkane	0.022	0.2	C10 alkane	0.091
31	C10 Cycloalkanes	c-alkane	0.017	0.2	C10 alkane	0.091
32	Butylcyclohexane	c-alkane	0.007	0.2	C10 alkane	0.091
33	Ethylmethylcyclohexanes	c-alkane	0.015	0.15	C9 alkane	0.068
34	Isopropylcyclohexane	c-alkane	0.007	0.15	C9 alkane	0.068
35	Trimethylcyclohexane	c-alkane	0.007	0.15	C9 alkane	0.068
36	C8 Cycloalkanes	c-alkane	0.006	0.107	C8 alkane	0.045
37	C7 Cycloalkanes	c-alkane	0.020	0.0696	C7 alkane	0.023
38	Cyclohexane	c-alkane	0.010	0.0392	none	0.000
39	C6 Cycloalkanes	c-alkane	0.007	0.0392	none	0.000
40	Alkanes, C14-16	n-alkane	0.110	0.321	C15 alkane	0.362
41	n-Pentadecane	n-alkane	0.006	0.321	C15 alkane	0.362
42	n-Tridecane	n-alkane	0.012	0.2	C13 alkane	0.241
43	n-Dodecane	n-alkane	0.071	0.15	C10 alkane	0.091
44	n-Undecane	n-alkane	0.085	0.107	C12 alkane	0.181
45	Isomers Of Undecane	n-alkane	0.027	0.107	C11 alkane	0.136
46	n-Undecane	n-alkane	0.008	0.107	C11 alkane	0.136
47	Isomers Of Decane	n-alkane	0.041	0.0696	C10 alkane	0.091
48	n-Decane	n-alkane	0.026	0.0696	C10 alkane	0.091
49	Other, Misc. VOC Compounds Aggregated In Profile	n-alkane	0.024	0.0696	C10 alkane	0.091
50	Voc Ingredients < 0.1%	n-alkane	0.023	0.0696	C10 alkane	0.091
51	N-Nonane	n-alkane	0.026	0.0392	C9 alkane	0.068
52	n-Octane	n-alkane	0.008	0.0154	C8 alkane	0.045

Rank	Chemical Name	Group	Emissions (kg/person/year)	VCPy SOA yield (g/g)	CB7r2_CF3 species[a]	CB7r2_CF3 SOA yield (g/g)
53	N-Octane	n-alkane	0.007	0.0154	C8 alkane	0.045
54	Propane	n-alkane	0.290	0	none	0.000
55	n-Butane	n-alkane	0.152	0	none	0.000
56	Hydrocarbon Propellant (LPG, Sweetened)	n-alkane	0.053	0	none	0.000
57	n-Heptane	n-alkane	0.037	0	C7 alkane	0.023
58	n-Hexane	n-alkane	0.011	0	none	0.000
59	Misc. esters	oxygenated	0.007	0.373	IVOA	0.343
60	2,2,4-Trimethyl-1,3-Pentanediol Isobutyrate (Texanol)	oxygenated	0.193	0.165	none	0.000
61	N,N-Diethyl-M-Toluamide	oxygenated	0.010	0.155	TOL	0.230
62	Diethyl Phthalate	oxygenated	0.011	0.148	IVOA	0.343
63	Decamethylcyclopentasiloxane	oxygenated	0.147	0.145	IVC1	0.101
64	Dimethylpolysiloxane	oxygenated	0.070	0.145	IVC1	0.101
65	Cyclotetrasiloxane	oxygenated	0.027	0.145	IVC1	0.101
66	Octamethylcyclotetrasiloxane	oxygenated	0.008	0.145	IVC1	0.101
67	Citronella Oil	oxygenated	0.009	0.14	TERP	0.481
68	Diethylene Glycol Monobutyl Ether	oxygenated	0.040	0.0739	IVC2	0.202
69	Glycol Ether Dpnb (1-(2-Butoxy-1-Methylethoxy)-2-Propanol)	oxygenated	0.013	0.0506	IVC1	0.101
70	Benzyl Alcohol	oxygenated	0.014	0.0504	IVC2	0.202
71	Diethylene Glycol Monoethyl Ether	oxygenated	0.024	0.0466	IVC2	0.202
72	Ethyl Cyanoacrylate	oxygenated	0.042	0.0418	none	0.000
73	Dipropylene Glycol Monomethyl Ether	oxygenated	0.012	0.0365	IVC1	0.101
74	N-Methylpyrrolidinone	oxygenated	0.008	0.0275	none	0.000
75	Propylene Glycol Butyl Ether (1-Butoxy-2-Propanol)	oxygenated	0.029	0.0242	IVC1	0.101
76	Ethylene Glycol Monobutyl Ether	oxygenated	0.073	0.0222	IVC2	0.202
77	Isobutyl Acetate	oxygenated	0.016	0.0185	none	0.000

Rank	Chemical Name	Group	Emissions (kg/person/year)	VCPy SOA yield (g/g)	CB7r2_CF3 species[a]	CB7r2_CF3 SOA yield (g/g)
78	N-Butyl Acetate	oxygenated	0.037	0.0179	none	0.000
79	Methyl Isobutyl Ketone (Hexone)	oxygenated	0.012	0.0173	none	0.000
80	Propylene Glycol Monomethyl Ether Acetate	oxygenated	0.008	0.0153	none	0.000
81	Ethanol	oxygenated	1.209	0	none	0.000
82	Acetone	oxygenated	0.841	0	none	0.000
83	Isopropyl Alcohol	oxygenated	0.510	0	none	0.000
84	Ethylene Glycol	oxygenated	0.254	0	none	0.000
85	Propylene Glycol	oxygenated	0.166	0	IVC1	0.101
86	Dimethyl Ether	oxygenated	0.094	0	none	0.000
87	Methanol	oxygenated	0.086	0	none	0.000
88	Glycerol	oxygenated	0.085	0	none	0.000
89	Methyl Ethyl Ketone (2-Butanone)	oxygenated	0.040	0	none	0.000
90	Methyl Acetate	oxygenated	0.033	0	none	0.000
91	Formic Acid	oxygenated	0.029	0	none	0.000
92	Witch Hazel	oxygenated	0.021	0	none	0.000
93	Ethyl Acetate	oxygenated	0.020	0	none	0.000
94	2-Amino-2-Methyl-1-Propanol	oxygenated	0.018	0	none	0.000
95	Sec-Butyl Alcohol	oxygenated	0.010	0	none	0.000
96	1,1-Difluoroethane (HFC-152a)	halocarbon	0.116	0	none	0.000
97	Methylene Chloride (Dichloromethane)	halocarbon	0.114	0	none	0.000
98	Parachlorobenzotrifluoride	halocarbon	0.028	0	none	0.000
99	1,1,1,2-Tetrafluoroethane (HFC-134a)	halocarbon	0.017	0	none	0.000
100	Ethyl-3-Ethoxypropionate	oxygenated	0.006	0.207	IVC1	0.101

[a]See Table 3-5 for the mapping of C7 to C15 alkanes to PAR, HPAR and/or IVOA